

A GRAVITY STUDY OF AN
ARCHEAN CRUSTAL SEGMENT NEAR
THUNDER BAY, ONTARIO

BY



SCOTT PHILIP CHEADLE

Submitted in partial fulfillment
of the requirements for the degree of

MASTER OF SCIENCE

Faculty of Science
Lakehead University
Thunder Bay, Ontario, Canada

May, 1982

ProQuest Number: 10611665

All rights reserved

INFORMATION TO ALL USERS

The quality of this reproduction is dependent upon the quality of the copy submitted.

In the unlikely event that the author did not send a complete manuscript and there are missing pages, these will be noted. Also, if material had to be removed, a note will indicate the deletion.



ProQuest 10611665

Published by ProQuest LLC (2017). Copyright of the Dissertation is held by the Author.

All rights reserved.

This work is protected against unauthorized copying under Title 17, United States Code
Microform Edition © ProQuest LLC.

ProQuest LLC.
789 East Eisenhower Parkway
P.O. Box 1346
Ann Arbor, MI 48106 - 1346

(c) Scott Philip Cheadle 1982

TABLE OF CONTENTS

	Page
ABSTRACT	i
ACKNOWLEDGEMENTS	iii
INTRODUCTION	1
GENERAL GEOLOGY	6
METAVOLCANIC ROCKS	8
METASEDIMENTARY ROCKS	9
GRANITIC INTRUSIVE ROCKS	11
ROCKS OF THE QUETICO BELT	12
STRUCTURE AND METAMORPHISM	15
GRAVITY SURVEY	21
DESCRIPTION OF THE REGIONAL BOUGUER ANOMALY FIELD	25
DESCRIPTION OF THE LOCAL BOUGUER ANOMALY FIELD	27
THE AEROMAGNETIC ANOMALY PATTERN	34
DENSITY STUDIES	38
MODELING METHODS AND RESULTS	45
DISCUSSION AND INTERPRETATION	63
CONCLUSIONS	78
APPENDIX A	
TABLE OF GRAVITY STATION DATA	83
APPENDIX B	
THE COMPUTER PROGRAMS AND MODEL DATA OUTPUT	104 & <i>Envelope</i>
REFERENCES	145

ABSTRACT

A gravity survey in an area involving portions of the Quetico and Shebandowan subprovinces of the Superior structural province resulted in the establishment of 350 new gravity stations in addition to 50 previously established stations.

For the purposes of this study the bedrock was divided into 4 major units including the metavolcanic rocks, metasedimentary rocks, assorted gneissic rocks and a group of intrusive igneous bodies.

Based on gravity modeling of these principal units, the following subsurface structure results. The metavolcanic rocks vary in depth extent from 6 km to 12 km and typically occupy a trough-shaped structure flanked by a domical feature of granitoid gneisses to the south. To the north of the metavolcanic unit, the metasedimentary rocks form a basin-like structure of variable depth extent. The contact between these two units is modeled as dipping steeply southward.

The Quetico granitoid gneisses to the north of the metasedimentary unit form a southward dipping wedge which extends to depths of 10 km in the model structure profiles. These gneisses are modeled as being underlain

by a denser substratum representative of more basic gneiss and amphibolite. The basal surface of this unit is gently convex upward, and the unit as a whole thickens toward the north and dips toward the south in a tapered wedge extending to a depth of 10 km. This unit is inclined slightly from east to west, and is exposed at the present erosion surface in the eastern portion of the study area only.

A number of quartz monzonite plutons have been emplaced near the northern portion of the metasedimentary unit and outcrops above the southern most edge of the dense substratum underlying the Quetico gneisses.

A tectonic model put forward synthesizes the available information regarding Archean crustal evolution and the data from this study. The proposed model consists of a basin-like structure (Quetico subprovince) which received sedimentary and volcanic debris from a mature volcanoplutonic terrane to the north (Wabigoon subprovince). Additional sedimentation into the basin was provided from the less mature volcanoplutonic terrane to the south (Shebandowan subprovince). Subsequent deformation accompanied by high grade metamorphism resulted in a general upwarping of the basin, producing the structures now observed in this part of the Quetico subprovince.

ACKNOWLEDGEMENTS

This thesis was supervised by Dr. M.M. Kehlenbeck and Dr. J.S. Mothersill, who provided much appreciated support and guidance throughout the course of the project. Thanks also to Dr. G.J. Borradaile for a number of helpful suggestions. I am grateful to M.D. Thomas of the Gravity and Geodynamics Division of the Earth Physics Branch, Department of Energy, Mines and Resources, and to Dr. G.F. West of the University of Toronto for providing a number of computer programs useful to this study. A special thanks also to Bonnie Morton of the Lakehead University Computer Center for much assistance in the implementation of these programs.

Many thanks to Sam Spivak, whose drafting skills and advice contributed greatly to this project. Finally, much credit for the execution and completion of this thesis is due to my wife Debi, whose contribution of assistance, patience and perseverance were above and beyond the call of matrimonial duty.

This study was in part funded by NSERC Grant No. 8379. We are also very grateful to the J.P. Bickel Foundation for funds made available for the acquisition of the gravity meter.

INTRODUCTION

In 1980, a gravity study was undertaken in the area north and west of Thunder Bay, Ontario. During 1980 and 1981, 350 new gravity stations were established between 89° and 90° longitude and 48°20' and 49° latitude. Access to the region was gained via Highways 11-17, 527, 102, 589 as well as numerous north-south and east-west trending secondary roads, and the shoreline of Dog Lake. The study area encompasses portions of the Wabigoon, Quetico and Shebandowan (Wawa) subprovince of the Superior Province of the Canadian Shield (Figure 1).

The aims of this study were threefold. The first objective was to collect the gravity data required to produce a detailed Bouguer gravity map of the study area. The second objective was to use computer modeling techniques as an aid to develop model subsurface structures of the various geological units based on the available geological and geophysical data. The third objective was to synthesize the results of the modeling procedure with currently available information from a number of sources regarding the tectonic development of the Archean crust in this part of the Superior province.

The Earth Physics Branch of the Department of Energy, Mines and Resources has published a regional

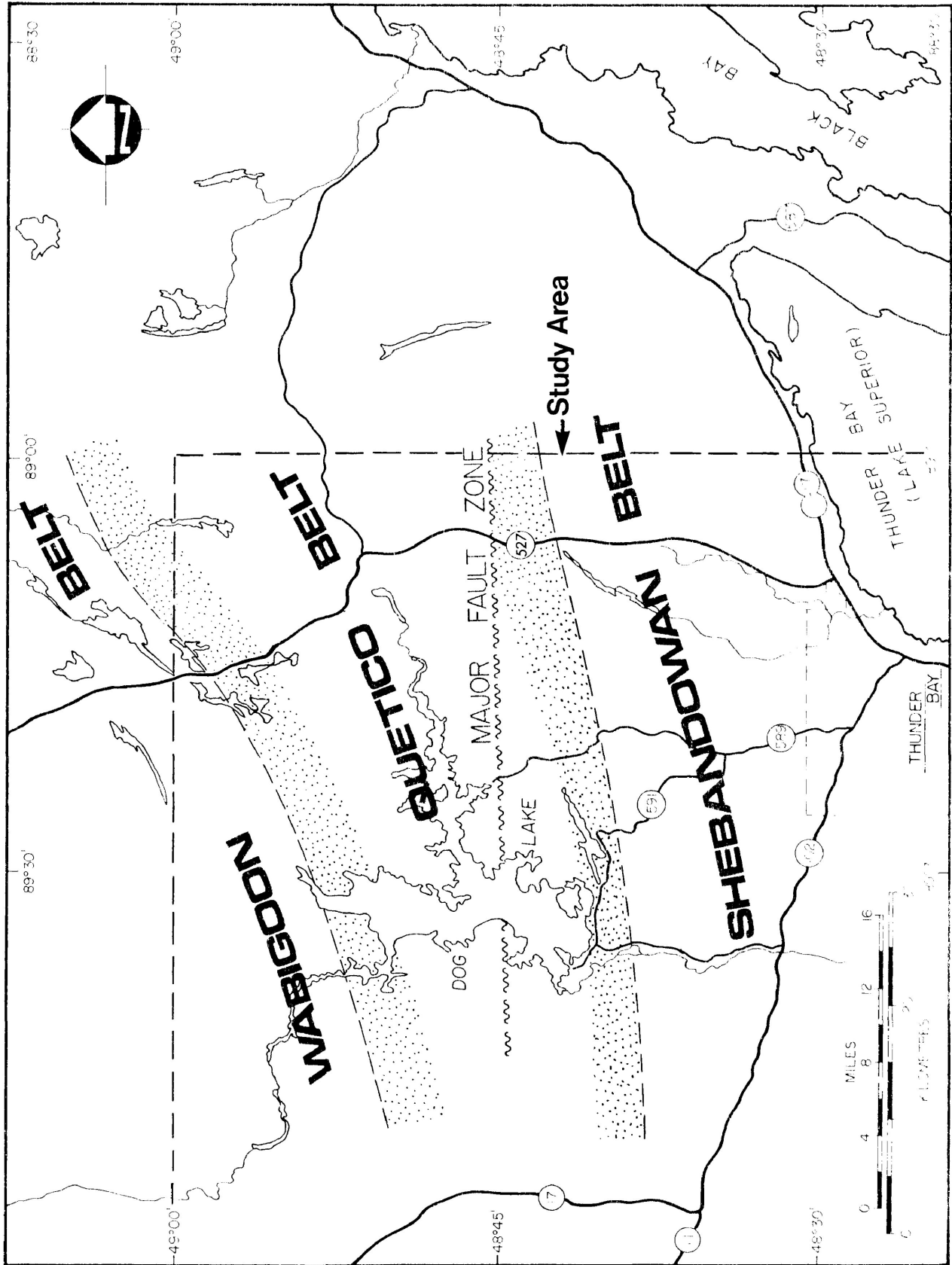


FIG.1 General Location Map

Bouguer gravity map series which includes coverage of this area (Figure 3). The general geology of the area is summarized on the Ontario Department of Mines Geology Compilation Map Series. The Ontario Department of Mines (presently the Ontario Geological Survey) has also published aeromagnetic maps of the region which provide coverage of the study area (Figure 6). A comparison of these sources of information demonstrates a generally good correspondence between the regional geology and the patterns of the regional geophysics.

The new gravity data collected during this study is combined with 50 gravity stations previously established in the area to compile a more detailed Bouguer gravity map of the area (Figure 4). These data, combined with the observed geology, density sampling and the aeromagnetic anomaly patterns, form the basis for the development and testing of model structures of the principal rock units recognized.

The usefulness of the gravity method as an aid to interpreting crustal structures in the Archean terrane has been demonstrated by a number of workers in a variety of situations. Brisbin and Green (1980) employed the gravity method to support a model of the Aulneau batholith of western Ontario extending to an average depth of 7 km., with a two pronged root structure extending to depths of

11 and 12 km. respectively. Adjacent mafic to ultramafic rocks were shown to not exceed 3 km. in thickness. Szewczyk and West (1976) used gravity modeling to demonstrate that while the Basket Lake intrusion near Ignace, Ontario extends to a depth of 8 km., the somewhat similar nearby Indian Lake intrusion is a thin sheet-like structure of only 2 km. in thickness. Adjacent metavolcanic units were modeled as varying from 3.2 km. to 7.7 km. in depth extent. Gupta, Thurston and Dusanowskyj (1982) tested a number of gravity models in their discussion of the constraints upon the development of metavolcanic and granitic structures in the Birch-Uchi greenstone belt of northern Ontario. Of 8 different model structures considered, based on both geophysical and various geological considerations they propose a shallow 5 km. depth extent for the metavolcanic units, which have apparently been affected by magmatic stoping processes.

This study will consider the subsurface configuration of the principal geological units in the area, which include the Shebandowan metavolcanic rocks, adjacent metasedimentary rocks, a number of small plutonic bodies and the gneissic rocks of the Quetico Belt. The resultant model structures will then be considered within the framework of several recent developments in the problem of Archean tectonism in

this part of the Superior province. Specifically, the Superior Geotraverse Project has provided a wealth of information about the structure, metamorphism and geophysics across the alternating subprovince belts of the western Superior province. Several workers including Tarling (1980) and West and Maraschel (1979, 1980) have explored the prevailing physical conditions and mechanics of tectonism during the Archean. This study will attempt to incorporate these concepts into a sequence of tectonic evolution which might result in the structural configuration suggested by the gravity models.

The gravity models which form the basis of the postulated tectonic development of the area are generally consistent with the volcanic-plutonic pattern suggested by West (1980) for the evolution of the Archean greenstone terranes and the adjacent metasedimentary gneiss belts. The proposed tectonic model is also consistent with the available geochronological data in that it supposes the Wabigoon Belt was at a more mature stage in the volcanic-plutonic cycle than the Shebandowan to the south during the initial development of the intervening Quetico belt. While it is recognized that there are undeniable ambiguities inherent in such broad schematic evolutionary models, it is felt that some attempt to synthesize the available geological evidence with the new geophysical data of this study is warranted.

GENERAL GEOLOGY

The study area covers in part three sub-provinces of the Superior Province as recognized by Stockwell (1970). The area to the north is characterized by rocks of the Wabigoon Belt, and the area to the south is typified by rocks of the Shebandowan - Wawa Belt. The central portion of the area is underlain by rocks of the Quetico Belt (Figure 1).

The general geology of the area is outlined on Ontario Department of Mines Geological Compilation Map 2065 (Pye and Fenwick, 1965). The most detailed published map and account of the geology within the area is that by MacDonald (1939). The general geology of the study area is presented in Figure 2.

For the purposes of the gravity study, it was expedient to divide the rocks into four major categories. These include the metavolcanic rocks, metasedimentary rocks, a variety of granitic rocks and a mixed group of gneisses and migmatites. Virtually all of the volcanic and sedimentary rocks in the area have been metamorphosed to some extent, typically greenschist facies. Henceforth for convenience the prefix "meta" will usually be dropped.

The dominant geological feature common to all but the intrusive granitic rocks is a ubiquitous east-west penetrative planar tectonic fabric which is expressed

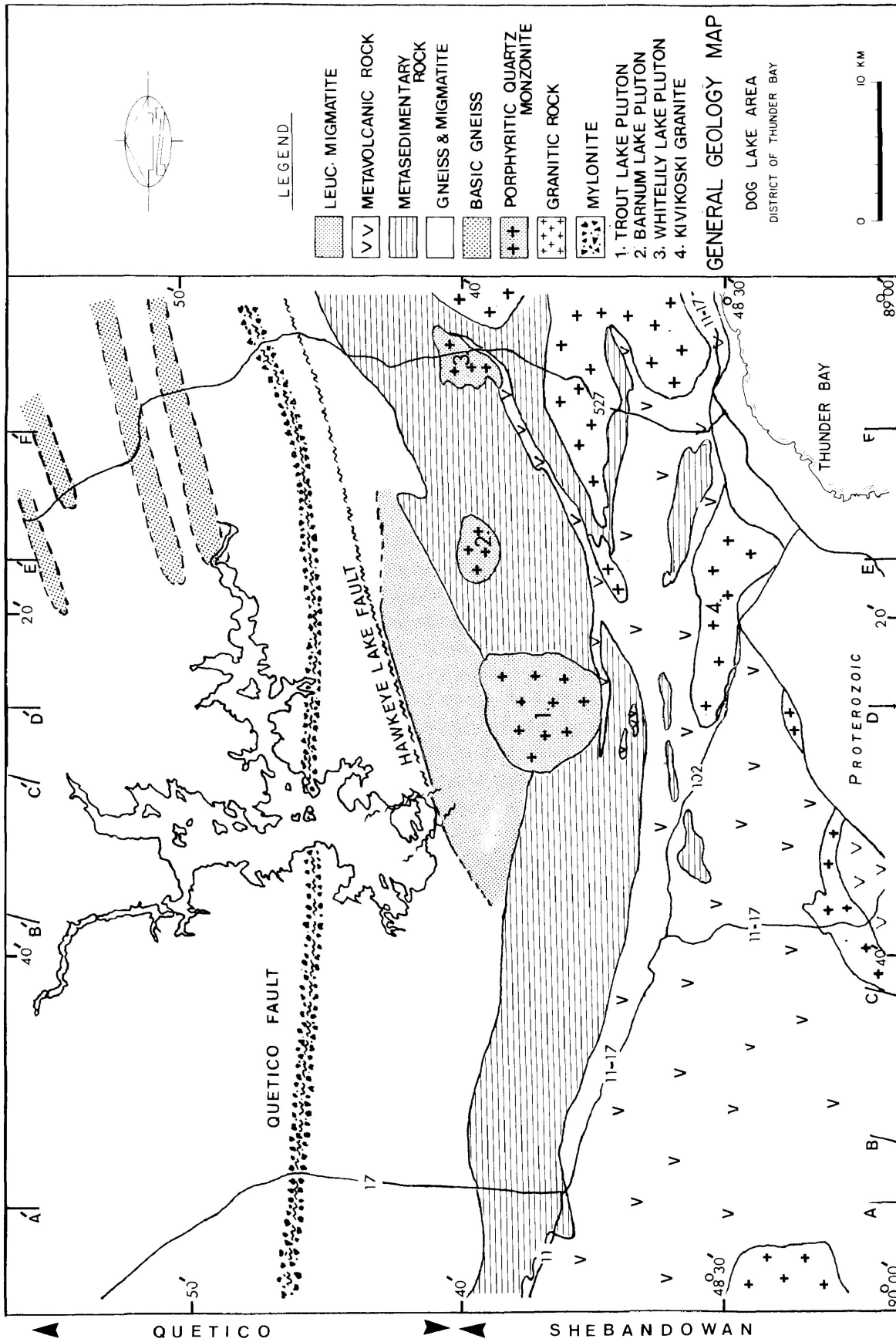


FIG.2 General Geology Map

differently in the various rock types. It appears as a cleavage, schistosity or gneissosity and is apparently the product of major tectonic events which affected the area in the Archean. Proterozoic rocks in the area are generally undeformed apart from some local faulting and gentle tilting.

THE METAVOLCANIC ROCKS

The Archean volcanic rocks of the area, commonly referred to as greenstones, consist of massive pillowed flows and pyroclastic strata. Compositions range from mafic to felsic in nature. The basaltic to andesitic compositions appear to be the most common of the volcanic suite (MacDonald, 1939). They exhibit a steeply dipping east-west cleavage and are typically chloritized, producing their characteristic dark green colour. Some exposures of these rocks show pillow structures which are generally deformed and elongated in an east-west direction. Where volcanic stratification can also be recognized, some pillows allow local top-direction determination.

The more felsic units are composed primarily of rhyolite and rhyolite porphyries (MacDonald, 1939). These felsic rocks are typically massive with a fine grained to cherty appearance. The porphyries have a similar ground-mass with quartz or feldspar phenocrysts, or both. A few exposures of the porphyritic rhyolite display flow banding (MacDonald, 1939).

Minor pyroclastic and fragmental rocks are associated primarily with the felsic units, although some basic agglomerate and tuff of andesitic association are reported by MacDonald (1939). Massive to stratified tuffs are generally felsic in nature and typically metamorphosed to a chlorite schist. These rocks are commonly accompanied by minor iron formation and chert layers (MacDonald, 1939).

Some chemical analyses of volcanic rocks near the extreme southwest corner of the area were performed by Shegelski (1980). He reports that in the Shebandowan Lake area, a suite of basaltic rocks outlines a typical island arc tholeiitic trend, and a chemically distinct suite of more silica-rich rocks outlines a calc-alkaline trend. A number of the latter group are rich in potassium and are considered by Shegelski (1980) to be members of a Shoshonite sequence. The relationship between this group of rocks and the main greenstone sequence has not yet been conclusively determined.

METASEDIMENTARY ROCKS

The main body of sedimentary rocks is exposed in a zone which parallels to the north the volcanic rocks. The principal type of sedimentary rocks in the area is a pelitic schist. These schists are typically fine grained wackes to mudstones usually deposited as laminated to thinly bedded turbidite sequences. These turbidites often

display graded bedding which enable younging directions to be determined. Schistosity is typically well developed by the preferred alignment of biotite or clay minerals. The schistosity generally parallels the bedding planes, which strike east to east northeast with steep to vertical dips.

In the vicinity of the Trout Lake and Barnum Lake quartz monzonite plutons, the bedding and schistosity of the intruded sedimentary rocks are conformable with the circular to elliptical intrusive contact outlines. The schistosity appears to become more intense northward away from the volcanic rocks to the south. This effect is most pronounced toward the interface with the Quetico Belt gneisses and migmatites, although primary sedimentary features are generally preserved in many exposures.

Several bodies of mixed coarse clastic sediments are found primarily within the volcanic units in the south central portion of the area, and their origin and structural and stratigraphic significance is not yet understood. They consist of conglomeratic, arkosic and greywacke rocks, and are generally poorly stratified. Fragments within conglomeratic pebbles are clearly granitic in origin but their source has yet to be determined.

In the extreme southwest portion of the area,

a unit of very fine grained and uniformly stratified slates is exposed along Hwy 11-17 near Shabaqua Corners. A similar unit is exposed just north of Kakabeka Falls between granitoid gneisses to the south and the volcanic rocks to the north. These rocks are clearly less intensely metamorphosed and deformed than the main body of turbidites.

GRANITIC INTRUSIVE ROCKS

A number of bodies of granitic rocks intrude the volcanic and sedimentary units of the area. Two masses of medium grained pink biotite-hornblende granite intrude the sedimentary and volcanic rocks in the eastern section of the map area. A mass of medium to coarse grained pink to red hornblende granite, herein called the Kivikoski Granite, intrudes the metavolcanic rocks of the south central portion of the map area.

The area near the contact zone between the sedimentary rocks to the south and the migmatized gneisses of the Quetico Belt to the north is the site of a zone intruded by a number of granitic plutonic bodies. Kehlenbeck (1977) reports chemical analyses of rocks collected from the Barnum Lake and Trout Lake plutons (the latter by personal communication) which occupy a central position in this zone. Both bodies are classified as porphyritic quartz monzonite, and display a classic porphyritic texture of

large euhedral megacrysts (1-2 cm) of microcline feldspar set in a medium grained groundmass of quartz dioritic composition.

The Whitelily Lake Pluton, exposed along Hwy. 527 to the east of Barnum Lake, appears to be similar to the Trout and Barnum plutons but has not been mapped in detail. The regional aeromagnetic map (Figure 6) clearly shows the above plutons as well defined positive anomalies of circular to elliptical outline. Similar but not as well defined anomalies to the west of Trout Lake suggest the presence of other intrusive bodies, some evidence for which can be noted in a few exposures along Hwy. 17 and the Silver Falls road due south of Dog Lake.

ROCKS OF THE QUETICO BELT

By far the most complex rocks of the study area both lithologically and structurally are those within the Quetico Gneiss Belt. For the purposes of this discussion, these rocks exclude those greywacke turbidites to the south which are typically of lower metamorphic grade, but are often included within the loosely defined boundaries of the Quetico Belt (eg. Pirie and Mackasey, 1978).

Rocks of the Quetico Belt include a heterogeneous group of migmatites, granitic and sedimentary gneisses and

a variety of minor constituents including mylonites amphibolites and pegmatites. The rocks are typically severely deformed and metamorphosed to upper amphibolite and locally granulite facies. Because of their heterogeneity and deformation, it is often difficult to delineate specific lithologic units within these rocks.

The most common rocks throughout the Quetico Belt in this area are pink to grey coloured quartzofeldspathic biotite gneisses. They vary from an equigranular massive texture to a more layered appearance depending on the degree of mineral segregation. Locally these gneisses form zones of migmatite resulting from varying degrees of partial melting. The migmatite typically is well separated into a light coloured granitic fraction, the leucosome (or neosome) and a darker and more dense fraction interpreted as the paleosome, as defined by Winkler (1976). It has been proposed that the leucosome of the migmatite was produced by partial melting of the gneiss, while the paleosome, commonly referred to as biotite schist, represents the remaining unmelted fraction. (Winkler, 1976). Gneisses in a zone along the southern perimeter of the Quetico Belt in this area have been extensively migmatized and provide a sharp contrast to the generally well preserved sedimentary rocks to the south. This effect is most pronounced immediately to the north of the Trout Lake and

and Barnum Lake Plutons, where a body of leucocratic migmatite is exposed in a zone parallel to the Hawkeye Lake Fault. Throughout the western and central parts of the Quetico Belt in this area, the gneisses and migmatites appear to be composed of equal fractions of leucocratic and biotite schist components. Toward the north and east of the map area, the gneisses and migmatites become more impoverished in leucosome and exposures of biotite schists are more extensive. In the northeast portion of the area, exposures of basic rocks are more common than elsewhere in the area. Layers of amphibolite and mafic-rich gneisses have been recognized which follow the regional trend of steep dips and east-west strike. These layers have been related by Urquhart and West (1975) to sharp linear aeromagnetic anomalies in that area. The possible significance of this association will be considered in greater detail in a later section.

Cataclastic rocks and mylonites are exposed in a zone approximately 1 km. in width which trends east-west through the Quetico Belt across the map area (Figure 2). This area of cataclasis is interpreted as the eastward extension of the Quetico fault system.

STRUCTURE AND METAMORPHISM

The rocks in the study area display a ubiquitous penetrative schistosity that strikes east to east northeast and possesses steep to vertical dips. This fabric appears to reflect the dominant deformation that has affected this area.

The volcanic rocks provide the least amount of information about the regional structure, owing principally to their macroscopic homogeneity. Mapping to date has not provided enough detail to outline the various layers of any mafic to felsic flow sequences. The few recognizable pillow structures and limited layering information indicate top directions both to the north and south. Unfortunately not enough exposures of this kind have been found to outline any recognizable fold structures.

Based on detailed field studies, Kehlenbeck (in prep.) has outlined at least two distinct episodes of folding in a sequence of sedimentary rocks in the vicinity of Hazelwood Lake. Measurements of bedding, cleavage and recording of younging directions from graded beds made it possible to delineate the deformational history there.

Kehlenbeck (in prep.) reports that these sedimentary strata were first folded about gently

plunging fold axes resulting in open upright folds with north-south striking axial surfaces. The F_1 structures were refolded about a subvertical fold axis contained in east-west striking axial surfaces, producing an axial planar cleavage. The refolded folds were subsequently subjected to a homogeneous strain which resulted in the local development of kink folds (Kehlenbeck in prep.).

Several workers consider the main deposition of sediments adjacent to the Quetico subprovince to have been contemporaneous with the volcanism in the Shebandowan-Wawa subprovince (Pirie and Mackasey, 1978). In this area, axial planar cleavage related to the tight east-west folding in the sedimentary rocks is continuous into the adjacent volcanic rocks, but no similar fold structures have yet been identified within these units.

Structures within the Quetico gneiss and migmatite terrane are at least as complex as those in the lower grade sediments to the south. Small scale ptygmatic and intrafolial folds are common within the gneisses, and the migmatites usually display a "marble-cake" appearance related to the effects of partial melting. The paucity of distinctive lithologic units

makes the identification of larger scale folds difficult. Lehto (1975) and Clendinning (1981) have outlined major fold structures in two localities within the Quetico Belt in the area. Both structures are reported to be folded about east-west axial surfaces with steep dips, with fold axes which plunge at shallow angles of between 15° - 30° to the east-northeast and west-southwest.

The most obvious structural features within the Quetico subprovince are a number of major faults, including the Quetico fault system. Several investigators consider the main motion on the Quetico fault to have been right lateral (Schwerdtner et al, 1979). The magnitude of the apparent transcurrent motion or any vertical displacement has not been determined owing to the consistent lack of crosscutting relationships of identifiable marker horizons.

The Hawkeye Lake fault is readily visible on aerial photographs as a deep topographic gash, now partly filled by Hawkeye Lake and feeder streams. There is also an apparent aeromagnetic lineament associated with the fault (Figure 6), but no distinctive fault zone textures are seen in the wallrock such as the mylonite related to the Quetico fault. The Hawkeye fault acts as a northern border to a zone of extensive partial melting

that is most pronounced south of Hawkeye Lake in the One Island to Two Island Lake area.

Lehto (1975) has described a pair of minor faults which strike north-northwest from the western terminus of the Hawkeye Lake. This subparallel pair of faults diverge to the north, and the apparent $\frac{1}{2}$ km. of horizontal motion has displaced the intervening block of bedrock to the north-northwest.

The volcanic rocks and the more southerly layers of sedimentary rock have been regionally metamorphosed to at least greenschist facies. There is a subtle northward increase in the metamorphic grade and texture visible in the sedimentary sequence. Rocks nearest the volcanic unit still display graded bedding of clay-rich pelites. Towards the north, the clay minerals are replaced by biotite, and the graded bedding becomes texturally reversed by the growth of coarse garnets in the former fine grained "tops" of the graded beds. Near the contact zone between the sedimentary rocks and the gneisses of the Quetico Belt, minor quartz veinlets appear interlaminated with the schistose sediments.

This gradual increase in metamorphic grade northward in the sedimentary rocks is brought to a sharp truncation in a narrow zone of several hundred meters

width across which one encounters the much higher grade and more severely deformed gneisses and migmatites which typify the Quetico subprovince.

Metamorphic mineral assemblages in the quartzofeldspathic gneisses and more basic rocks within the Quetico Belt suggest that upper amphibolite and occasionally granulite facies grade conditions affected the rocks presently exposed. Pirie and Mackasey (1978) have documented an axis effect based on the patterns of metamorphic assemblages they perceived at several localities along the length of the Quetico Belt. They have outlined a general scheme which finds the highest metamorphic grades toward the centre of the belt. Grades decrease towards the periphery which includes the metasedimentary units in their model. This pattern appears to operate in a general way in this area, as documented by Perry (1976). Local fluctuations from the pattern across the belt are probably related to the present structural disposition of the area.

Kehlenbeck (1976) has detailed the facies changes and lithologies of the gneisses and schists that form the northern boundary zone of the Quetico Belt. The zone is characterized by Kehlenbeck as a complex front of increasing metamorphic grade southward from the volcanic and sedimentary assemblages typical of the Wagiboon Belt

into the rocks of the Quetico Belt. This transition appears to have been complicated by multiphase deformation and heating accompanied by partial melting indicative of a possible increase in geothermal gradients southward (Kehlenbeck, 1976).

THE GRAVITY STUDY

During the 1980 and 1981 field seasons, 350 new gravity stations were established (Figure 5). All readings were taken with a Scintrex CG-2 Prospecting Gravimeter, with a calibration constant of 0.10846 mGals per division.

The majority of the station elevations were determined by automatic levelling from available Ministry of Transportation and Communication geodetic benchmarks. Closed loops revealed elevations were accurate to ± 0.75 meters over distances up to 12 km. For 90 stations, the elevations were directly available at benchmarks surveyed by the M.T.C. or the Geodetic Survey of Canada along Highways 11-17, 102, 527, 589 and 591 (Figure 5). In less accessible locations, elevations were determined by barometry, using a Taylor recording barograph at a base station for pressure drift corrections. The elevations determined in this manner are repeatable to within ± 1.5 meters.

The effect of gravimeter drift was controlled by the repetition of base station readings at four hour intervals. Standard data correction techniques were employed to reduce the data to a sea level datum (Telford et al., 1976). A free air correction of 0.09406 mGal/ft.

and a Bouguer correction of -0.03400 mGal/ft. were used based on the generally accepted upper crustal density value of 2.67 gm/cm³ (Gibb, 1968). The low topographic relief of the region obviated the application of terrain corrections.

The station interval along the roads and lakes worked is typically 1 km., but varies from a minimum of 0.5 km. to a maximum of 3.5 km. The wider station spacing is typical of the stations established at M.T.C. benchmarks along Hwy. 11-17, 102 and 527 (Figure 5).

Innes (1960) reported on approximately 55 previously established gravity stations in the vicinity of Thunder Bay. Three of these stations are included in the network of gravity base stations established by the Earth Physics Branch of the Department of Energy, Mines and Resources. These stations, described by Innes (1960) as located at the Port Arthur Baptist Church and the C.P.R. dock (in the north ward of Thunder Bay), and Lakehead Airport (in the south ward of Thunder Bay) were used as stations in a calibration loop to confirm the precision of the gravimeter dial calibration constant. Fifty of the stations described by Innes (1960) are included along with the 350 new stations of this study to produce a Bouguer anomaly map of the area (Figure 4 and 5).

The base station at the Baptist Church (located at the corner of Red River Road and Algoma Street in

Thunder Bay's north ward) was used to establish a loop of secondary base stations at benchmarks strategically located throughout the study area. The initial value of observed gravity reported by Innes (1960) for the Baptist Church station was 980,823.3 mGals, with a Bouguer anomaly value of -74.8 mGals. These values were based on the 1930 International Geodetic Association formula for the theoretical value of gravity at sea level. The 1930 calculation for $G_T = 978.049 (1 + 0.0052884 \sin^2 \theta - 0.0000059 \sin^2 \theta)$ where θ is the station latitude.

Recent Earth Physics Branch computer listings give an adopted value of 980,807.0 mGals for the observed value of gravity at the Baptist Church station, and a Bouguer anomaly of -81.3 mGals. These values are based on the more recent 1967 Geodetic Reference System formula for theoretical sea level gravity given by

$$G_T = 978.031846 (1 + 0.005278895 \sin^2 \theta + 0.000023462 \sin^4 \theta).$$

A correction is also applied to bring the original national base station network into agreement with the 1971 International Gravity Standardization Net. This adjustment, the Potsdam correction, has an average value of -14.7 mGals. A complete summary of the new international gravity base station network was published by Woollard (1979).

Theoretical sea level values of gravity for this area calculated by the 1967 GRS formula differ from the 1930 IGA values by -9.6 mGals at 48 degrees latitude to -9.4 mGals at 49 degrees. The present survey has used the older system adopted by Innes (1960) so that the resultant Bouger anomaly map would closely conform to values recorded on the regional Gravity Map Series published by the Earth Physics Branch of the E.M.R. Comparing values on Gravity Map no. 83 for this area with the recent computer listing of Bouguer anomaly values for those stations shows that a simple correction of -6.1 mGals applied to the map values combines the Potsdam correction and new latitude corrections and will bring them into good agreement with the new gravity system. This correction can be applied locally with an accuracy of ± 0.1 mGal.

Station locations were plotted on 1:50,000 scale topographic maps, with a plotting accuracy of ± 0.001 degrees of latitude. This is equivalent to a maximum error in gravity determination of ± 0.1 mGals. Errors in gravity values due to inaccuracy of elevations are typically less than ± 0.2 mGals. Repeated readings at specific stations yielded values which varied no more than ± 0.1 mGal. The cumulative maximum error for any station is considered to be less than 0.8 mGal, and is

probably less than 0.5 mGal at those stations established at M.T.C. benchmarks. All error estimates are relative to the assumed value of gravity at the Baptist Church base station, which is rated on the E.M.R. computer listings of gravity station data as accurate to 1 mGal.

DESCRIPTION OF THE REGIONAL BOUGUER ANOMALY FIELD

Before discussing the more detailed local gravity anomaly field (Figure 4) a review of patterns revealed on the regional gravity map is valuable. A portion of the E.M.R. Gravity Map Series No. 83 (Figure 3) shows several major gravitational features. Two centres of relatively high anomaly values occur near Lac des Milles Lac and in the area between Shebandowan Lake and the townsite of Kaministikwia. Both of these anomalies appear to be associated with extensive exposures of primarily metavolcanic rocks.

To the south and southwest of the Shebandowan-Kaministikwia anomaly, a broad east-west linear zone of relatively low gravity anomaly values is associated with exposures of granitoid gneisses. Typical values in and near Thunder Bay of -75 mGals extend westward parallel to the southern border of the study area. To the southwest of the Shebandowan-Kaministikwia anomaly,

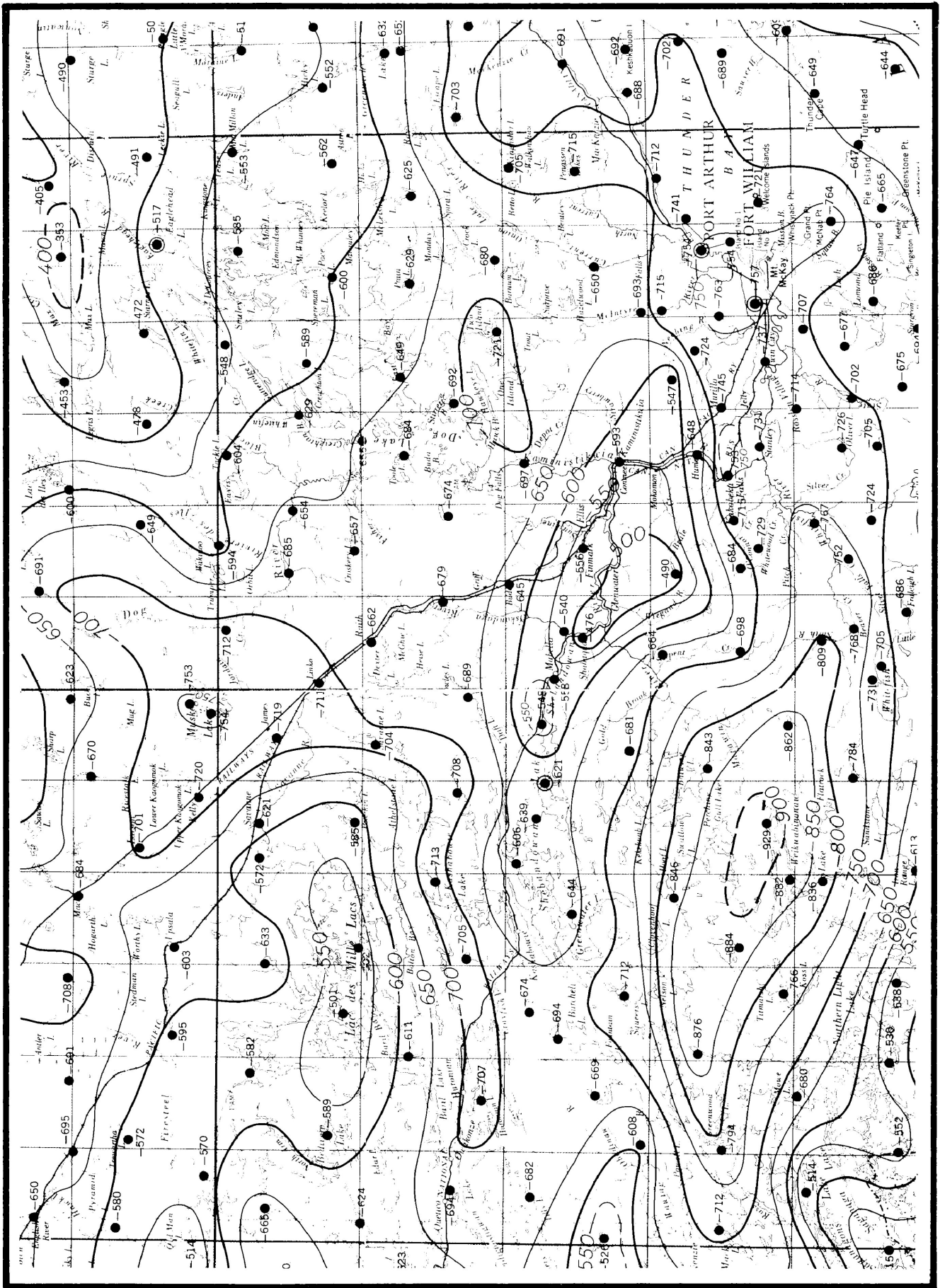


FIG.3 Regional Bouguer Gravity Map (from E.M.R. Gravity Map Series No. 83)

this pattern develops into an anomaly of elliptical outline. Values in the centre of this anomalous area decrease to less than -90 mGal (Figure 3).

A trend of low gravitational values extends to the west and east-southeast of the Dog Lake area, and is associated with the gneissic rocks of the Quetico Belt. Values in this zone are typically between -65 mGal and -70 mGal, with a small anomaly of elliptical outline with values less than -70 mGal located in the One Island - Two Island Lakes area. The broad zone of low values extends westward where it narrows between the Lac des Milles Lac and Shebandowan-Kaministikwia anomalies. This pattern appears to correspond to the narrowing of the Quetico Belt between the Wabigoon Belt and the Shebandowan Belt. To the north and northeast of the Dog Lake area, gravity values increase in an area characterized by metavolcanic and metasedimentary rocks of the Wabigoon subprovince (Figure 3).

DESCRIPTION OF THE LOCAL BOUGUER ANOMALY FIELD

Figure 4 shows the Bouguer anomaly field outlined by the 350 new gravity stations established during this study and the 50 stations previously established in the area. In general, there appears to be a good correlation

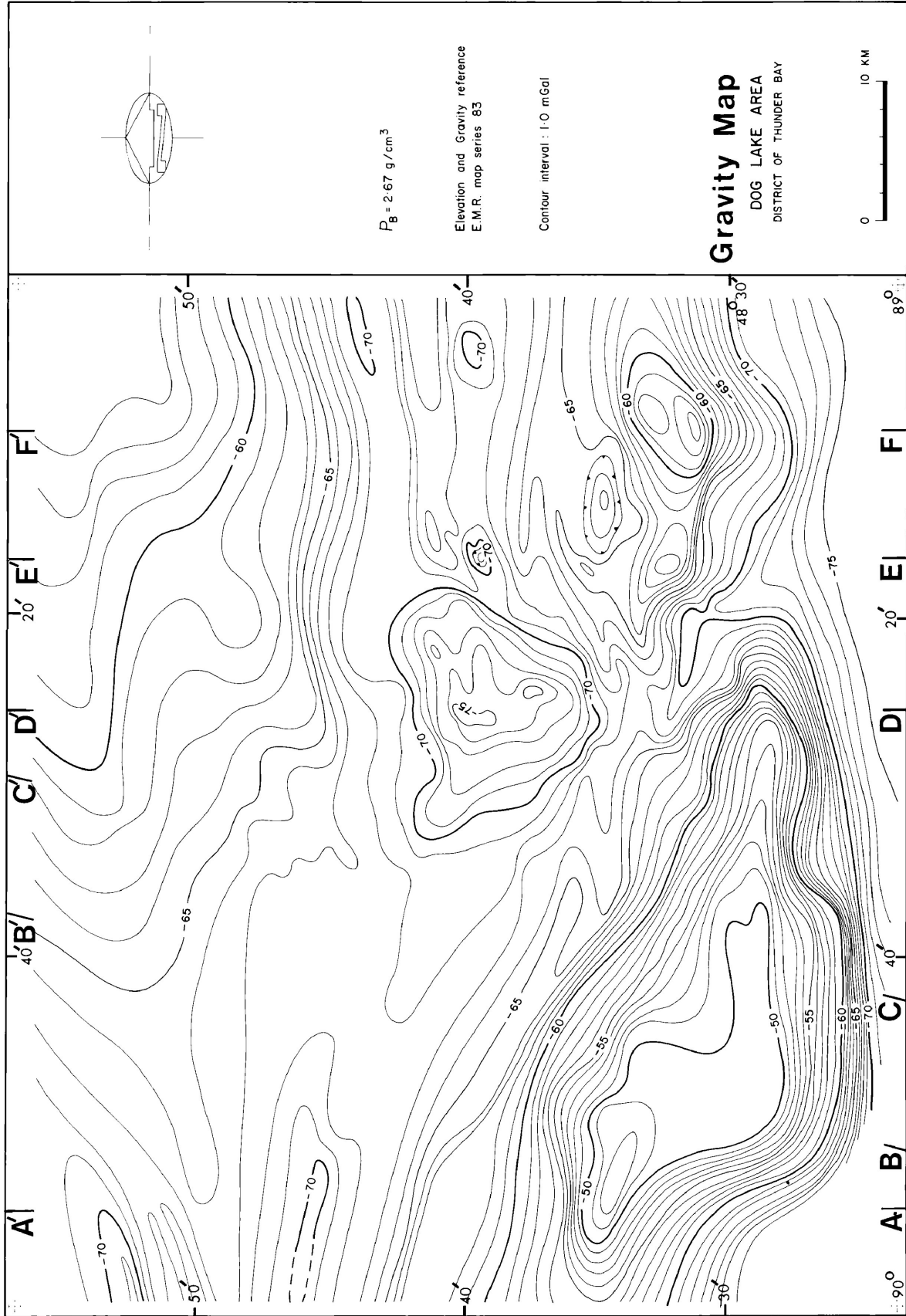


FIG.4 Bouguer Anomaly Map

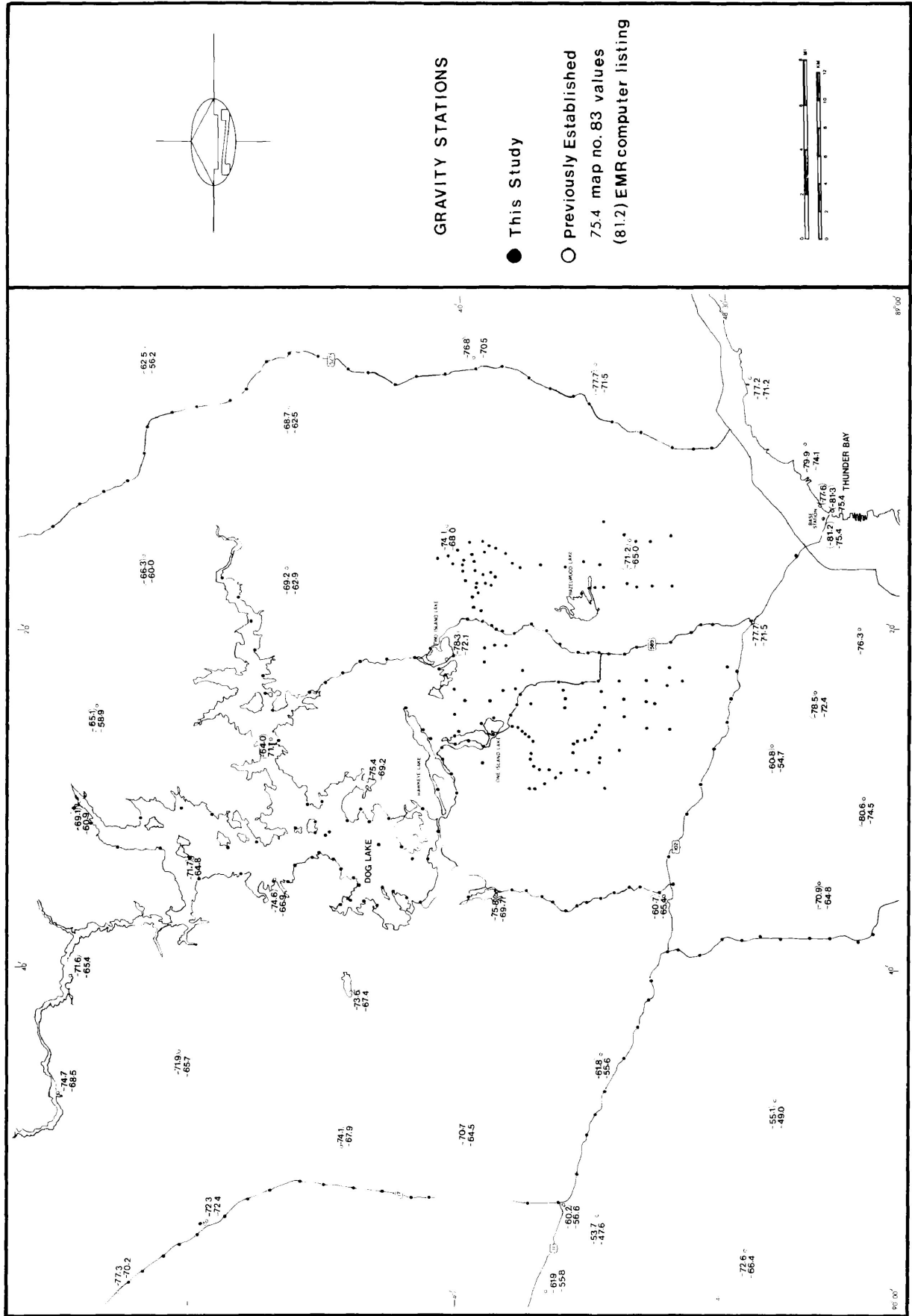


FIG.5 Gravity Station Location Map

between the gravity anomaly pattern (Figure 4) and the observed geology (Figure 2).

The highest values of gravity occur in the southwestern portion of the study area underlain by volcanic rocks of the Shebandowan subprovince. This anomaly, which is centered near the junction of Hwys. 11 and 17 with values as high as -47 mGal, extends to the west toward Shebandowan Lake and east to where it appears to terminate south and east of the Kivikoski Granite.

A second centre of relative gravity highs is located in the southeast section of the area, which is also underlain by volcanic rocks. The values outlining this anomaly are a maximum at -57 mGal. The volcanic rocks collected from this area appear from specific gravity measurements to be generally less dense than those apparently responsible for the Shebandowan-Kaministikwia anomaly. Although the volcanic rocks appear as a continuous belt from the western anomaly through to the east in surface exposure, the gravity anomaly pattern indicates a break between the two centres related either to a subsurface density contrast, the Kivikoski Granite or both.

The most significant gravity low on the Bouguer anomaly map (Figure 4) is centered over the Trout Lake

Pluton and extends northward into an area underlain by leucocratic migmatite and gneiss. This anomalous area typified by values of -70 mGal to -75 mGals is terminated to the north by the Hawkeye Lake fault (Figure 2, 4). One interesting feature is a small "lobe" of low gravity values which is directly associated with a wedge of rocks displaced to the northwest along the minor fault pair on the south shore of Dog Lake.

Smaller gravity lows are associated with the Barnum Lake Pluton and Whitelily Lake Pluton, with values typically between -70 mGal and -73 mGal over these bodies.

The two major faults in the area are both partially coincident with somewhat steeper gravity gradients than those over surrounding areas. In the eastern portion of the area, near Hwy. 527, values of -70 mGals over a zone of migmatization increase sharply to the north in the vicinity of the confluence of the Hawkeye Lake fault and the Quetico fault zone. As these faults diverge to the west, the steeper gradients remain associated with the Quetico fault only as far as Dog Lake. The anomaly pattern in the area of Dog Lake is relatively flat over the Quetico fault, while to the west near Hwy. 17, an east-west linear zone of low values of -70 mGal appears

associated with the Quetico fault zone. Clearly the character of the anomaly associated with the Quetico fault changes from east to west. Gradients of gravity are steep across the Hawkeye Lake fault which strikes along the northern boundary of the low anomaly to the north of the Trout Lake Pluton. This pattern also appears to terminate at the southeast corner of Dog Lake (Figure 4).

To the north of the Quetico fault zone, values of gravity increase, particularly in the area northeast of Dog Lake. Values in this area climb to -56 mGal, in apparent association with the increased occurrence of more basic gneisses and amphibolite. This broad anomaly pattern narrows and subsides to the west, with values between -65 mGal and -70 mGal.

The general anomaly pattern shows a subtle "trough" of relatively low values which extends east to west as far as Dog Lake along the interface between recognizable sedimentary rocks and strongly migmatized gneisses. This zone of low values between -68 mGal and -70 mGal veers gently to the northwest in the western section of the study area, and appears to connect with the linear low associated with the Quetico fault near Hwy. 17 as previously described.

Immediately to the south of this linear low, a

subtle parting of the gravity contours along Hwy. 17 just north of the exposures of sedimentary rocks creates a small plateau of values of -62 mGal. This area is underlain at the surface by the leucocratic gneisses and migmatites typical of the southern portion of the Quetico Belt. This pattern suggests that somewhat denser rocks than those exposed at the surface may possibly extend northward beneath the southern boundary of the Quetico gneisses in this localized area.

The pattern of gravity values over several of the granitic intrusive bodies other than the porphyritic quartz monzonite plutons provides some suggestion as to their subsurface extent. The largest body of granitic rocks is exposed in the eastern section of the study area, and values of gravity along Hwy. 527 across this body show little or no apparent deflection due to this body. This exposure of granite narrows somewhat about 6 km. to the west of Hwy. 527, and values of gravity decrease more noticeably over the granitic mass in this area centered just southeast of Hazelwood Lake (Figure 2, 4).

The anomaly pattern related to the Kivikoski Granite to the south of the Trout Lake Pluton appears to create a break between the areas of higher values associated with volcanic rocks to the east and west. The relatively low gravity values associated with this body of granite

decrease to a minimum of less than -70 mGal, centered in an area 2 km. north of the exposure of granite. This may suggest a possible northward dip of this body.

THE AEROMAGNETIC ANOMALY PATTERN

The aeromagnetic anomaly pattern (Figure 6) shows a high degree of correlation with the trends observable on the Bouguer anomaly map (Figure 4). The most intense magnetic response is in the southwest section of the area which is typified by exposures of volcanic rocks which contain scattered exposures of iron formation. The latter locally enhance the typically high magnetic susceptibility of the basic volcanic rocks. The magnetic anomaly over the volcanic rocks in the more easterly section of the area is more subdued, a further indication of the relative paucity of more basic compositions in these rocks.

The Whitelily Lake, Barnum Lake and Trout Lake plutons (from east to west) are each clearly outlined by circular to elliptical anomalies. There is also a subtle decrease westward of the intensity of these anomalies. To the west of the Trout Lake Pluton, rather vague outlines of similar anomalies suggest the presence of plutonic bodies that either have not been recognized as such or are not exposed at the present level of erosion. The anomalies of this kind to the extreme west of the area are located in the same area in which the "trough"

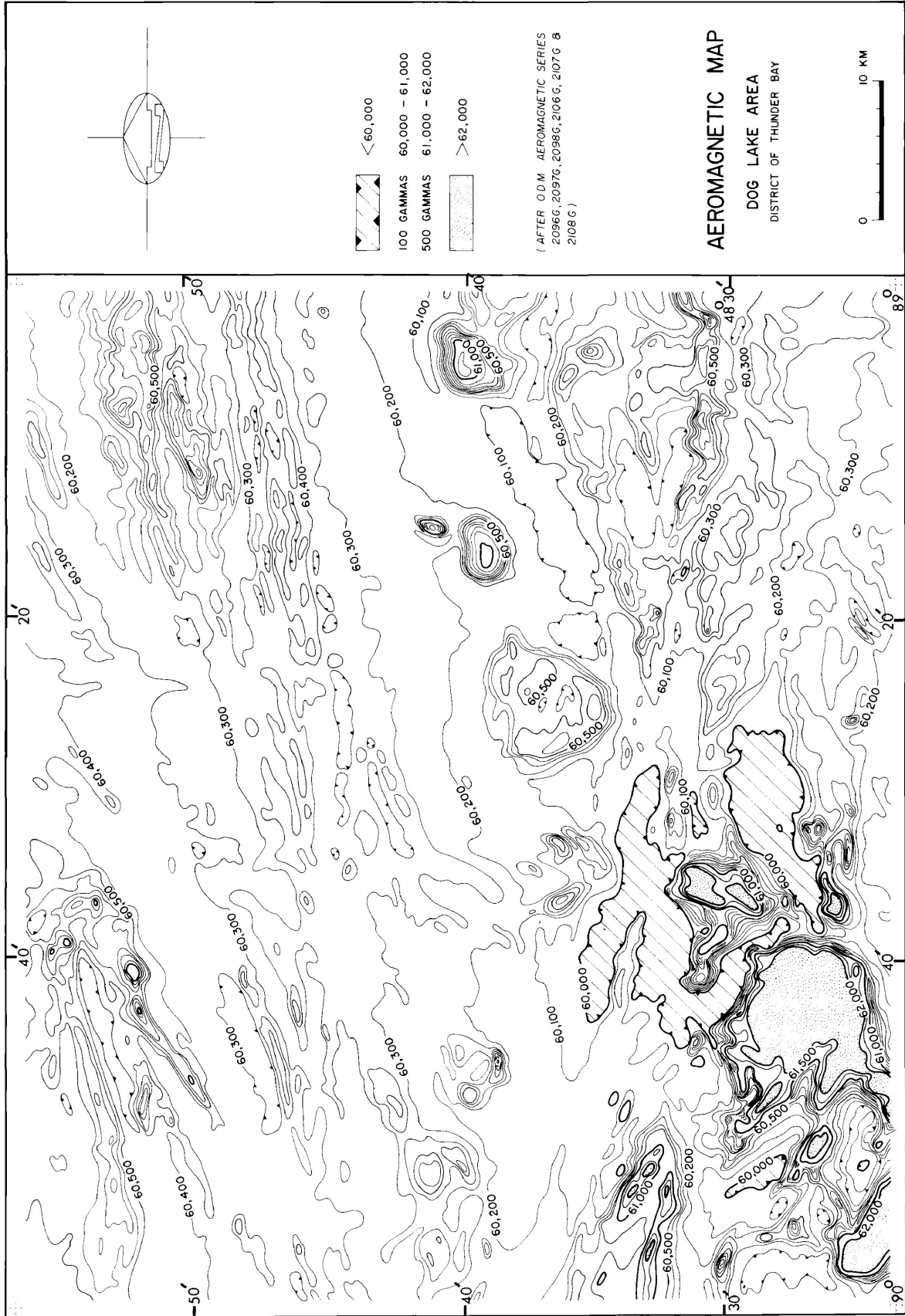


FIG.6 Aeromagnetic Anomaly Map

of gravity lows associated with partial melting and migmatization are located. With respect to the anomaly due west of Trout Lake, localized exposures of granitic material intruding the sedimentary rocks and deviations from the east-west bedding strike in this area suggest the nearby presence of possible intrusive rocks.

To the north of the main zones of plutons, the magnetic contour lines parallel the Hawkeye Lake and Quetico faults. Like the pattern of gravity, this trend is only well developed east of Dog Lake and becomes more irregular toward the west. In the eastern half of the area north of the Quetico fault zone, there is an area of east-west trending linear magnetic anomalies. These long, narrow anomalies are located in the same area that the layers of basic gneiss and amphibolite are exposed interlayered with the gneisses, migmatites and biotite schist more typical of the Quetico Belt. Urquhart and West (1975) eliminated the possibility that these anomalies are due to dyke swarms that reach the surface, and modeled the anomalies in this area as due to vertical sheets of varying width (in the hundreds of feet) and rather high susceptibilities, measured in the range up to 23×10^{-4} emu.

This zone of linear anomalies extends to the

east out of the mapped area for a distance of 10-15 km. and similarly subsides toward the west in the vicinity of Dog Lake. This pattern intensifies again to some extent west of Dog Lake in the same area that the pattern of gravity contours narrow between the low associated with the Quetico fault zone to the south and a low in the northwest corner of the area. The latter low appears to be related to intrusive rocks in the area of Muskeg Lake (Figure 3).

DENSITY STUDIES

During the course of this gravity study, 194 rock samples were collected for specific gravity measurements. A Mettler balance was adapted to measure the dry weight of samples in air and their saturated weight in distilled water. The specific gravity is given by $\text{spec. grav.} = \text{wt. in air} / (\text{wt. in air} - \text{wt. in water})$. The results are considered to be reliable to $\pm 0.01 \text{ gm/cm}^3$. Four principal rock types were considered, with the results summarized in Figure 7.

The porphyritic quartz monzonites were collected from the Trout Lake and Barnum Lake Plutons. Thirty-seven samples produced a range of density values from 2.60 gm/cm^3 to 2.75 gm/cm^3 , with an average of 2.66 gm/cm^3 . The density values from each of the plutons separately also had averages of 2.66 gm/cm^3 , and were therefore grouped together. The denser samples were typically those taken from near the periphery of the intrusions, while the lighter samples were collected from the central part of the Trout Lake Pluton. The average value of 2.66 gm/cm^3 was used in the modeling of these bodies.

The metasedimentary rocks were collected from outcrops throughout the area. Twenty-four samples weighed exhibit a sharp peak at 2.75 gm/cm^3 , with the distribution skewed slightly toward the denser samples. The average

value of 2.76 gm/cm^3 was used for modeling. Nineteen samples of "Coutchiching mica schist" collected by Innes (1960) from the Thunder Bay to Rainy Lake area showed an average of 2.75 gm/cm^3 . One hundred and sixty-two samples of metasedimentary rocks from Manitoba studied by Gibb (1968) had an average of 2.76 gm/cm^3 , as did similar metasedimentary rocks from the Sturgeon Lake area (Dusanowskyj et al., 1975).

Samples of metavolcanic rocks were collected from outcrops throughout their exposure in the area. Forty-two samples were determined with a very wide range of values from 2.64 gm/cm^3 to 3.06 gm/cm^3 . The majority of the samples were between 2.70 gm/cm^3 and 2.80 gm/cm^3 , which is typical for andesitic compositions. The calculated average of 2.78 gm/cm^3 is probably not representative of a typical greenstone belt assemblage. Innes (1960) determined an average of 2.96 gm/cm^3 for 84 samples of "Keewatin greenstones", which were apparently mostly basaltic in composition. Gibb (1968) sampled 51 Precambrian greenstone volcanic rocks and arrived at an average of 2.85 gm/cm^3 . Dusanowskyj et al., (1975) weighed some 450 samples from the metavolcanic exposures around Sturgeon Lake and found an average of 2.91 gm/cm^3 , with some 306 mafic samples averaging 2.95 gm/cm^3 .

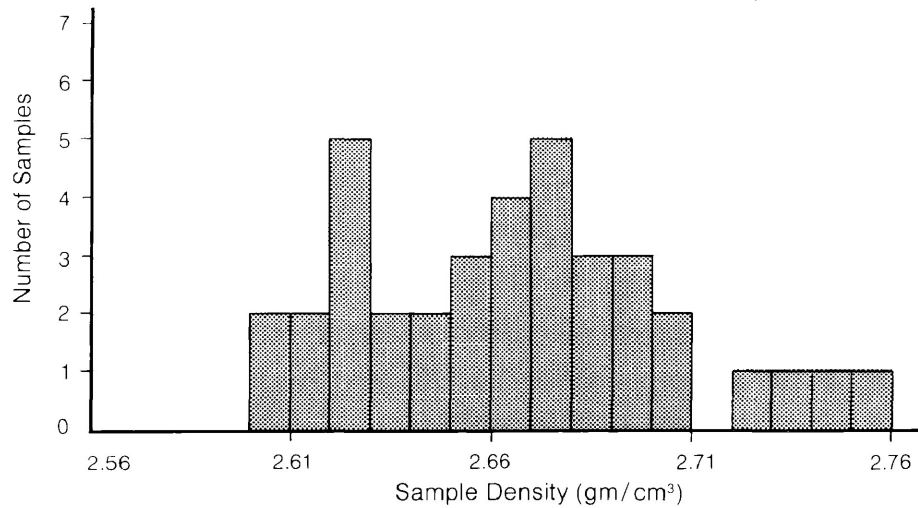
Szewczyk and West (1976) sampled 27 metavolcanic

DENSITY DISTRIBUTION HISTOGRAMS

A.

PORPHYRITIC QUARTZ MONZONITE

37 SAMPLES - AVERAGE DENSITY = 2.66 gm/cm³



B.

METASEDIMENTARY ROCKS

24 SAMPLES - AVERAGE DENSITY = 2.76 gm/cm³

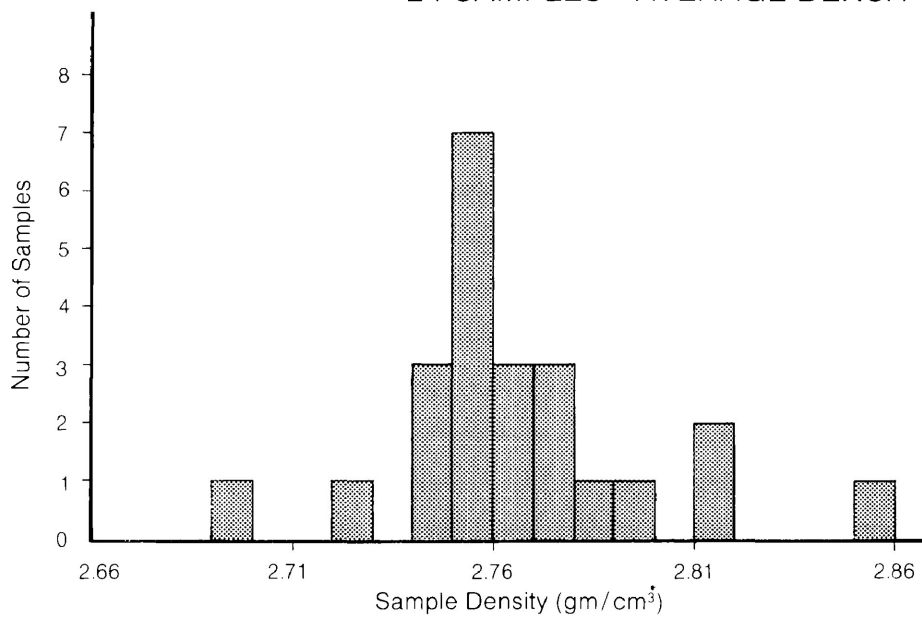


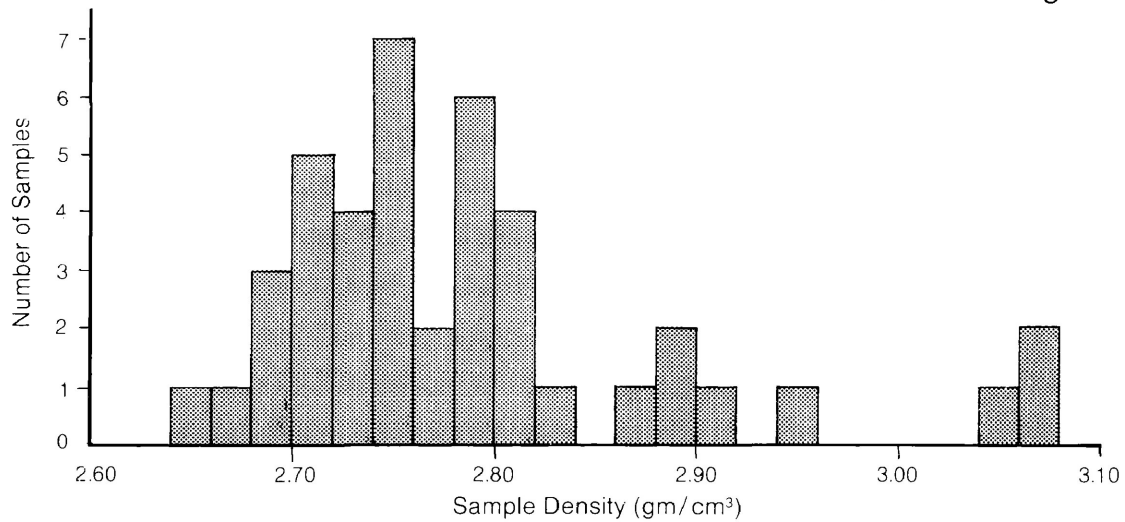
FIG. 7A) and B) Frequency Distribution of Sample Densities

DENSITY DISTRIBUTION HISTOGRAMS

C.

METAVOLCANIC ROCKS

42 SAMPLES - AVERAGE DENSITY = 2.78 gm/cm³



D.

MIGMATITE and GNEISS

86 SAMPLES - AVERAGE DENSITY = 2.68 gm/cm³

LEUCOSOME - 42 SAMPLES

- AVERAGE = 2.63 gm/cm³

MELANOSOME - 44 SAMPLES

- AVERAGE = 2.74 gm/cm³

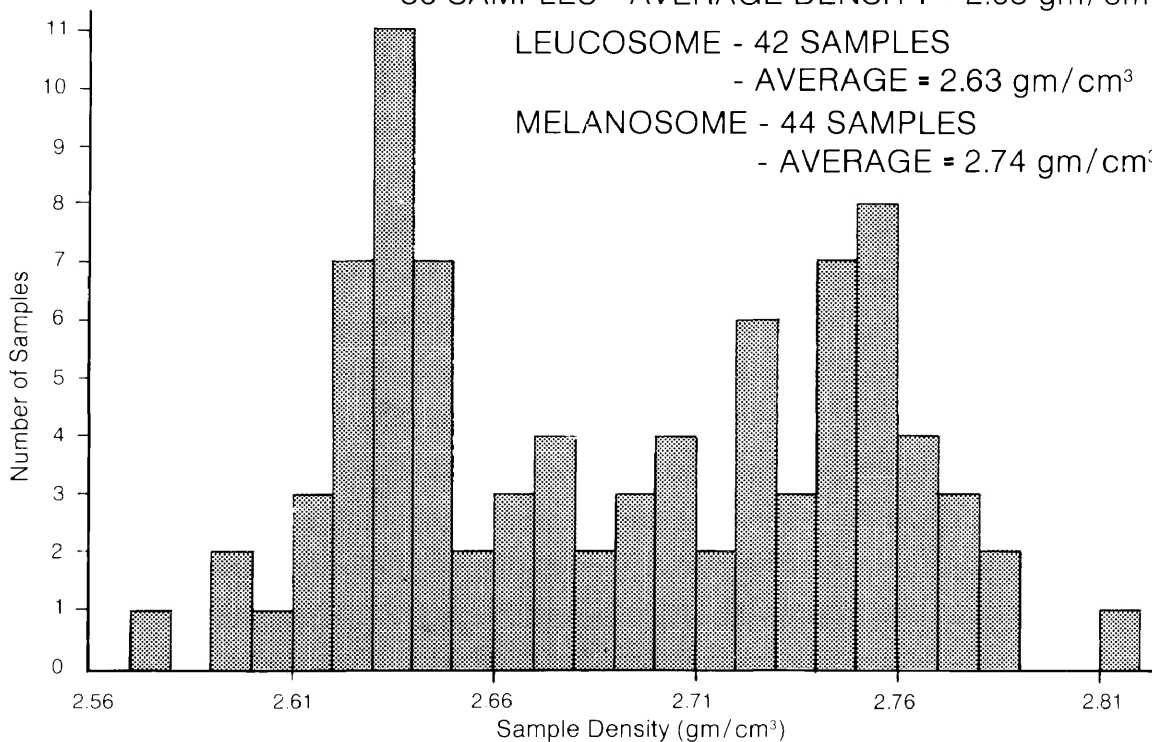


FIG. 7C) and D) Frequency Distribution of Sample Densities

rocks from the Ignace area, and found a strongly bimodal density distribution, with peaks at approximately 2.78 gm/cm^3 and 3.0 gm/cm^3 , with an overall average of 2.87 gm/cm^3 . Considering the wide range of values and their bimodal distribution, Szewczyk and West (1976) concluded that their average density was somewhat unrepresentative of an overall formational density, and chose to use Gibb's (1968) 2.85 gm/cm^3 as a model density.

This study appears to have sampled mainly rocks which would be typical of the less dense peak of the bimodal pattern found by Szewczyk and West (1976), with only 8 samples of 42 denser than 2.85 gm/cm^3 . It appears that the sampling of the metavolcanic rocks along exposures on Hwy. 11-17 and 102 has inadvertently followed the east-west strike of more andesitic to felsic layers, and resulted in a bias in the density distribution. Sampling across strike in other areas revealed a more representative range of density values. Considering the apparent abundance of denser samples recovered by Innes (1960) from the same metavolcanic units, an average density of 2.85 gm/cm^3 as determined by Gibb (1968) was used for the modeling of the volcanic structures in the western part of the area. In the eastern part of the area, there is less evidence of more basic rocks, and a density of 2.80 gm/cm^3

was employed in the modeling procedure.

Eighty-six samples of migmatite and gneiss were obtained from outcrops within the accepted boundaries of the Quetico Belt in this area. A strong bimodal density distribution is revealed for this diversified group of rocks. Every attempt was made to sample both the leucocratic and biotite schist components in proportion to their apparent exposure in outcrop. As a result, roughly equal numbers of the leucocratic and biotite schist samples were collected. An average density of 2.68 gm/cm^3 was found for all samples. An average of 2.63 gm/cm^3 characterizes 42 samples of the more leucocratic rocks with densities less than 2.68 gm/cm^3 , and an average of 2.74 gm/cm^3 was found for 44 samples, mostly biotite schist, denser than 2.68 gm/cm^3 (loosely referred to as "melanosome" in Figure 7D).

Szewczyk and West (1976) obtained an average of 2.68 gm/cm^3 for 108 samples of gneiss and migmatite from the Ignace area, which cover the same general range of density values but do not exhibit the same bimodal distribution. This pattern appears to reflect the scale of segregation of leucosome and paleosome of the migmatites considered by this study. While the segregation is on a scale large enough to collect hand samples of each component, it is not broad enough to warrant any attempt at modeling

the two components as distinct lithologic units. It is on this basis that the overall average density of 2.68 gm/cm^3 is used to model the gneisses and migmatites exposed at the surface throughout the Quetico Belt.

Five samples of basic gneiss and amphibolite were collected from the east-central part of the Quetico Belt in the map area. The basic gneiss samples had an average density of 2.79 gm/cm^3 and the amphibolites a density of 3.00 gm/cm^3 .

MODELING METHODS AND RESULTS

Models of the subsurface distribution of the various rock units previously discussed were generated based on the observed surficial geology, the measured density data and the gravity anomaly pattern determined by this survey. To this end, two computer programs were utilized to compute gravity values for model subsurface structures and to compare those model values with the observed values.

A three-dimensioned program based on an algorithm written by Y. Lamontagne was kindly provided by Dr. Gordon West of the University of Toronto. This program defines model structures as stacks of vertically sided prisms or horizontal sheets of polygonal outlines. The thickness, depth and density of each prism is uniquely assigned, and the position of each prism is outlined by the definition of the vertices of its polygonal plan.

A second program is an interactive $2\frac{1}{2}$ -dimensional inversion scheme originally written by John Snow and available in its present form from the Earth Science Laboratory of the University of Utah Research Institute. This routine defines model structures as vertical cross sections of polygonal plan. The $2\frac{1}{2}$ -dimensional designation comes from the ability to uniquely define the strike length into and out of the cross sectional plane of each polygon in the model. The search and

inversion capabilities of the program are made possible by the input of parameters which define the degree of manipulation of the vertice coordinates and/or density desired.

The modeling technique in general began by defining a crude 3 dimensional model that followed the surface geology as closely as feasible, and densities were assigned to the modeled rock units based on the results of the density studies and some reasonable assumptions. The background density employed for the modeling was 2.68 gm/cm^3 , which is the average density of the granitoid gneisses along the southern border of the study area and the gneisses and migmatites exposed throughout the Quetico Belt. The model volcanic units to the west have a cap layer of density 2.80 gm/cm^3 , which is close to the measured average of these rocks, but are underlain by a substructure with a density of 2.85 gm/cm^3 which is assumed to be a more typical value representative of greenstone sequences. The volcanic units to the east have been modeled with a density of 2.80 gm/cm^3 as there is much less evidence of more basic compositions there to justify the higher assumed value of 2.85 gm/cm^3 .

The zone of leucocratic migmatite north of the Trout Lake and Barnum Lake Plutons is modeled with

a density of 2.64 gm/cm^3 , and granitic units are variously modeled with densities of 2.63 gm/cm^3 and 2.65 gm/cm^3 . The sedimentary rock units and the porphyritic quartz monzonite plutons are modeled with densities of 2.76 gm/cm^3 and 2.66 gm/cm^3 respectively.

The other assumption made concerning density distribution is that the gneiss and migmatite exposed in portions of the Quetico Belt are underlain by a unit with density greater than 2.68 gm/cm^3 . This assumption is based on the exposure of basic gneiss and amphibolite in the northern and eastern part of the map area, and the continuation of gravity and magnetic patterns related to these limited exposures toward the western part of the Quetico Belt. The measured density value of several samples of basic gneiss have an average of 2.79 gm/cm^3 , while samples of amphibolite have a value of 3.00 gm/cm^3 . Gibb (1968) measured an average of 2.79 gm/cm^3 for 260 basic sedimentary gneissic samples. Including some of the denser amphibolites within this unit, an overall formational density of 2.80 gm/cm^3 was assigned to this unit.

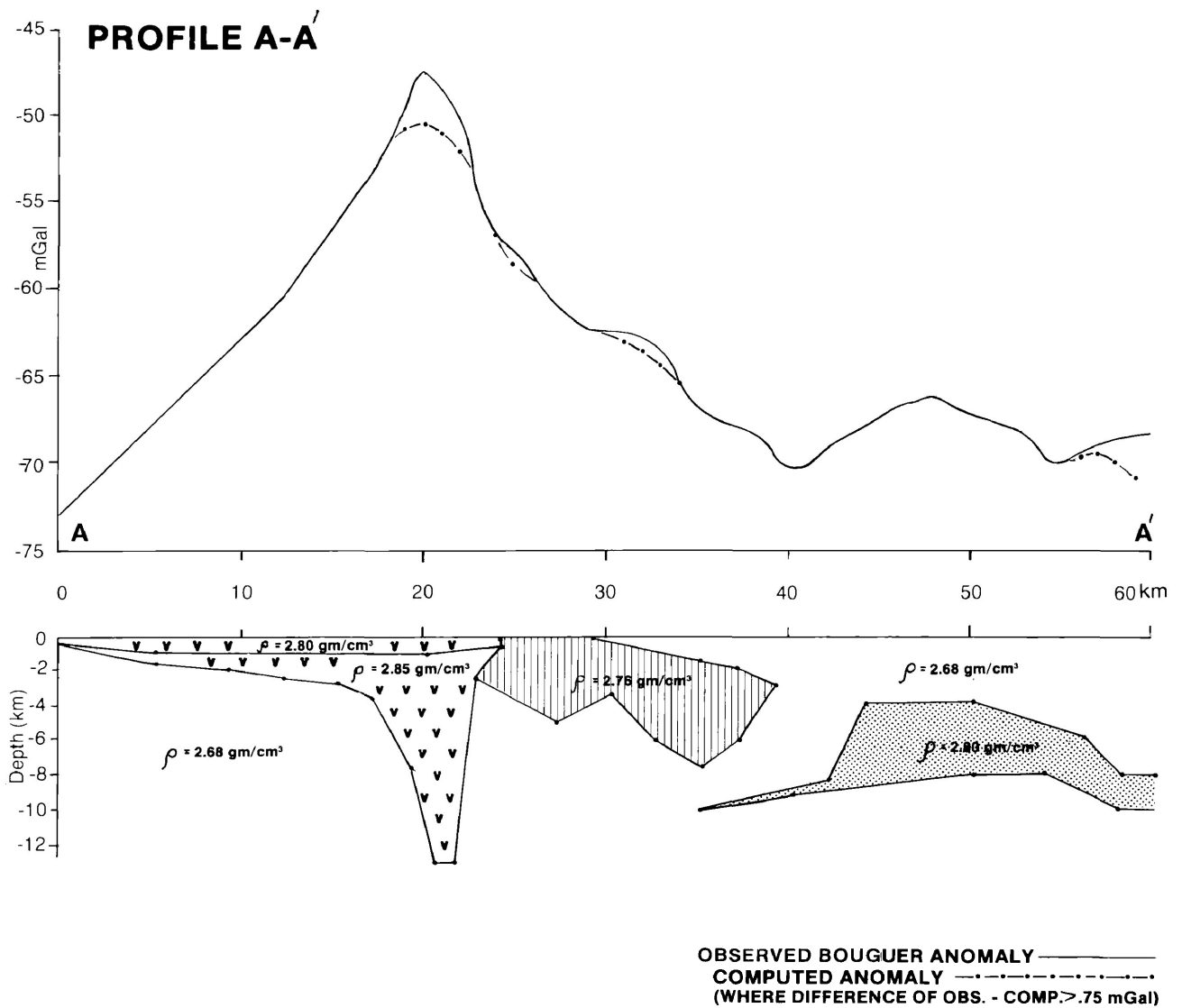
The modeling procedure was initiated by the application of the 3-D program to simplified block

models. After several attempts, a configuration was found that generated values which crudely simulated the observed anomaly trends. The $2\frac{1}{2}$ -D program was then utilized to refine this model along six critical profiles (Figure 4, 8, 9). The general east-west strike of the regional structures allowed the exploitation of north-south cross sectional profiles to simulate the 3-dimensional structure in $2\frac{1}{2}$ -dimensions with a reasonable degree of reliability. (see Appendix B)

The search and inversion capabilities optionally available with the $2\frac{1}{2}$ D program were utilized only to a limited extent. Search parameters are necessary to control the manipulation of each individual vertice of each polygon within the model, and often the selection of values for these critical parameters was rather time consuming. The limited data editing functions of the program itself are also somewhat primitive in comparison with the system file editor capabilities available on the DEC VAX 11 computer on which all computations were performed. It was found that the model data file could be manually edited much faster with the VAX-11 editor. The program was then used to calculate the forward problem in $2\frac{1}{2}$ -dimensions, and the results examined. A complete cut-and-try cycle of editing and computation could be performed in fifteen to thirty minutes depend-

ing on the complexity of the model. The cut-and-try method has the advantage in this case of keeping geological "sense" in the control of the investigator as opposed to the automatic model manipulation generated by the inversion and search algorithms. The Marquardt inversion algorithm in general requires a good model fit to start with or computational stability problems arise.

The resultant $2\frac{1}{2}$ -D model structures and comparative profiles of the observed and computed gravity values are summarized in Figures 8 and 9. The computed values of gravity for the model structures presented can be seen to agree well with the profiles of the new gravity data. The modeled structures were configured to reduce the discrepancy between the computed and observed values to within the range of error expected in the observed data, 0.8 mGal. All model structures were constructed based on the exposure of the various rock units at the surface and the assumption that there is no variation in density for the model units with depth. This assumption does not apply in the case of the volcanic unit in the western portion of the area as previously described. The model structures represent the lateral and depth extent of the density contrasts between the various rock units



SYMBOL KEY

METAVOLCANIC ROCK		GNEISS	
METASEDIMENTARY ROCK		BASIC GNEISS	
LEUC. MIGMATITE		GRANITIC ROCK	
PORPHYRITIC QUARTZ MONZONITE			

FIG. 8A - Observed and 2½ - D Model Gravity Profiles

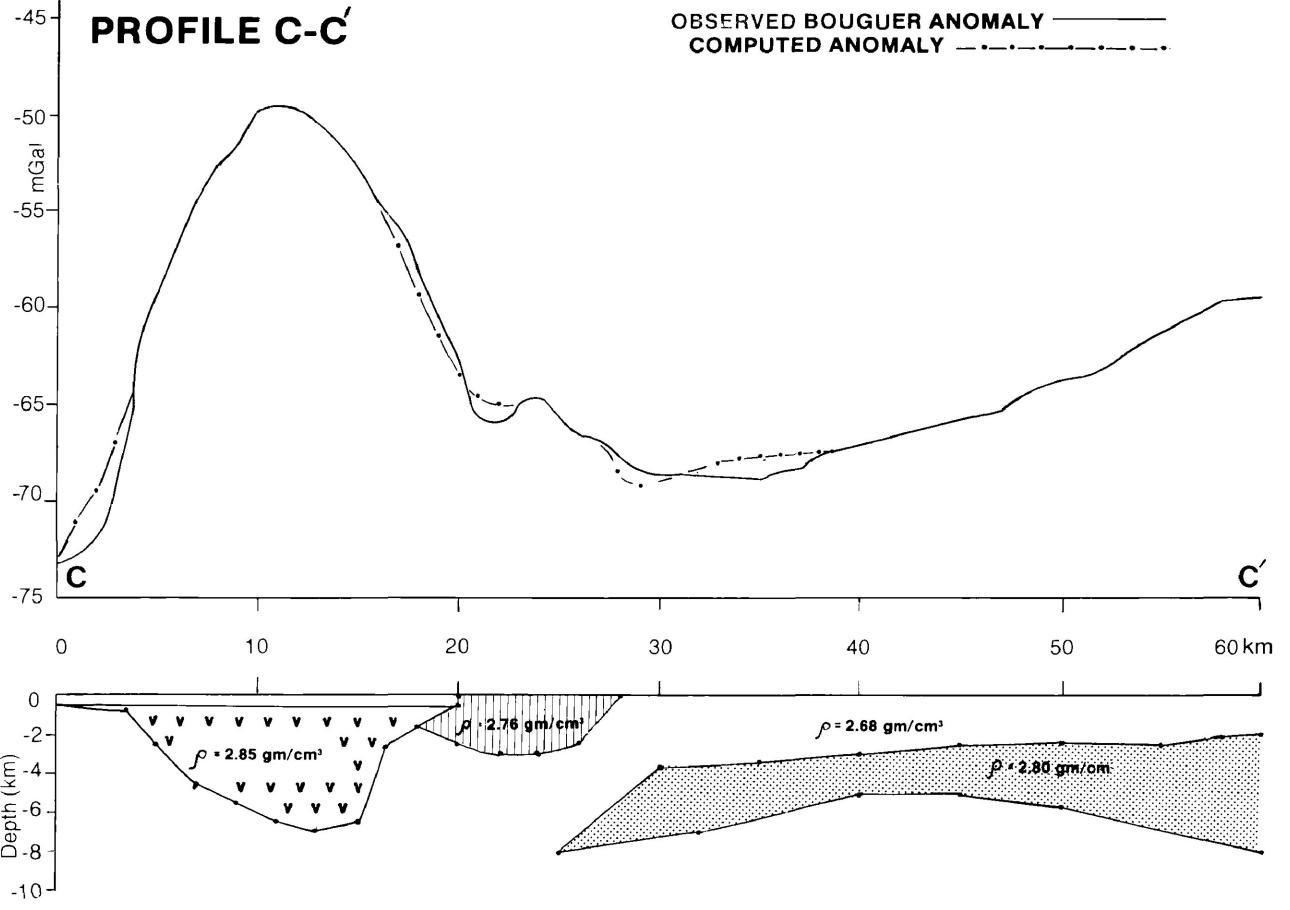
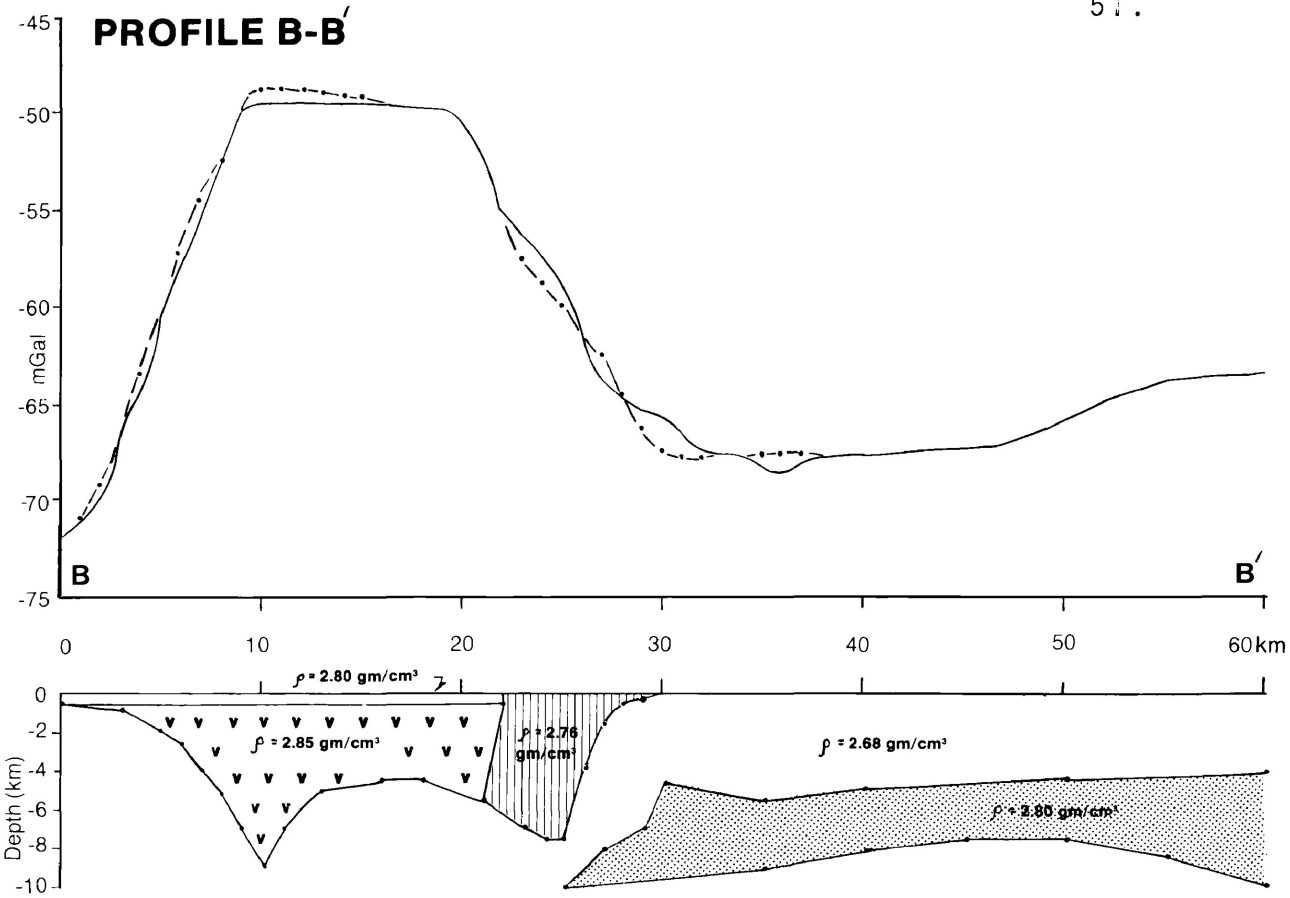


FIG. 8B and C - Observed and 2 1/2 - D Model Gravity Profiles

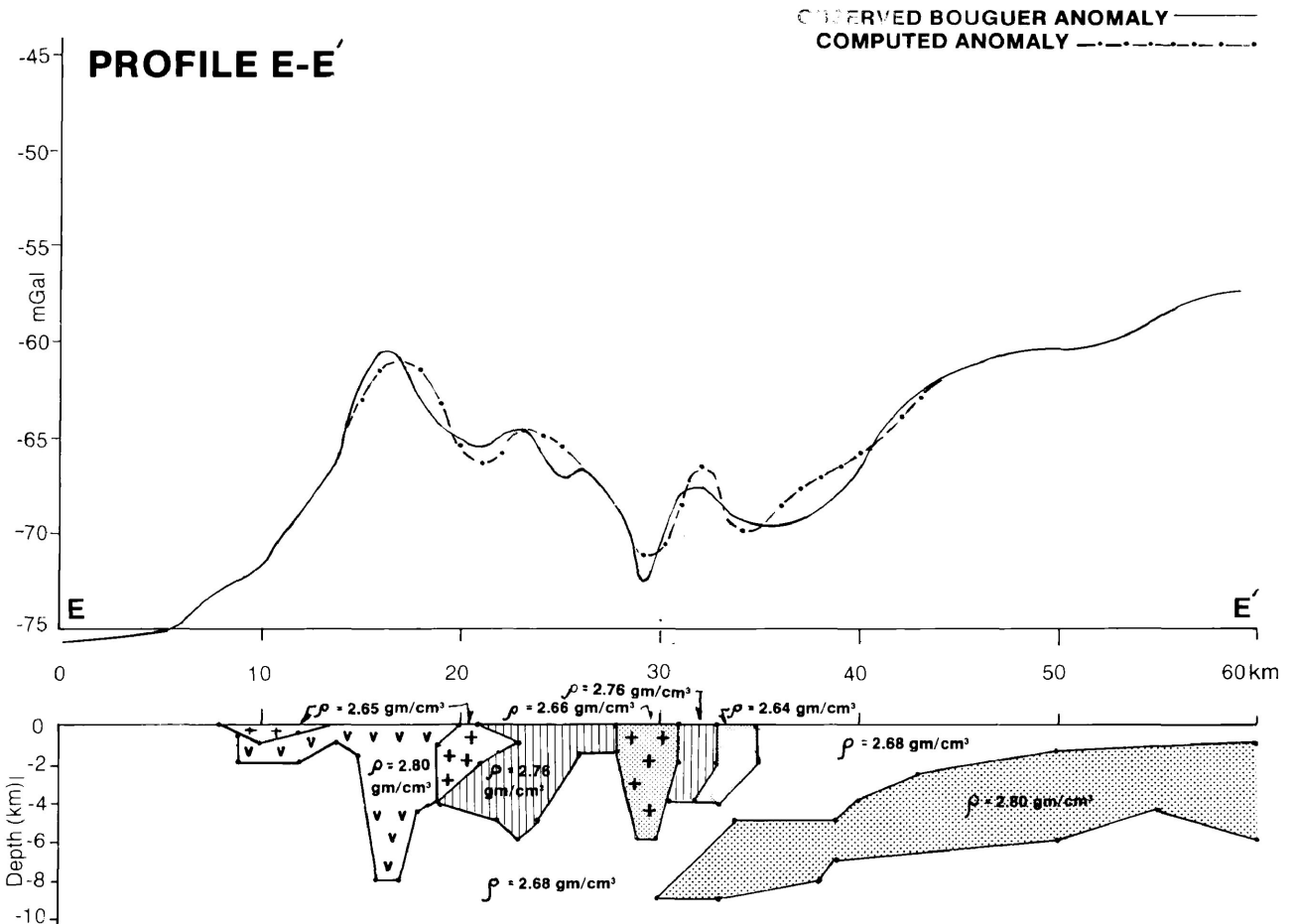
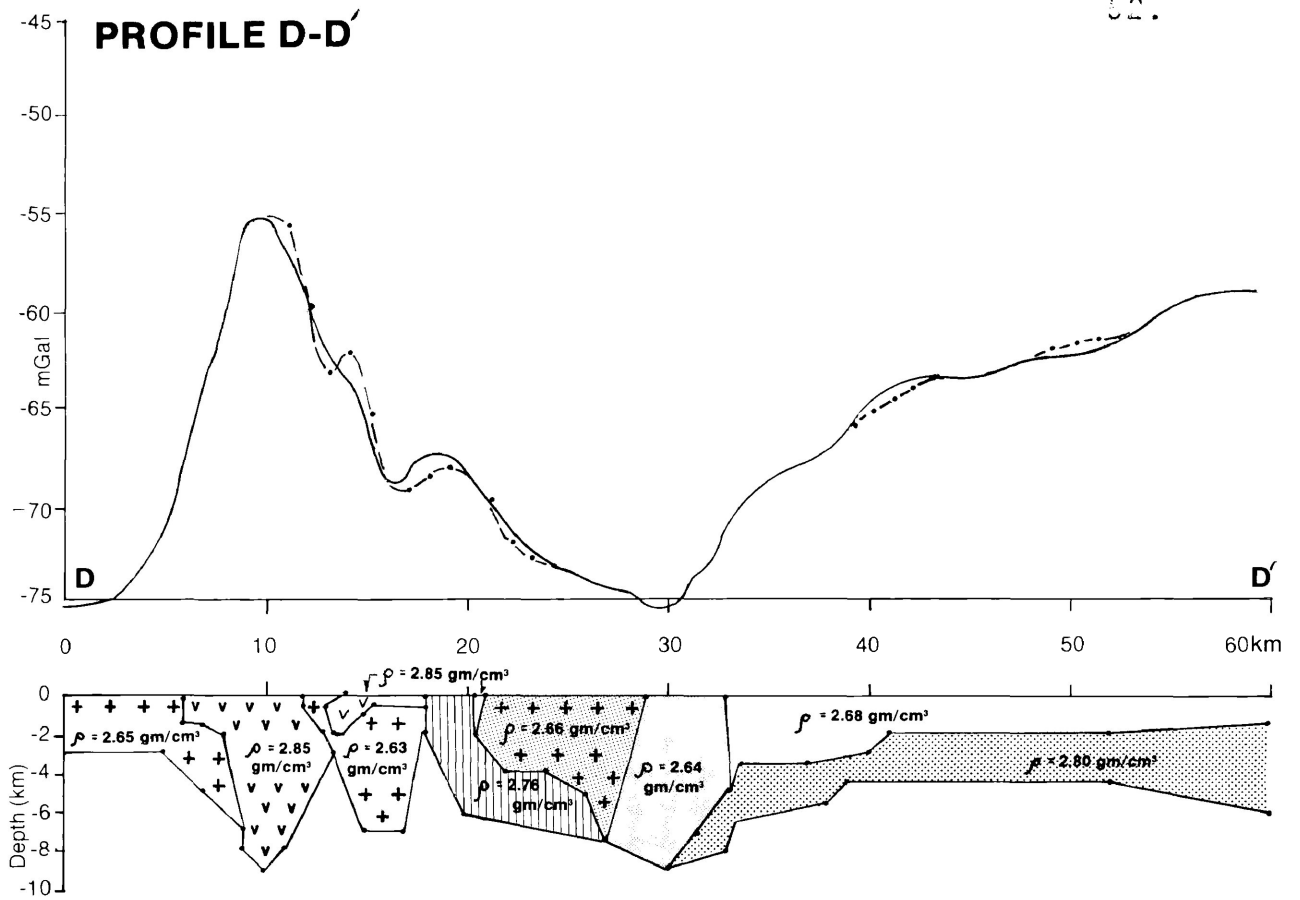


FIG. 8D and E - Observed and 2 1/2 - D Model Gravity Profiles

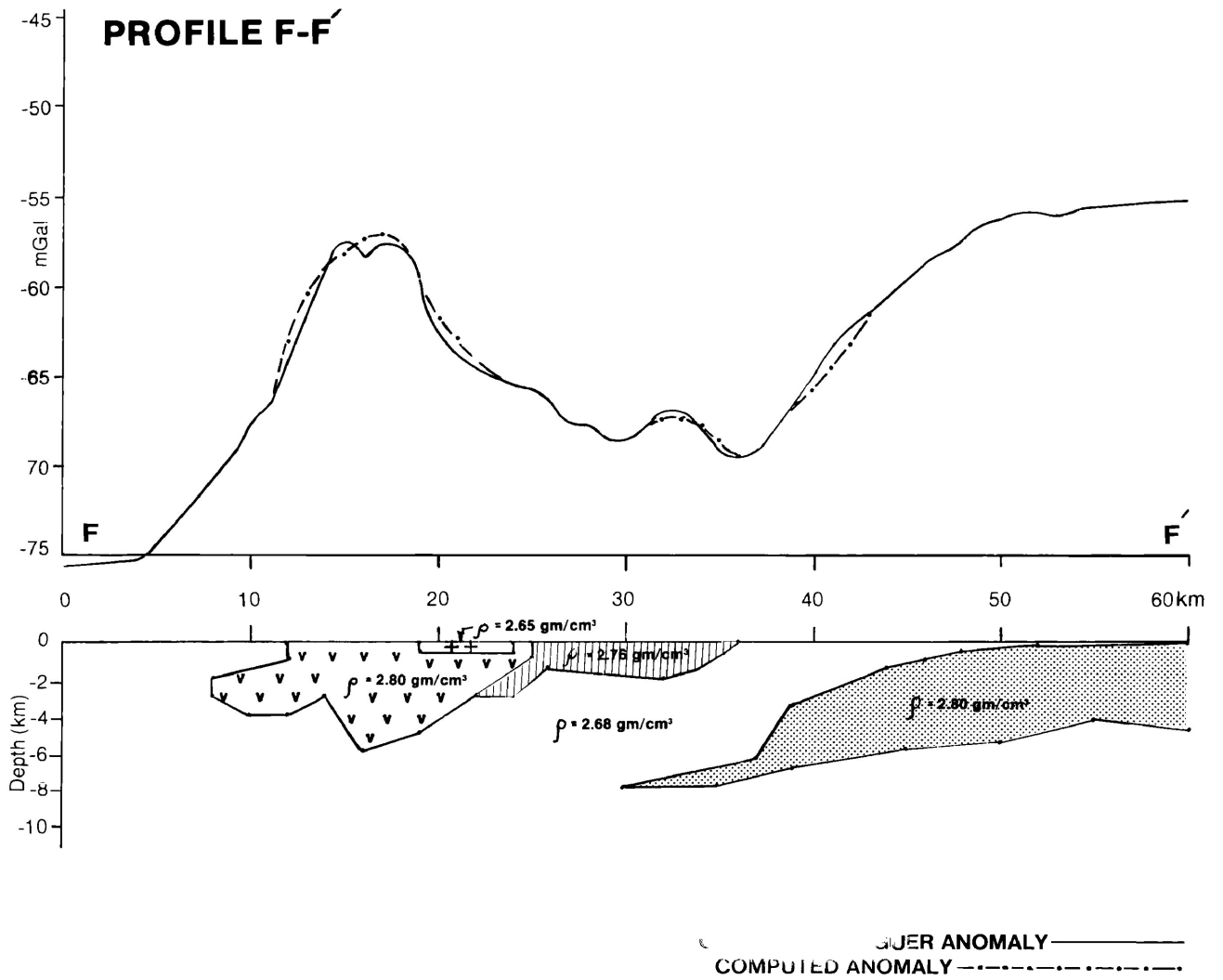


FIG. 8F - Observed and 2½ - D Model Gravity Profiles

represented. It must be considered that a variety of configurations of these density contrasts could produce similar computed results. It is the responsibility of the investigator to develop geologically reasonable models from the many solutions possible.

The density contrast representative of the volcanic unit is modeled as a basinal or keel-like structure which typically extends to depths of between 6 and 10 km. on profiles B-B' to F-F' (Figure 8). The sharp keel-shaped structure modeled on profile A-A' is shown extending to a depth of 13 km. and still does not adequately reproduce the peak gravity values observed. Local layers of rock denser than 2.85 gm/cm^3 may be responsible for the narrow peak along this profile.

The generally synformal shape of the model volcanic structure in cross-section is flanked to the south by a broad domical structure considered to be representative of the granitoid gneisses exposed along the southern border of the map area. To the north of the volcanic structure, the density contrast representative of the greywacke turbidite metasedimentary rock unit is modeled as outlining a basin-like structure of variable depth extent. The modeled sedimentary structure

is shown as deepening somewhat in some cases away from the adjacent volcanic unit, producing a domical appearance to the background rock unit of density 2.68 gm/cm^3 which is shown as underlying the volcanic and sedimentary structures depicted.

Where in immediate juxtaposition, the contact between the model volcanic and sedimentary structures appears to be steeply dipping toward the south. The model sedimentary units vary considerably in depth extent from profile to profile, ranging from 3 km. to 8 km. The model sedimentary unit appears to shallow to the east from profile A-A' to C-C' along the northern flank of the volcanic structure in the west half of the area. This sedimentary structure also appears to shallow to the east from profile D-D' to F-F' along the flank of the more easterly model volcanic unit. Along profile A-A', the density contrast representative of the sedimentary unit is depicted as extending 10 km. to the north beneath a thin tapered layer of rock of density 2.68 gm/cm^3 considered here to represent the gneisses and migmatites of the Quetico Belt.

On all the profile cross-sections, the model sedimentary unit is flanked to the north by a thick

south dipping wedge-shaped structure representative of the gneiss and migmatite. This wedge-shaped structure is modeled as an arcuate zone convex to the south. This unit is shown as located on profile A-A' (Figure 8) between kilometer 40 and 45, and is depicted as swinging south on profiles B-B' and C-C' to kilometer 28 to 30. The wedge-shaped structure then appears to be located more toward the north again through D-D' to F-F', where the somewhat shallower dipping structure is located between kilometer 36 to 45. On profiles D-D' and E-E', part of this "gneissic" wedge is modeled as a less dense unit (2.64 gm/cm^3) representative of the zone of leucocratic migmatite, shown between kilometer 29 and 34.

Profiles D-D' and E-E' also are shown with a number of structures representative of intrusive granitic rocks. A 7 km. deep plug of rock of density 2.63 gm/cm^3 is modeled as occupying a central position within an domical structure of the unit of density 2.68 gm/cm^3 , here considered to represent granitoid gneiss. Where exposed at the surface between kilometer 12 and 14 on D-D', this model granitic plug is considered to represent the Kivikoski granite. The extent of this

unit in cross-section was suggested by the gravity low to the north of the granitic exposure shown on profile D-D' (Figure 8) and on the Bouguer gravity map (Figure 4). The result of the modeling procedure in this profile section shows a relatively thin unit representative of the volcanic rock of density 2.85 gm/cm^3 underlain between kilometer 14 and 18 by the granitic plug. A somewhat similar but less extensive unit representative of granitic rock is shown on profile E-E', modeled as separating the volcanic and sedimentary units between kilometer 19 and 21. This granitic unit shown on E-E' is continuous with the thin sheet of granite modeled on profile F-F' between kilometer 19 and 24.

The Trout Lake Pluton is modeled in cross-section on profile D-D' between kilometer 22 and 29. This unit of density 2.66 gm/cm is representative of the quartz monzonite porphyry, shown as overlying to some extent the enveloping model sedimentary unit. This pluton is also shown as being bordered to the north by the model unit of leucocratic migmatite. While the contact is depicted as dipping steeply to the south, the low density contrast between the two units prevents a clear resolution of the orientation of this interface.

A steep to vertical contact is considered the most reasonable arrangement based on the steep dip of the sedimentary bedding planes near the contact and the aeromagnetic anomaly pattern (Figure 6).

The Barnum Lake Pluton is represented on profile E-E' between kilometer 28 and 31 as a 6 km. deep plug with a density of 2.66 gm/cm^3 . This porphyritic quartz monzonite unit is modeled as enveloped to the north and south by sedimentary units, to a depth of 2 km. on the south flank and 4 km. on the north flank.

The gneiss and migmatite of the Quetico Belt represented by the unit of density 2.68 gm/cm^3 is shown on all profiles as being underlain by a model unit of density 2.80 gm/cm^3 . This unit is intended to represent a zone dominated by basic gneiss and amphibolite but not necessarily exclusive of less dense granitoid gneiss. In general, this unit is modeled to be very close to the surface in the east along profile F-F' and inclined at a shallow angle toward the west. The unit typically is modeled as more sharply inclined to the south and tapering to a truncated edge which defines the base of the wedge-shaped unit representative of gneiss and migmatite as previously described.

The basal surface of the modeled dense substratum is typically gently convex upward, and the unit as a whole appears to thicken toward the north particularly along the more easterly profile sections. On several profiles, D-D' and E-E' in particular, the dense layer is modeled as having been dislocated along steeply dipping planes. Such apparent vertical displacements, suggested by the increase of the gradient along several of the gravity profiles located at 33 km. and 40 km. coincide with the exposure at the surface of the Hawkeye Lake and Quetico faults respectively. Sharp changes in the angle of the southward dip of this unit on profiles A-A' and F-F' also coincide with the position of the Quetico fault. Based on the model results and the gravity profile pattern, no effect of apparent fault related displacement is shown on profiles B-B' and C-C'.

The structures suggested by the 2½-dimensional modeling program were tested with the 3-dimensional program. Forty-nine prisms of varying density, thickness and polygonal outline were arranged to simulate the cross-sectional structure along the various profile planes suggested by the 2½-D models. The configuration of the 3-D polygonal prism model, while necessarily simplified in comparison, reproduces the anomaly pattern of observed gravity reasonable closely in the same profile planes utilized in the 2½-D program.

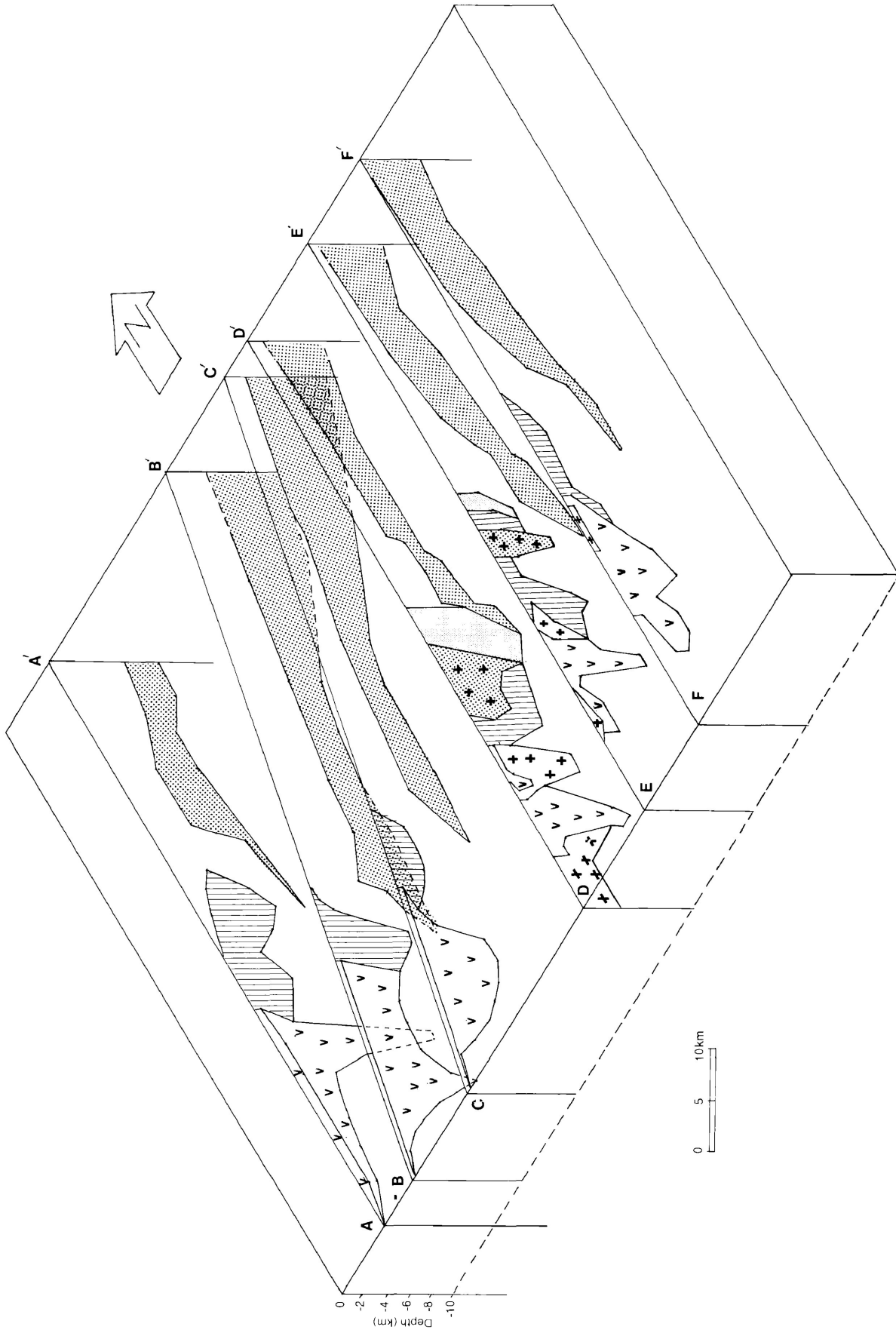


FIG.9 Projection of 2¹/₂-D Model Structure Profiles (SAME SYMBOL KEY AS FIG.8)

The fit of the computed data based on the 3-D program is not able to achieve the same degree of statistical fit as the more easily manipulated 2½-D model sections, but seldom deviates more than 2 to 3 mGals in the areas of poorest fit. Without regard to sign the average difference between the observed data and the data computed for the 3-dimensional model is 0.9 mGal, which is considered acceptable in consideration of the expected error range of up to 0.8 mGal for the observed gravity values. The poorest average profile fit is +1.4 mGal while the most successful profile fit is -0.1 mGal. (see Appendix B)

The 3-D model structures, while difficult to illustrate meaningfully, generally confirm the structural trends outlined by the model profiles from the 2½-D program (Figure 9). One point of interest that is difficult to resolve in 2½-D is the relationship between the Trout Lake and Barnum Lake Plutons. While the gravity pattern suggests a possible subsurface connection between the two, the aeromagnetic data and the 3-dimensional models of these units suggest they are separate bodies, but share a common base within the model wedge of leucocratic migmatite to the north.

The 3-dimensional model of the Trout Lake

Pluton generally confirms the north-south cross-sectional plan suggested by the $2\frac{1}{2}$ -dimensional model. In an east-west profile cross-section, the pluton is modeled with steeply inward dipping contacts. The Barnum Lake Pluton is modeled as a tapering plug with a steep inclination toward the west to a depth of approximately 5 km., in good agreement with the $2\frac{1}{2}$ -dimensional model and a magnetic study of the body (Cheadle, 1980).

The Whitelily Pluton just to the east of profile section F-F' (Figure 8, 9) is modeled as a simple prism of 4 km. depth which closely reproduces the anomaly perturbation associated with that body. Similar gravity perturbations along profiles A-A' and C-C' also appear to be related to similar intrusive bodies, as suggested by the aeromagnetic anomaly pattern (Figure 6). While no attempt was made to model these units either in $2\frac{1}{2}$ -D or 3-D, the domical structure of density 2.68 gm/cm^3 underlying the model sedimentary unit in profile A-A' at 30 km. coincides closely with the suspected plutonic body in that location.

DISCUSSION AND INTERPRETATION

The model structures suggested by the observed geology and the gravity and aeromagnetic anomaly patterns will be considered in terms of modern theories of Archean crustal evolution (Figures 8, 9, 10).

In general, the model profiles share a common pattern. A domical structure of granitoid rocks along the southern border of the area abutts a trough or keel structure of volcanic rocks. A basin-like structure of sedimentary rocks adjacent to the volcanic unit deepens away from the volcanic trough and is truncated on its northern boundary by a thick south-dipping wedge of granitoid gneisses and migmatites. This wedge of gneiss and migmatite is underlain by a layer predominantly composed of dense basic gneiss and amphibolite. An apparent series of small plutons originating from the base of the migmatite wedge and the southern edge of the basic layer intrude upward through the northern edge of the sedimentary unit. The basic substratum is always thinnest along its southern edge, and variably thickens and/or domes upward toward the north. This layer also appears gently inclined toward the west (Figures 8, 9).

Theories regarding crustal evolution abound, and are summarized in a number of publications (Windley, 1977; Condie, 1981). Several recent papers have dealt with the evolution of the physical conditions which ultimately control the mechanics of Archean tectonic activity.

Tarling (1980) has proposed a model of lithospheric evolution based on postulated changes in geothermal gradients, mantle convection rates and their effects on the tectonic regimes prevalent during geological time. Tarling has characterized the Archean as a period during which rapid mantle convection and high radioactive heat flux produced geothermal gradients considerably steeper than those known presently. Initially, a thin primitive lithosphere somewhat similar to modern oceanic lithosphere hosted a small area of proto-continental blocks. During the Archean between 3.8 b.y. and 2.5 b.y., Tarling proposes that the two dominant Archean crustal rock types, greenstone volcanics and granitoid gneisses were emplaced as a slowly cooling and thickening oceanic lithosphere resulted in segregation of lithospheric components by partial melting at increasing depths beneath subduction sites.

Initially, the angle of subduction of the thin

(30 km.) oceanic lithosphere beneath early volcanic arcs was shallow, and dehydration and partial melting at depths of approximately 100 km. produced generally sodic differentiates of granodiorite. Tarling suggests that as the subducting lithosphere thickened to 40 km, the depth of complete dehydration would increase to 200 km, at which depth more potassic melts would be produced. He also proposes that as these proto-continental blocks thickened, isostatic compensation over large distances would be able to support greater accumulations of sediment which presumably would be rich in heat producing elements such as K, Th and U.

Tarling suggests that by the end of the Archean 2.7 - 2.5 b.y ago subduction was extended to depths of 300 km beneath a thickening continental lithosphere as the isopeistic level deepened. He proposes that the end of the Archean was marked by the stabilization of amphibolites at the base of the continental crust. The release of water and other volatiles from this widespread phase change would result in the accumulation of granitic material rich in radiogenic elements in the upper crust. Tarling also proposes that the depletion of volatiles would increase the solidus temperature of the continental block, and quickly increase its rigidity in comparison

with oceanic lithosphere. The continental lithosphere would thicken rapidly from 50 km. to over 200 km., and end the rapid horizontal tectonism of the Archean in favour of more enhanced vertical tectonism and granitic diapirism which characterizes the Proterozoic period of continental stability (Tarling, 1980).

West (1980) has proposed a similar model for crustal evolution during the Archean based in part on finite element modeling of the formation of observed greenstone synform-granitoid gneiss dome structures (West and Mareschal, 1979; Mareschal and West, 1980).

West (1980) described in some detail the mechanisms by which the Archean continental crustal features developed in an environment of high heat flow and locally copious volcanism. West proposes that as successive layers of volcanic rocks and associated supracrustals become buried, they would undergo partial melting resulting in shallow granitic bodies and a deeper mafic residuum. Continued burial would lead to melting of this residuum at a depth of approximately 50 km. producing a tonalitic magma and an ultramafic residue. The granitoid magma would rise to form an intermediate crustal layer while the ultramafic material would in part return to the mantle convection cycle (West, 1980).

West has shown that local effusive volcanism onto this developing granitoid crust would create a

thermal blanketing effect and an unstable density and viscosity contrast between the volcanic material and the underlying granitoid layer. West and Mareschal (1979, 1980) used thermal constraints and finite element modeling techniques to explore the possible mechanical results of such an arrangement under a variety of postulated geothermal gradients and viscosity conditions. The results tended to be generally insensitive to changes in the initial parameters suggesting a possible explanation for the similarity of Archean structures which must have developed over a broad time interval and variable local conditions.

In West and Mareschal's model study, an initial perturbation at the volcanic-granitoid interface would evolve slowly until the radioactive heat flux generated in the granitoid layer and trapped by the thick cool volcanic blanket would cause softening in the substratum. The viscosity difference combined with the density inversion would cause the volcanic material to begin to sink at the site of the initial perturbation, forming a synformal trough flanked by upwelling orthogneissic dome structures. They suggest that the doming exerts some lateral compression which contributes to a vertical elongation which develops in the trough-like volcanic structure. They also propose that

geothermal gradients would be depressed in the vicinity of the infolding volcanic pile.

West (1980) proposes that this mechanism could eventually ingest the volcanic material by complete diapiric overturn, which would trigger another cycle of partial melting and further thickening of the continental lithosphere and concentration of radiogenic elements near the surface. Volcanism, ingestion and partial melting could proceed in cycles as long as the temperature and pressure conditions postulated for the Archean crust persisted. Eventually, the decrease of crustal geothermal gradients and the events described by Tarling (1980) at the beginning of the Proterozoic would diminish the capacity of the crust to sustain the gravity driven ingestion of greenstone volcanic material. Greenstone style volcanism itself seems to have diminished sharply after the Archean, possibly due to the increased angle of subduction of a thin oceanic lithosphere beneath the greatly thickened continental lithosphere (Tarling, 1980).

It is apparent from the model cross-sections (Figures 8, 9) that the volcanic structures and adjacent granitoid gneisses in the study area conform well with the form predicted by the West-Mareschal model. Lateral compression and synformal infolding between the upwelling

gneissic domes would contribute to the strong east-west striking and near vertical foliation apparent in the volcanic and adjacent rocks. The depression of geothermal gradients near the volcanic keels predicted by their model would also adequately explain the pattern of increasing metamorphism away from the volcanic unit in this area.

A principal result of the evolution of continental crust as envisaged by both West (1980) and Tarling (1980) is the accumulation of radiogenic granitophile elements near the surface and the increased ability of the thickening crust to support significant thicknesses of sediment rich in those elements. West (1980), Condie (1980) and others (Goodwin, 1977) consider the gneiss and migmatite belts of the Superior province to have been basins which received the sedimentary material eroded during adjacent continental crustal emergence. Allis and Garland (1979) recorded heat flow measurements within the Quetico Belt and other locations throughout the Superior province. Their results showed anomalously high heat flow and relatively high K and Th contents in the rocks of the Quetico Belt.

While Condie (1981) considers that the high grade linear belts were such basins, he points out that one difficulty with such a concept is the apparently

great depth of burial implied by metamorphic mineral assemblages now exposed. Condie (1981) invokes several possible schemes including underplating and upcurrents of mantle convection to explain the phenomenon. West's (1980) model suggests a somewhat simpler explanation that seems to agree well with the structures implied by the gravity models. West describes the results of a thick accumulation of sediments on an Archean crust. A thermal blanketing effect could again develop but because of the diminished density inversion, diapiric overturn would not necessarily occur as it would in the case of volcanic material. Only if the pile were thick enough that metamorphism converted the base of the pile to a dense substratum of basic gneiss would any degree of diapirism take place.

West (1980) postulates that the Quetico Belt and its counterparts elsewhere in the Superior province, (i.e. English River Belt) may have developed in basins, possibly rift related, that developed prior to a volcanic-plutonic cycle of cratonization. Sedimentation from the emergent cratonic block or belt would fill the basin and in approximately 30 m.y. crustal softening beneath the pile, uplift and compressive cratonization stresses would result in the observed gneiss-migmatite belt (West, 1980).

There is some suggestion from radiometric age determination and paleomagnetic drift data that the alternating high-grade and low-grade belt pattern in the Superior province progressed chronologically from north to south, such that the Wabigoon Belt may be somewhat older than the Shebandowan Belt (Goodwin, 1976; Dunlop, 1979). In this case, the Wabigoon volcanic-plutonic terrane would be the initial source of material into a marginal basin to the south. The basin would be floored by lavas and greywacke turbidite sequences. As the cycle of gneissic diapirism and plutonism described by West (1980) proceeded to the north, the sediments would become progressively more quartzofeldspathic in nature and rich in granitophile radiogenic elements (Figure 10).

Dunlop (1979) has suggested that based on paleomagnetic models, the Shebandowan-Wawa Belt may have been emplaced after the Wabigoon Belt. Consider this second developing cratonic arc approaching from the south, shedding a second cycle of turbidite sediments into the basin. Thermal anisotropy in these laminated sediments would partially trap heat generated in the underlying (and interlayered) quartzofeldspathic pile. The lavas and turbidites at the base of the pile would have been metamorphosed to amphibolites and basic gneiss

and biotite schist. This pile as a whole would contribute to thermal softening of the underlying granitoid crust as described by West (1980). Thermal gradients through the basin would be artificially steepened while in the adjacent volcanic terrane they would be decreased, providing for the pattern of metamorphism noted.

Heating and softening in both the basement gneiss and the sedimentary basin would develop in a regime of north-south compressive stresses. Without a significant density contrast to perpetuate downsagging, partial melting, tight folding and diapric uplift possibly accompanied by nappe style tectonics would result in the formation of the metasedimentary-gneiss-migmatite belt observed.

Several features of the observed geology and geophysics help support this hypothesis. The predominantly granitic gneisses and migmatites that are exposed throughout the Quetico Belt are unlikely to have evolved solely from the greywacke turbidite sequences which flank the belt. Allis and Garland (1979) found that the rocks richest in K, Th and U are located in the Quetico Belt and parts of the Wabigoon Belt to the north, where extensive outcropping of granitic rock is exposed, suggesting a possible source for the quartzofeldspathic

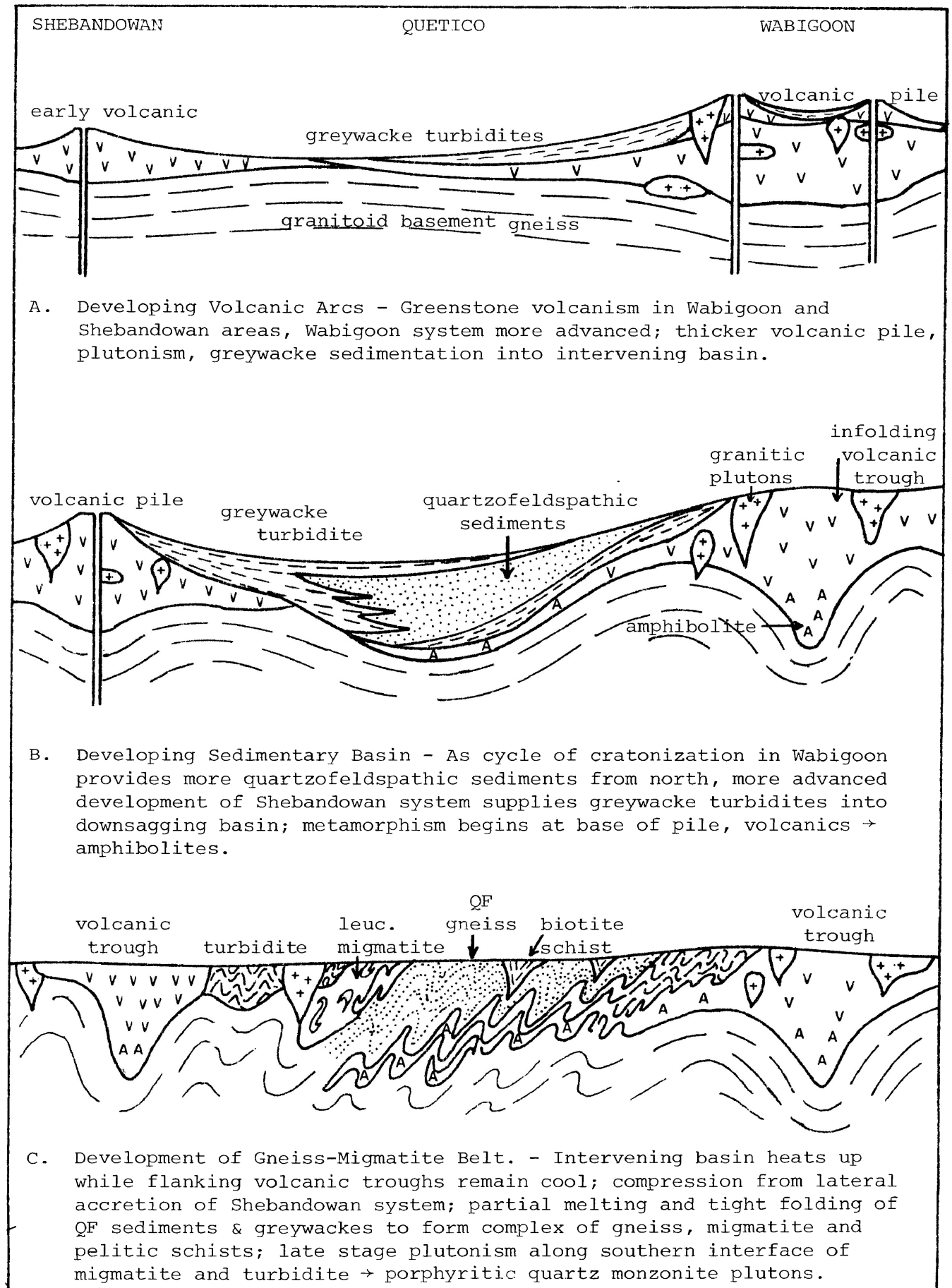


FIG.10 Postulated Sequence of Tectonic Development

sediments now exposed as granitic gneiss within the Quetico Belt.

The layers of amphibolite and basic gneiss that form the dense substratum of the belt of migmatite and gneiss tends to thicken somewhat toward the north, while it dips and thins sharply toward the south. Kehlenbeck (1976) has described a gradational metamorphic interface between the Quetico Belt rocks and the Wabigoon Belt rocks to the north. In contrast, the transition between the Quetico Belt rocks and lower grade turbidite sediments to the south is sharper, and corresponds spatially with the truncation of the southern edge of the basic layer which underlies the gneisses and migmatites. This arrangement suggests that the substratum and possibly the bulk of the original sedimentation into the basin were more intimately related to the Wabigoon Belt cycle of cratonization and that the later turbidite sedimentation and compressional stresses were related to the subsequent lateral accretion of the Shebandowan-Wawa terrane.

At some stage of deposition into the original basin, the quartzofeldspathic sediments considered to have originated in the north would become interlayered with the clay-rich turbidites being shed from the south.

Granitic gneisses and migmatites are interlayered with layers of mica schists within the Quetico Belt presently, and this arrangement is considered to represent the metamorphosed equivalent of the former interlayering. It is postulated that eventually greywacke turbidites related to an active cycle of cratonization and volcanism in the Shebandowan Belt would bury the sagging basin. If these sediments are considered as a cap to the basinal sediments, present patterns of exposure within the Quetico, which suggest somewhat lower grade keels of preserved pelitic schists, would be consistent with the style of second order diapirism postulated as a mechanism of uplift operative in high grade Archean terranes (Schwerdtner et al, 1979).

The Quetico fault and the Hawkeye Lake fault appear to have exploited the structures suggested by the gravity modeling. In the case of the Hawkeye Lake fault, it forms an apparent northern border to a zone of extensive partial melting. This area would represent the zone of maximum mixing of the wet clay-rich turbidites and the quartzofeldspathic sediments, providing H₂O and other volatiles to support melting at relatively low temperatures. Thick remnants of dark biotite schist within the migmatized area possibly

reflecting a primary stratigraphic change between the greywacke turbidites and more quartzofeldspathic material are more predominant toward the north near the Hawkeye Lake fault zone. The interface between the relatively weak zone of biotite schist and the more crystalline gneisses to the north would provide a convenient plane on which vertical displacements suggested by the gravity model could occur without requiring significant brittle failure.

The Quetico fault zone is identified by its cataclastic and mylonitic textures, and is consistent with the concept that the main motion on the fault system postdates the principal metamorphic and deformation events (Schwerdtner et al, 1979). A difficulty arises in that the large transcurrent motions ascribed to the fault system do not appear to have obviously affected the dense substratum of the Quetico Belt, which is transected on profiles B-B' to E-E'. Apparent vertical displacements on the fault are found only on profiles D-D' and E-E', which could be ascribed to a scissor style motion. On profiles A-A' and F-F', the fault plane appears to coincide with the southward dip and truncation of the dense layer. A possible solution to the problem is that displacements on the fault in its present state were not as great as

suggested by some authors (Dunlop, 1979) but rather formed in an environment of oblique compressional stress as suggested by Schwerdtner et al (1979). This stress is accommodated by the structural grain already in place and thus exploits the most suitable path or plane of least resistance provided by the available structures. The timing of the main fault motion may have been such that only late stage tectonic adjustments were accommodated by the present fault system and that these adjustments migrated along the system as required by the overall tectonic regime. This scheme does not rule out major transcurrent displacements occurring along the fault line before the last cycle of cratonization and final accretion were completed.

CONCLUSIONS

Three hundred and fifty new gravity stations have been established. Based on these values and the values of 50 gravity stations previously established by the Earth Physics Branch of E.M.R. a new Bouguer gravity map of the study area has been constructed (Figure 4). New stations established at or near the sites of the previously occupied stations have values in good agreement with the earlier recorded values, typically within 1.0 mGal. The new stations themselves are expected to be reliable to within 0.8 mGals based on estimates of errors.

Based on measurements of specific gravity of 194 selected rock samples, representative densities have been determined for the major rock units recognized for the purposes of this study. Two and one half and three dimensional gravity modeling programs were utilized to test various subsurface configurations of the density contrasts which represent the major rock units (Figures 8, 9).

The model structures suggested by the pattern of Bouguer gravity have been related to several aspects of theoretical concepts of tectonic evolution which may have affected this area. Scale material modeling by

Ramberg (1967) and finite element numerical modeling by West and Mareschal (1979, 1980) have suggested the mechanical results of a dense layer of material (representative of volcanic rock) overlying a layer of less dense material (representative of granitoid rock). The underlying material is shown to upwell diapirically into antiformal structures which flank an infolded or ingested trough of the denser material. The model structures of this study representative of the volcanic rock units and surrounding granitoid rocks conform closely to this structural arrangement.

Several other elements suggested by the model structures of this study may reflect aspects of the tectonic history of the area. Most workers presently recognize the Quetico Belt as a high grade metasedimentary belt. Several workers also suggest that the east-west linear subprovince belt pattern of the Superior Province developed progressively from north to south, so that the Wabigoon volcanic-plutonic belt to the north of the Quetico gneiss belt may have been formed somewhat earlier than the Shebandowan subprovince to the south (Goodwin, 1976; Dunlop, 1979). The pattern of gravity, observed geology and the aeromagnetic anomalies suggests a layer of rocks more dense than the typical quartzofeldspathic

gneiss and migmatite underlies those rocks in the northern portion of the Quetico Belt adjacent to the Wabigoon Belt. This layer has been modeled as dipping southward and becoming truncated beneath the apparent interface between the high grade gneisses typical of the Quetico Belt and the lower grade metasedimentary rocks to the south. While exposures of biotite schist appear to be high grade equivalents of greywack turbidite, the more quartzofeldspathic gneisses within the high grade terrane of the Quetico Belt appear to be of a more granitoid parentage.

The apparent arrangement of the various rock units is outlined by the model structures presented. The dense substratum representative of amphibolite and basic gneisses of probable volcanic origin appear to be associated with a cycle of volcanism to the north, while the apparently overlying quartzofeldspathic gneisses represent high grade metasediments associated with the subsequent cycle of plutonism. The turbidite sedimentary rocks and the higher grade biotite schists may represent the products of a cycle of sedimentation associated with volcanism within what is now the Shebandowan Belt to the south.

The proposed model of tectonic evolution is

based on the results of the gravity derived model structures and a synthesis of current concepts regarding the development of observed patterns of geology within this area of the Superior Province. The Quetico Belt is assumed to represent a sedimentary basin initially offshore to the south relative to a developing craton comprising the Wabigoon Belt and the other subprovinces to the north. This downsagging basin is postulated to have evolved into what might resemble an interarc basin as the developing volcanic terrane now represented by the Shebandowan Belt was accreted laterally and possibly obliquely from the south. The subsequent horizontal compression is possibly responsible for the pervasive east-west planar tectonic fabric and pattern of deformation noted throughout the area.

Geothermal gradients in the vicinity of the model volcanic troughs within the Shebandown Belt may have potentially been depressed by the apparent infolding of cold volcanic material. Geothermal gradients within the proposed sedimentary basin to the north may have been considerably steeper, in part due to the concentration of radiogenic elements within the quartzofeldspathic sediments. This northward steepening of thermal gradients would help explain the pattern of

metamorphism from the low grade metavolcanic rocks in the south of the study area toward the center of the Quetico Belt, where metamorphic grades are generally highest. High heat flow within the proposed basin and the apparent regional compression contributed to a general softening, diapirism, partial melting and upwarping, resulting in the complex features presently exposed in what is now referred to as the Quetico Belt.

APPENDIX A

TABLE OF GRAVITY STATION DATA

Station No.	Elev.(ft. above S.L.)	G Theoretical + 980,000 mGals	G measured + 980,000 mGals	Bouguer Anomaly mGals	Latitude + 48° north
Spruce River Road Series (Hwy. 527)					
SP0	992.8	945.4	885.4	-60.0	48° .508
1	1125.9	946.5	890.0	-56.5	.520
2	1191.0	947.6	889.3	-58.3	.533
3	1225.6	949.3	891.9	-57.4	.552
4	1295.2	950.9	888.3	-62.6	.570
5	1319.0	952.3	888.1	-64.2	.585
6	1596.2	953.2	888.5	-64.7	.595
7	1515.9	954.4	889.1	-65.3	.608
8	1572.7	955.7	888.5	-67.2	.623
9	1567.7	957.2	889.1	-68.1	.640
10	1493.8	958.7	889.1	-69.6	.657
11	1515.4	960.4	893.3	-67.1	.675
12	1560.3	962.0	895.2	-66.8	.693
13	1481.9	963.2	894.1	-69.1	.707
14	1336.6	964.7	894.5	-70.2	.723

Station No.	Elev. (ft. above S.L.)	G Theoretical + 980,000 mGals	G measured + 980,000 mGals	Bouguer Anomaly mGals	Latitude + 480 north
SP15	1542.1	965.9	896.4	-69.5	48.737
16	1579.3	967.5	900.7	-66.8	.755
17	1587.5	969.1	905.4	-63.7	.773
18	1563.3	970.5	908.9	-61.6	.788
19	1535.6	971.5	912.1	-59.4	.800
20	1527.8	972.4	914.0	-58.4	.810
21	1560.1	974.4	917.0	-57.4	.832
22	1567.1	975.7	920.1	-55.6	.847
23	1541.4	977.2	921.0	-56.2	.863
24	1428.9	977.4	920.5	-56.9	.865
25	1498.4	978.1	921.0	-57.1	.873
26	1527.8	979.4	922.2	-57.2	.888
27	1563.1	980.9	924.2	-56.7	.905
28	1528.4	982.3	924.9	-57.4	.920
29	1534.0	983.8	926.2	-57.6	.937
30	1498.5	985.2	928.5	-56.7	.953
31	1499.6	986.5	931.2	-55.3	.967

Station No.	Elev.(ft. above S.L.	G Theoretical + 980,000 mGals	G measured + 980,000 mGals	Bouguer Anomaly mGals	Latitude + 48° north
SP32	1476.7	987.9	934.0	-53.9	48.983
33	1465.8	988.7	934.0	-54.7	.992
34	1593.4	990.5	937.5	-53.0	490.012
35	1558.4	992.1	940.9	-51.2	49.030
36	1530.0	993.6	945.0	-48.6	49.047
37	1562.5	995.1	949.0	-46.1	49.063
38	1528.9	996.3	951.3	-45.0	49.077

Linko - Jumbo Series (Hwy. 17 - 102)

LJ1	1553.9	978.7	908.5	-70.2	48° .880
2	1541.8	978.0	906.5	-71.5	.872
3	1545.6	977.2	908.8	-68.4	.863
4	1552.5	976.0	909.1	-66.9	.850
5	1602.9	975.1	906.6	-68.5	.840
6	1591.7	973.9	907.8	-66.1	.827
7	1581.3	973.7	907.5	-66.2	.824
8	1653.3	972.7	906.6	-66.1	.813

Station No.	Elv. (ft. above S.L.)	G Theoretical + 980,000 mGals	G measured + 980,000 mGals	Bouguer Anomaly mGals	Latitude + 48° north
LJ9	1677.3	971.3	903.8	-67.5	48° .798
10	1634.7	970.0	901.9	-68.1	.783
11	1616.1	968.5	898.7	-69.8	.766
12	1466.9	967.0	896.8	-70.2	.750
13	1408.3	965.3	897.2	-68.1	.731
14	1496.7	963.6	896.4	-67.2	.712
15	1571.4	961.9	896.3	-65.6	.692
16	1441.3	960.5	898.4	-62.1	.677
17	1374.3	958.6	895.9	-62.7	.656
18	1400.1	957.0	895.4	-61.6	.638
19	1388.0	955.2	896.3	-58.9	.618
20	1261.5	953.6	897.0	-56.6	.600
21	1405.9	952.7	901.2	-51.5	.590
22	1424.3	952.2	902.7	-49.5	.584
23	1453.9	951.6	902.6	-49.0	.578
24	1296.8	951.0	899.4	-51.6	.571
25	1296.0	950.1	900.0	-50.1	.561
26	1193.2	949.5	898.0	-51.5	.554
27	1094.9	948.8	895.0	-53.8	.546

Station No.	Elev.(ft. above S.L.	G Theoretical + 980,000 mGals	G measured + 980,000 mGals	Bouguer Anomaly mGals	Latitude + 48° north
LJ28	1096.5	948.7	893.9	-54.8	48° .545
29	1145.3	974.9	893.1	-54.8	.536
31	1184.9	947.6	886.4	-61.2	.533
32	1455.5	946.6	884.4	-62.2	.522
33	1505.4	949.9	884.3	-61.6	.514
34	1434.8	945.2	884.3	-60.9	.506
35	1317.5	944.5	882.4	-62.1	.498
36	1216.0	944.2	877.3	-66.9	.495
37	1156.8	944.0	877.2	-66.8	.493
39	1020.0	943.0	871.2	-71.8	.482
43	861.0	940.7	866.9	-73.8	.457

Trout Series

T1	1439.6	951.8	884.9	-66.9	.580
2	1452.6	951.6	884.3	-67.3	.577
3	1457.6	951.6	883.2	-68.4	.577

Station No.	Elev. (ft. above S.L.)	G ^{Theoretical} + 980,000 mGals	G ^{measured} + 980,000 mGals	Bouguer Anomaly mGals	Latitude + 48° north
T5	1444.1	951.8	882.3	-69.5	48° .579
6	1399.7	951.9	881.7	-70.2	.581
7	1394.2	952.1	881.5	-70.6	.583
9	1333.9	951.7	883.0	-68.7	.578
10	1334.1	951.7	884.3	-67.4	.578
12	1292.4	951.5	884.0	-67.5	.576
14	1299.0	952.2	884.9	-67.3	.584
16	1320.1	953.1	883.0	-70.1	.594
17	1347.0	953.9	883.1	-70.8	.603
18	1342.4	954.5	882.4	-72.1	.610
19	1345.8	955.1	883.0	-72.1	.616
20	13.83.7	955.3	882.8	-72.5	.619
21	1354.2	955.6	882.7	-72.9	.622
22	1338.7	955.6	882.7	-73.1	.622
23	1363.5	955.4	881.9	-73.5	.620
24	1391.3	955.7	881.5	-74.2	.623
26	1458.0	955.9	881.9	-74.0	.625
27	1562.0	956.1	882.0	-74.1	.628

Station No.	Elev. (ft. above S.L.)	G Theoretical + 980,000 mGals	G measured + 980,000 mGals	Bouguer Anomaly mGals	Latitude + 48° north
T28	1352.4	954.2	884.0	-70.2	48° .606
29	1378.2	954.8	884.2	-70.6	.613
30	1374.0	955.5	884.3	-71.2	.621
31	1384.0	955.6	884.4	-71.2	.622
32	1527.4	956.1	882.0	-74.1	.628
33	1598.9	956.4	882.3	-74.1	.631
34	1379.0	952.6	881.1	-71.5	.588
36	1424.0	952.9	881.3	-71.6	.592
37	1447.4	953.2	880.8	-72.4	.595
38	1477.5	953.2	881.1	-72.1	.595
41	1397.8	951.8	886.0	-65.8	.579
43	1463.4	952.5	885.6	-66.9	.587
44	1515.9	952.9	885.5	-67.4	.592
45	1511.4	953.9	885.4	-68.5	.603
46	1511.7	956.6	887.8	-68.8	.633
47	1523.7	957.1	887.9	-69.2	.639
48	1577.4	957.5	888.1	-69.4	.643
49	1582.1	957.9	888.3	-69.6	.648

Station No.	Elev. (ft. above S.L.)	G Theoretical + 980,000 mgals	G measured + 980,000 mgals	Bouguer Anomaly mgals	Latitude + 480 north
T50	1564.8	958.2	888.3	-69.9	480.651
51	1484.9	958.4	888.8	-69.6	.653
52	1490.7	958.8	889.5	-69.3	.658
53	1494.3	958.9	890.4	-68.5	.659
54	1552.9	958.6	889.3	-69.3	.655
55	1607.0	958.7	888.9	-69.8	.657
56	1592.6	958.7	888.7	-70.0	.656
57	1585.4	959.3	890.1	-69.2	.663
58	1652.0	959.4	890.9	-68.5	.664
59	1651.3	959.4	891.0	-68.4	.664
60	1624.3	959.5	891.0	-68.5	.665
61	1596.9	959.4	890.0	-69.4	.664
62	1584.3	958.9	889.4	-69.5	.659
63	1624.5	958.6	889.2	-69.4	.655
64	1628.2	958.2	888.8	-69.4	.651
65	1576.1	957.8	888.1	-69.7	.647
66	1616.7	957.5	888.0	-69.5	.643
67	1634.5	957.8	888.0	-69.8	.647

Station No.	Elev.(ft. above S.L.)	G Theoretical + 980,000 mGals	G measured + 980,000 mGals	Bouguer Anomaly mGals	Latitude + 48° north
T68	1592.1	957.9	889.9	-68.0	48° .648
69	1567.6	957.6	889.9	-67.7	.644
70	1567.8	957.0	889.6	-67.4	.638
71	1633.8	956.7	889.8	-66.9	.634
72	1577.5	958.3	889.4	-68.9	.652
73	1584.7	959.0	890.4	-68.6	.660
74	1600.9	959.7	891.8	-67.9	.668
75	1553.5	956.8	882.6	-74.2	.635
76	1541.1	956.5	882.3	-74.2	.632
77	1551.7	956.3	882.1	-74.1	.630
78	1500.3	956.4	882.6	-73.8	.631
79	1586.5	957.1	883.5	-73.6	.639
80	1537.1	957.7	883.7	-74.0	.646
81	1438.6	952.9	882.8	-70.1	.592
82	1474.0	954.0	882.4	-71.6	.604
83	1451.0	953.7	881.6	-72.1	.601
84	1462.7	953.6	880.9	-72.7	.600

Station No.	Elev.(ft. above S.L.)	G Theoretical + 980,000 mGals	G measured + 980,000 mGals	Bouguer Anomaly mGals	Latitude + 48° north
T85	1459.9	953.6	881.5	-72.1	480.600
86	1454.5	953.6	880.1	-73.5	.600
87	1509.8	954.7	886.9	-67.8	.612
88	1513.2	955.5	887.4	-68.1	.621
89	1511.4	956.9	887.7	-69.2	.637
90	1550.0	956.1	890.4	-65.7	.628
91	1650.0	958.8	887.7	-71.1	.658
92	1610.0	958.7	888.8	-69.9	.657
93	1615.0	960.9	894.7	-66.2	.681
94	1650.0	960.4	892.1	-68.3	.675
95	1620.0	959.9	891.7	-68.2	.670
96	1595.0	958.2	885.7	-72.5	.651
97	1550.0	957.9	883.9	-74.0	.648
98	1470.8	959.8	886.2	-73.6	.669
99	1469.7	959.1	884.4	-74.7	.661
100	1468.9	958.3	883.9	-74.4	.652
101	1472.4	958.4	883.6	-74.8	.653

Station No.	Elev. (ft. above S.L.)	G Theoretical + 980,000 mGals	G measured + 980,000 mGals	Bouguer Anomaly mGals	Latitude + 48° north
T102	1650.0	959.2	886.8	-72.4	48° .662
103	1465.0	961.2	888.0	-73.2	.685
104	1465.0	962.0	890.1	-71.9	.693
105	1460.0	950.6	882.5	-68.1	.566
106	1425.0	951.1	884.5	-66.6	.572
107	1375.0	949.7	885.9	-63.8	.556
108	1500.0	950.3	882.2	-68.1	.563
109	1395	950.5	882.9	-67.6	.565
110	1440	950.3	882.4	-67.9	.563
111	1545	949.1	881.1	-68.0	.549
112	1515	956.1	884.0	-72.1	.628
113	1565	955.6	879.9	-75.7	.622
114	1480	957.7	882.5	-75.2	.645
115	1425	960.8	890.7	-70.1	.680
116	1540	959.7	887.4	=72.3	.668
117	1510	960.2	888.1	-72.1	.673
118	1470	960.6	889.4	-71.2	.678
119	1560	960.6	887.4	-73.2	.678

Station No.	Elev. (ft. above S.L.)	G Theoretical + 980,000 mgals	G measured + 980,000 mgals	Bouguer Anomaly mgals	Latitude + 48° north
T120	1425	962.7	893.9	-68.8	48° .701
121	1500	961.6	890.4	-71.2	.689
122	1500	961.3	890.2	-71.1	.686
123	1550	958.4	885.5	-72.9	.653
124	1595	958.2	884.2	-74.0	.651
125	1580	958.1	884.9	-73.2	.650
126	1560	957.7	885.5	-72.2	.645
127	1550	957.0	885.5	-71.5	.638
128	1520	959.3	885.7	-73.6	.663
129	1500	960.4	886.9	-73.5	.675
130	1500	960.0	885.6	-74.4	.671
131	1550	959.7	884.4	-75.3	.668
132	1565	959.9	885.1	-74.8	.670
133	1425	952.7	888.2	-64.5	.590
134	1385	961.7	893.1	-68.6	.690
136	1135	945.4	874.2	-71.2	.508
137	1260	946.6	875.8	-70.8	.522
138	1290	947.8	878.8	-69.0	.535

Station No.	Elev. (ft. above S.L.)	G Theoretical + 980,000 mGals	G measured + 980,000 mGals	Bouguer Anomaly mGals	Latitude + 48° north
T139	1290	947.8	880.1	-67.7	48° .535
140	1435	948.1	880.5	-67.6	.638
141	1480	947.7	878.5	-69.2	.534
142	1455	948.5	880.4	-68.1	.543
143	1350	949.0	882.5	-66.5	.549
144	1435	949.0	881.3	-67.7	.549
145	1425	952.4	888.6	-63.8	.586
146	1470	952.1	887.5	-64.6	.583
147	1470	951.5	887.0	-64.5	.577
148	1510	950.1	885.7	-64.4	.561
149	1620	949.6	886.5	-63.1	.555
150	1530	948.8	887.8	-61.0	.546
151	1420	947.6	886.8	-60.8	.533
152	1330	946.2	881.0	-65.2	.517
153	1345	947.1	874.8	-72.3	.527
154	1150	944.6	876.5	-68.1	.499
155	1475	949.0	882.8	-66.2	.549
156	1385	950.3	884.5	-65.8	.563

Station No.	Elev. (ft. above S.L.)	G Theoretical + 980,000 mGals	G measured + 980,000 mGals	Bouguer Anomaly mGals	Latitude + 48° north
T157	1470	959.8	886.2	-73.6	480.669
158	1220	946.0	876.4	-69.6	.515
159	1160	956.0	885.4	-70.6	.627
160	1155	955.1	886.2	-68.9	.617
161	1140	954.0	885.9	-68.1	.604
162	1155	953.6	886.7	-66.9	.600
163	1105	952.7	887.2	-65.5	.590
164	1080	951.5	883.0	-68.5	.577
165	1075	950.3	884.7	-65.6	.563
166	1075	949.6	884.4	-65.2	.555
167	1140	948.8	885.4	-63.4	.546
168	1085	947.8	885.5	-62.3	.535
169	1070	946.8	883.9	-62.9	.524
170	1050	946.0	879.4	-66.6	.515
171	1380	967.8	904.0	-63.8	.758
172	1445	967.2	900.3	-66.9	.752
173	1440	966.0	897.3	-68.7	.738
174	1490	965.1	895.5	-69.6	.728

Station No.	Elev. (ft. above S.L.)	G Theoretical + 980,000 mGals	G measured + 980,000 mGals	Bouguer Anomaly mGals	Latitude + 48° north
T175	1490	960.8	886.7	-74.1	48° .680
176	1455	959.9	887.3	-72.6	.670
177	1575	958.2	888.0	-70.2	.651
178	1575	955.1	888.2	-66.9	.617
179	1445	953.6	888.7	-64.9	.600
180	1380	952.5	886.9	-65.6	.588
181	1300	951.6	884.9	-66.7	.578
Kakabeka Series					
K1	1332.0	947.2	893.4	-53.8	48° .529
2	1310.0	945.9	894.8	-51.1	.514
3	1384.0	944.6	895.0	-49.6	.500
4	1295.0	943.6	893.5	-50.1	.488
5	1359.0	942.8	893.1	-49.7	.479
6	1342.0	941.7	889.6	-52.1	.467
7	1169.0	939.7	884.6	-55.1	.445
8	1042.0	938.9	879.3	-59.6	.436

Station No.	Elev.(ft. above S.L.)	G Theoretical + 980,000 mGals	G measured + 980,000 mGals	Bouguer Anomaly mGals	Latitude + 48° north
K9	944.0	936.9	866.5	-70.4	48° .414
10	856.0	935.9	861.6	-74.3	.402
Silver Falls Series					
SF1	1025	947.6	889.8	-57.8	.533
2	1030	948.3	887.6	-60.7	.541
3	1010	949.3	886.2	-63.1	.552
4	1020	950.0	885.3	-64.7	.560
5	1020	950.9	884.2	-66.7	.570
6	1030	951.6	884.8	-66.8	48° .578
7	1035	952.4	887.1	-65.3	.586
8	1080	952.9	888.3	-64.6	.592
9	1030	953.6	888.8	-64.8	.600
10	1025	954.3	888.3	-66.0	.608
11	1020	954.9	888.6	-66.3	.614
12	1045	955.7	889.5	-66.2	.623
13	1050	956.6	888.6	-68.0	.633
14	1025	957.5	889.4	-68.1	.643
15	1025	958.9	890.5	-68.4	.659

Station No.	Elev.(ft. above S.L.)	G Theoretical + 980,000 mGals	G measured + 980,000 mGals	Bouguer Anomaly mGals	Latitude + 480 north
Dog Lake Series					
D1	1385	96.7	893.1	-68.6	48° .690
2	1383	963.1	895.5	-67.6	.706
3	1383	965.0	897.6	-67.4	.727
4	1381	966.2	898.6	-67.6	.740
5	1382	965.6	897.9	-67.7	.734
6	1382	965.1	897.7	-67.4	.728
7	1382	967.4	900.9	-66.5	.754
8	1381	969.9	903.0	-66.9	.782
9	1381	969.1	902.2	-66.9	.773
10	1381	968.8	901.9	-66.9	.770
11	1386	967.8	901.5	-66.3	.759
12	1384	966.4	899.5	-66.9	.743
13	1383	966.2	899.4	-66.8	.740
14	1381	965.4	898.5	-66.9	.732
15	1381	964.1	896.7	-67.4	.717
16	1382	963.8	896.1	-67.7	.714
17	1383	962.5	894.6	-67.9	.699

Station No.	Elev. (ft. above S.L.)	G Theoretical + 980,000 mGals	G measured + 980,000 mGals	Bouguer Anomaly mGals	Latitude + 48° north
D18	1381	960.7	889.2	-71.5	48° .679
19	1382	961.3	892.3	-69.0	.686
20	1381	962.0	892.9	-69.1	.694
21	1383	964.1	896.0	-68.1	.717
22	1381	966.8	899.9	-66.9	.747
23	1383	967.0	900.4	-66.6	.750
24	1382	967.6	901.1	-66.5	.756
25	1381	967.6	901.2	-66.4	.756
26	1384	968.0	901.2	-66.8	.761
27	1381	967.2	901.0	-66.2	.752
28	1381	965.7	897.7	-68.0	.735
29	1383	964.5	896.9	-67.6	.722
30	1382.5	963.5	894.8	-68.7	.710
31	1382	962.7	893.9	-68.8	.701
32	1383	965.0	897.4	-67.6	.727
33	1381	974.5	909.7	-64.8	.833
34	1384	972.5	907.6	-64.9	.811

Station No.	Elev. (ft. above S.L.)	G Theoretical + 980,000 mGals	G measured + 980,000 mGals	Bouguer Anomaly mGals	Latitude + 480 north
D35	1381	968.7	902.7	-66.0	48° .769
36	1381	970.5	908.4	-62.1	.789
37	1381	973.0	912.2	-60.8	.816
38	1381	972.1	911.9	-60.2	.806
39	1381	971.2	910.7	-60.5	.796
40	1382	971.0	910.2	-60.8	.794
41	1381	970.5	908.9	-61.6	.789
42	1382	970.0	907.0	-63.0	.783
43	1384	969.7	905.7	-64.0	.780
44	1384	961.6	890.8	-70.8	.689
45	1381	971.8	906.0	-65.8	.803
46	1382	974.1	909.1	-65.0	.829
47	1382	976.4	913.4	-63.0	.854
48	1381	978.8	916.3	-62.5	.881
49	1383	981.1	920.2	-60.9	.907
50	1383	980.0	919.0	-61.0	.895
51	1381	977.5	915.8	-61.7	.867

Station No	Elev. (ft. above S.L.)	G Theoretical + 980,000 mGals	G measured + 980,000 mGals	Bouguer Anomaly mGals	Latitude + 480 north
D52	1383	975.2	912.0	-63.2	48 ⁰ .841
53	1384	973.4	909.7	-63.7	.821
54	1383	970.9	904.7	-66.2	.793

APPENDIX B

THE COMPUTER PROGRAMS AND MODEL DATA OUTPUT

The 2½-D program utilized extensively in this study was originally based on several algorithms written by John Snow while a graduate student at the University of Utah. These algorithms formed the basis for the computation of the forward gravitational problem, the search function and the Marquardt inversion scheme. Because of the length of the GRAV2D listing, only a brief summary of its function will be given here.

The model is defined by entering the density contrast and x and z coordinates which define the vertices of each polygon. The strike of each polygon in and out of the profile plane is also defined. The forward problem is the simple computation of the gravitational attraction over the model polygons along a specified profile. The measure of fit between the observed values and the computed values for each calculated value is determined at a specified station interval along the profile. This measure of fit, the objective function, is a sum of squares measure given by

$$\begin{aligned} \text{SSR}(\theta) &= \sum_{i=1}^{\text{Nstations}} (\text{Observed}_i - \text{Computed}_i)^2 \\ &= \sum_{i=1}^{\text{Nstat}} (O_i - C_i)^2 \end{aligned}$$

Simply put, the search function is utilized

to locate minima in the forward problem by changing the value of a specified parameter by a specified step size and the forward problem is re-evaluated. If there is an improvement in the objective function, the step size is doubled and the forward problem is again computed. If there is a worsening of the objective fit, the direction of the step changes in the particular parameter value is reversed and the objective function is again re-evaluated.

The expression of the objective function in the general case of the search function is given by

$$C_i = \sum_{j=1}^{\text{No.Polygon}} \phi(j) \sum_{k=1}^{\text{No.Sides}(j)} Z_{ijk}(X_K, Z_K)$$

so that

$$SSR(\theta) = \sum_{i=n_1}^{n_2} (O_i - \sum_{j=1}^{\text{NPOLY}} \phi_j \sum_{n=1}^{\text{NSIDES}(j)} Z_{ijk})^2$$

where $\phi(j)$ is the density contrast of the j th polygon and Z_{ijk} represents the integral over one side of the j th polygon with respect to the i th station. In the case where only polygon vertices are changed, as was the case in this study, the objective function is expressed as

$$SSR(\theta) = \sum_{n_1}^{n_2} (O_i - (A_i + \sum_{j=1}^m \phi_j \sum_{k=1}^1 Z_{ijk}))^2$$

where n_1 , n_2 represents the specified data window, and

A_i is the contribution of the fixed part of the model. The objective function is seen to change as those 1 intergrads of the m polygons which change.

Once a realistic minimum is found the Marquardt inversion algorithm can be used. Based on a

linearization or derivative method, the theoretical anomaly C_i^T can be given by $C_i^T = C_i^{\circ} + \sum_{m=1}^m \frac{\partial C_j^{\circ}}{\partial \theta_m} \Delta \theta_m$

where C_i° is an initial estimate of C_i^T (typically derived by the search routine) and $\Delta \theta_m$ are the parameters of the model to be changed. When the observed anomaly is substituted for C_i^T , then

$$G_i = O_i - C_i^{\circ} = \sum_{m=1}^M \frac{\partial C_j}{\partial \theta_m} \Delta \theta_m$$

The derivative with respect to changing vertices is expressed as

$$\frac{\partial C_i}{\partial X_{jk}} = \frac{C_i(X_{jk} + \Delta X) - C_i(X_{jk})}{\Delta X}$$

for horizontal derivations, and

$$\frac{\partial C_i}{\partial Z_{jk}} = \frac{C_i(Z_{jk} + \Delta X) - C_i(Z_{jk})}{\Delta X}$$

for vertical derivatives.

The inversion algorithm involves Jacobian matrix functions to solve for the partial derivations of the computed anomaly C_i at each station i with

respect to those parameters which are changed during the inversion modeling process, $\frac{\partial C_i}{\partial \theta_m}$. Again, in this study density ϕ_j was typically held constant, and only the derivatives with respect to the vertices $\frac{\partial C_i}{\partial X_{jk}}$ and $\frac{\partial C_i}{\partial Z_{jk}}$ are involved.

For a formalized analysis of the search and inversion techniques, which become detailed beyond the scope of this appendix, the reader is directed to the program documentation GRAV2D: An Interactive 2½ Dimensional Gravity Modeling Program by Carleen Nutter (1980). The following sample terminal session, like the brief outline of the program function above, is taken directly from the program documentation. While this sample terminal session and the following sample output from this study will adequately familiarize the user with the program, several points should be mentioned. While the VAX-II 780 system will very nearly reproduce the values listed by the sample terminal session, minor system differences between Lakehead University and the University of Utah result in a small variance in the roundoff error at the third or fourth decimal place of calculated values. It should be cautioned that because of the highly iterative nature of the search and inversion functions, this program can rapidly erode a student user's computer

time budget. A recent bulletin from the Earth Science Laboratory in Utah has pointed out that while the program professes a capability to handle models with topography, apparently only flat earth modeling should be computed with this program. Finally, at the time this author modified the GRAV2D program for implementation on the VAX-II 780 program, ancillary hardware for the various plotting options of the program did not exist. It is understood that plotting and graphics devices will eventually be available, and future user's are invited and encouraged to enable the plotting routines as their usefulness in this type of study are obvious.

SAMPLE TERMINAL SESSION #1

The following terminal session demonstrates the use of the program from initial model through the inversion process. It also demonstrates the INPUT, EDIT, EXECUTE, LIST, PLOT, and FMAIN functions. The terminal session is summarized in the following steps:

- STEP 1 - Station distances are stored in a file, IN-STATIONS. A theoretical model is stored in file IN-MODEL. A forward problem will be calculated using the station distances and theoretical model to obtain theoretical gravity data. This data will be used as sample field data in STEP 2.
- STEP 2 - Use theoretical data from STEP 1 as observed data in new problem. Perturb the theoretical model from STEP 1 to obtain an initial guess. Normally STEP 1 would not be done, but actual field data would be used and the initial guess would be an attempt to describe the earth cross section where the data was obtained.
- STEP 3 - Compute a forward problem with the initial guess and observed gravity values to find the error. Obtain a plot (Fig. 1).
- STEP 4 - Do a 1D direct search. Note the change in the error and get a plot of new model (Fig. 2).
- STEP 5 - Do an inversion. Note error and get a plot (Fig. 3).
- STEP 6 - Store the newest model and results on the merge file.

A composite of the three plots is included for easier comparison (Fig. 4).

OK, SLIST IN-MODEL

```

1
16, -. 5, 10., 10., 0
-100. 000, 0. 000, 0, 0
118. 500, 0. 000, 0, 0
118. 500, 0. 010, 0, 0
16. 25, 0. 01, 0, 0
15. 5, 2., 0, 0
13. 5, 2., 0, 0
12. 0, 4. 75, 0, 0
9. 5, 5., 0, 0
8. 50, 2. 92, 0, 0
7. 5, 3. 0, 0, 0
6. 5, . 125, 0, 0
5., . 25, 0, 0
4. 5, 1. 42, 0, 0
2. 5, 1. 5, 0, 0
2., . 01, 0, 0
-100. 0, . 01, 0, 0
-100. 0, . 00, 0, 0

```

```

-----
! file containing model      !
! data in format required  !
! by INPUT                  !
-----

```

OK, SLIST IN-STATIONS

THEORETICAL MODEL FROM SNOW

```

1
1
90
0., 0. 0, 0.
0., 0. 2, 0.
0., 0. 4, 0.
0., 0. 6, 0.
0., 0. 8, 0.
0., 1. 0, 0.
0., 1. 2, 0.
0., 1. 4, 0.
0., 1. 6, 0.
0., 1. 8, 0.
0., 2. 0, 0.
0., 2. 2, 0.
0., 2. 4, 0.
0., 2. 6, 0.
0., 2. 8, 0.
0., 3. 0, 0.
0., 3. 2, 0.
0., 3. 4, 0.
0., 3. 6, 0.
0., 3. 8, 0.
0., 4. 0, 0.
0., 4. 2, 0.
0., 4. 4, 0.
0., 4. 6, 0.
0., 4. 8, 0.
0., 5. 0, 0.
0., 5. 2, 0.
0., 5. 4, 0.

```

```

-----
! file containing station   !
! data in format required  !
! by INPUT-observed gravity !
! values are zeros         !
-----

```

0. , 5. 6, 0.
0. , 5. 8, 0.
0. , 6. 0, 0.
0. , 6. 2, 0.
0. , 6. 4, 0.
0. , 6. 6, 0.
0. , 6. 8, 0.
0. , 7. 0, 0.
0. , 7. 2, 0.
0. , 7. 4, 0.
0. , 7. 6, 0.
0. , 7. 8, 0.
0. , 8. 0, 0.
0. , 8. 2, 0.
0. , 8. 4, 0.
0. , 8. 6, 0.
0. , 8. 8, 0.
0. , 9. 0, 0.
0. , 9. 2, 0.
0. , 9. 4, 0.
0. , 9. 6, 0.
0. , 9. 8, 0.
0. , 10. 0, 0.
0. , 10. 2, 0.
0. , 10. 4, 0.
0. , 10. 6, 0.
0. , 10. 8, 0.
0. , 11. 0, 0.
0. , 11. 2, 0.
0. , 11. 4, 0.
0. , 11. 6, 0.
0. , 11. 8, 0.
0. , 12. 0, 0.
0. , 12. 2, 0.
0. , 12. 4, 0.
0. , 12. 6, 0.
0. , 12. 8, 0.
0. , 13. 0, 0.
0. , 13. 2, 0.
0. , 13. 4, 0.
0. , 13. 6, 0.
0. , 13. 8, 0.
0. , 14. 0, 0.
0. , 14. 2, 0.
0. , 14. 4, 0.
0. , 14. 6, 0.
0. , 14. 8, 0.
0. , 15. 0, 0.
0. , 15. 2, 0.
0. , 15. 4, 0.
0. , 15. 6, 0.
0. , 15. 8, 0.
0. , 16. 0, 0.
0. , 16. 2, 0.

0., 16. 4, 0.
 0., 16. 6, 0.
 0., 16. 8, 0.
 0., 17. 0, 0.
 0., 17. 2, 0.
 0., 17. 4, 0.
 0., 17. 6, 0.
 0., 17. 8, 0.
 0., 18. 0, 0.

OK, GRAV2D

TERMINL-OPTION # (I)= 0
 1 HARD COPY 80 COLUMN
 2 TEKTRONIX 4014
 3 CRT 80 COLUMN

```
-----
! enter program and input !
! 0 to obtain list of    !
! possible options      !
-----
```

TERMINL-OPTION # (I)= 3
 *** GRAV2D MASTER ***
 MASTER--OPTION # (I)= 2
 INPUT WORK FILE HEADER (80 CHAR.)
 EXAMPLE OF TERMINAL SESSION
 DO YOU WANT TO INPUT STATION DATA FROM FILE?
 YES
 INPUT FILENAME (16 CHAR)
 IN-STATIONS
 INPUT PROFILE ID.
 INPUT CODE FOR UNITS: 1 = KILOMETERS
 2 = METERS
 3 = KILOFEET
 INPUT STATION NO. OR MATCH PT.
 INPUT NO. OF STATIONS
 INPUT OBS. GRAVITY, DIST., ELEV. FOR 90 STATIONS
 DO YOU WANT TO INPUT MODEL DATA FROM FILE?
 YES
 INPUT FILENAME (16 CHAR)
 IN-MODEL
 INPUT NO. OF POLYGONS
 FOR POLYGON 1, INPUT:
 # OF SIDES(I), DENSITY CONTRAST, STRIKE OUT, STRIKE IN, DENSITY SEARCH #(I)
 FOR 17 VERTICES, INPUT:
 HORZ. COORD., VERT. COORD., VERT. SEARCH #(I), HORZ. SEARCH #(I)
 DO YOU WANT TO INPUT SEARCH DATA FROM FILE?
 NO
 INPUT # ITERATIONS FOR INVERSION
 0
 INPUT TOTAL # OF VERTEX SEARCH DIRECTIONS
 0
 INPUT TOTAL # OF DENSITY CONTRAST SEARCH DIRS.
 0
 INPUT HOR. SCALE, VER. SCALE(CURVES), VER. SCALE(MODEL)
 3.
 30.
 1.75

MASTER--OPTION # (I)= 5
 XQT-----OPTION # (I)= 0
 1 RETURN TO MASTER
 2 XQT SEARCH
 3 XQT INVERSION

```
-----
| FORWARD PROBLEM |
|   STEP 1   |
|-----
```

XQT-----OPTION # (I)= 2
 OUTPUT--OPTION # (I)= 1
 THE TOTAL SUM OF SQUARES (SSR) = 104375.641
 0 SEARCHES LEFT

XQT-----OPTION # (I)= 1
 MASTER--OPTION # (I)= 4
 LIST----OPTION # (I)= 2

WORK FILE HEADER:

EXAMPLE OF TERMINAL SESSION

DATE: 07/02/80 15:12

THE TOTAL SUM OF SQUARES IS 104375.641

LIST----OPTION # (I)= 3

* STATION DATA *

THEORETICAL MODEL FROM SNOW

UNITS OF DISTANCE IS KILOM

STATION # OR MATCH PT IS 1

THE TOTAL SUM OF SQUARES IS 104375.641

INPUT RANGE OF STATIONS TO BE PRINTED

AS START INDEX, END INDEX

0,0 WILL PRINT ALL

0,0

Type <CR> to continue

STATION	DISTANCE TO STATION	ELEVATION	COMPUTED GRAVITY	OBSERVED GRAVITY	DIFFERENCE OBS-COMP
1	0.000	0.000	0.000	0.000	0.000
2	0.200	0.000	-0.274	0.000	0.274
3	0.400	0.000	-0.633	0.000	0.633
4	0.600	0.000	-1.029	0.000	1.029
5	0.800	0.000	-1.497	0.000	1.497
6	1.000	0.000	-2.067	0.000	2.067
7	1.200	0.000	-2.770	0.000	2.770
8	1.400	0.000	-3.664	0.000	3.664
9	1.600	0.000	-4.854	0.000	4.854
10	1.800	0.000	-6.562	0.000	6.562
11	2.000	0.000	-9.789	0.000	9.789
12	2.200	0.000	-14.024	0.000	14.024
13	2.400	0.000	-16.657	0.000	16.657
14	2.600	0.000	-18.590	0.000	18.590
15	2.800	0.000	-20.056	0.000	20.056
16	3.000	0.000	-21.173	0.000	21.173
17	3.200	0.000	-22.015	0.000	22.015
18	3.400	0.000	-22.627	0.000	22.627

Type <CR> to continue

19	3.600	0.000	-23.038	0.000	23.038
20	3.800	0.000	-23.256	0.000	23.256
21	4.000	0.000	-23.277	0.000	23.277
22	4.200	0.000	-23.081	0.000	23.081
23	4.400	0.000	-22.632	0.000	22.632

24	4.600	0.000	-21.883	0.000	21.883
25	4.800	0.000	-20.796	0.000	20.796
26	5.000	0.000	-19.474	0.000	19.474
27	5.200	0.000	-18.411	0.000	18.411
28	5.400	0.000	-17.937	0.000	17.937
29	5.600	0.000	-17.995	0.000	17.995
30	5.800	0.000	-18.517	0.000	18.517
31	6.000	0.000	-19.510	0.000	19.510
32	6.200	0.000	-21.074	0.000	21.074
33	6.400	0.000	-23.504	0.000	23.504
34	6.600	0.000	-27.095	0.000	27.095
35	6.800	0.000	-30.578	0.000	30.578
36	7.000	0.000	-33.522	0.000	33.522
37	7.200	0.000	-36.059	0.000	36.059
38	7.400	0.000	-38.283	0.000	38.283
Type<CR> to continue					
39	7.600	0.000	-40.252	0.000	40.252
40	7.800	0.000	-42.009	0.000	42.009
41	8.000	0.000	-43.582	0.000	43.582
42	8.200	0.000	-44.992	0.000	44.992
43	8.400	0.000	-46.256	0.000	46.256
44	8.600	0.000	-47.387	0.000	47.387
45	8.800	0.000	-48.395	0.000	48.395
46	9.000	0.000	-49.283	0.000	49.288
47	9.200	0.000	-50.068	0.000	50.068
48	9.400	0.000	-50.743	0.000	50.743
49	9.600	0.000	-51.315	0.000	51.315
50	9.800	0.000	-51.786	0.000	51.786
51	10.000	0.000	-52.156	0.000	52.156
52	10.200	0.000	-52.423	0.000	52.428
53	10.400	0.000	-52.603	0.000	52.603
54	10.600	0.000	-52.680	0.000	52.680
55	10.800	0.000	-52.660	0.000	52.660
56	11.000	0.000	-52.545	0.000	52.545
57	11.200	0.000	-52.335	0.000	52.335
58	11.400	0.000	-52.031	0.000	52.031
Type<CR> to continue					
59	11.600	0.000	-51.634	0.000	51.634
60	11.800	0.000	-51.147	0.000	51.147
61	12.000	0.000	-50.572	0.000	50.572
62	12.200	0.000	-49.912	0.000	49.912
63	12.400	0.000	-49.172	0.000	49.172
64	12.600	0.000	-48.355	0.000	48.355
65	12.800	0.000	-47.468	0.000	47.468
66	13.000	0.000	-46.517	0.000	46.517
67	13.200	0.000	-45.509	0.000	45.509
68	13.400	0.000	-44.448	0.000	44.448
69	13.600	0.000	-43.341	0.000	43.341
70	13.800	0.000	-42.188	0.000	42.188
71	14.000	0.000	-40.991	0.000	40.991
72	14.200	0.000	-39.742	0.000	39.742
73	14.400	0.000	-38.433	0.000	38.433
74	14.600	0.000	-37.047	0.000	37.047
75	14.800	0.000	-35.564	0.000	35.564

76	15.000	0.000	-33.955	0.000	33.955
77	15.200	0.000	-32.181	0.000	32.181
78	15.400	0.000	-30.176	0.000	30.176
Type<CR> to continue					
79	15.600	0.000	-27.931	0.000	27.931
80	15.800	0.000	-25.286	0.000	25.286
81	16.000	0.000	-22.077	0.000	22.077
82	16.200	0.000	-17.785	0.000	17.785
83	16.400	0.000	-13.204	0.000	13.204
84	16.600	0.000	-10.795	0.000	10.795
85	16.800	0.000	-9.042	0.000	9.042
86	17.000	0.000	-7.663	0.000	7.663
87	17.200	0.000	-6.535	0.000	6.535
88	17.400	0.000	-5.591	0.000	5.591
89	17.600	0.000	-4.785	0.000	4.785
90	17.800	0.000	-4.090	0.000	4.090

LIST----OPTION # (I)= 4

* MODEL DATA *

POLYGON NO. 1 DENSITY = -0.50000

STRIKE LENGTH 1 = 10.00000

STRIKE LENGTH 2 = 10.00000

SEARCH NO. = 0

X VERTICE	Z VERTICE	VERT. SEARCH NO.	HOR. SEARCH NO.
-100.000	0.000	0	0
118.500	0.000	0	0
118.500	0.010	0	0
16.250	0.010	0	0
15.500	2.000	0	0
13.500	2.000	0	0
12.000	4.750	0	0
9.500	5.000	0	0
8.500	2.920	0	0
7.500	3.000	0	0
6.500	0.125	0	0
5.000	0.250	0	0
4.500	1.420	0	0
2.500	1.500	0	0
2.000	0.010	0	0

Type <CR> to continue

-100.000	0.010	0	0
-100.000	0.000	0	0

Type <CR> to continue

LIST----OPTION # (I)= 5

* SEARCH DATA *

NO. OF ITERATIONS FOR INVERSION IS 0

TOTAL NO. OF VERTEX SEARCH DIRECTIONS IS 0

TOTAL NO. OF DENSITY CONTRAST SEARCH DIRECTIONS IS 0

LIST----OPTION # (I)= 6

* PLOT DATA *

HORIZONTAL SCALE (UNITS/INCH) = 3.00000

VERTICAL SCALE FOR CURVES (MILLIGALS/INCH) = 30.00000

VERTICAL SCALE FOR MODEL (UNITS/INCH) = 1.75000

LIST----OPTION # (I)= 1

MASTER--OPTION # (I)= 3

```

EDIT----OPTION # (I)=    3
  ESTAT---OPTION # (I)=    0
    1 RETURN TO EDIT OPTIONS
    2 EDIT PROFILE ID.
    3 EDIT UNITS OF DIST.
    4 EDIT STATION #/MATCH PT.
    5 EDIT NO. OF STATIONS
    6 EDIT DISTANCES
    7 EDIT ELEVATIONS
    8 EDIT OBS. GRAVITY VALUES

```

```

      ESTAT---OPTION # (I)=    8
CHANGE-OBSERVED GRAVITY
 0.000000E-01 0.000000E-01 0.000000E-01 0.000000E-01 0.000000E-01
 0.000000E-01 0.000000E-01 0.000000E-01 0.000000E-01 0.000000E-01
 0.000000E-01 0.000000E-01 0.000000E-01 0.000000E-01 0.000000E-01
 0.000000E-01 0.000000E-01 0.000000E-01 0.000000E-01 0.000000E-01
 0.000000E-01 0.000000E-01 0.000000E-01 0.000000E-01 0.000000E-01
 0.000000E-01 0.000000E-01 0.000000E-01 0.000000E-01 0.000000E-01
 0.000000E-01 0.000000E-01 0.000000E-01 0.000000E-01 0.000000E-01
 0.000000E-01 0.000000E-01 0.000000E-01 0.000000E-01 0.000000E-01
 0.000000E-01 0.000000E-01 0.000000E-01 0.000000E-01 0.000000E-01
 0.000000E-01 0.000000E-01 0.000000E-01 0.000000E-01 0.000000E-01
 0.000000E-01 0.000000E-01 0.000000E-01 0.000000E-01 0.000000E-01
 0.000000E-01 0.000000E-01 0.000000E-01 0.000000E-01 0.000000E-01
 0.000000E-01 0.000000E-01 0.000000E-01 0.000000E-01 0.000000E-01
 0.000000E-01 0.000000E-01 0.000000E-01 0.000000E-01 0.000000E-01
 0.000000E-01 0.000000E-01 0.000000E-01 0.000000E-01 0.000000E-01
 0.000000E-01 0.000000E-01 0.000000E-01 0.000000E-01 0.000000E-01
 0.000000E-01 0.000000E-01 0.000000E-01 0.000000E-01 0.000000E-01
 0.000000E-01 0.000000E-01 0.000000E-01 0.000000E-01 0.000000E-01
 0.000000E-01 0.000000E-01 0.000000E-01 0.000000E-01 0.000000E-01

```

```

PARAMETER # (I)=-1
#    1  OLD = 0.000000E-01  NEW =
0.
#    2  OLD = 0.000000E-01  NEW =          |   STEP 2   |
-.294          | Change observed |
#    3  OLD = 0.000000E-01  NEW =          | values from 0's |
-.633          | to previously  |
#    4  OLD = 0.000000E-01  NEW =          | calculated theo- |
-1.029         | retical values |
#    5  OLD = 0.000000E-01  NEW =
-1.499
#    6  OLD = 0.000000E-01  NEW =
-2.067
#    7  OLD = 0.000000E-01  NEW =
-2.77
#    8  OLD = 0.000000E-01  NEW =
-3.664
#    9  OLD = 0.000000E-01  NEW =
-4.854
#   10  OLD = 0.000000E-01  NEW =
-6.562
#   11  OLD = 0.000000E-01  NEW =
-9.789

```

# 12	OLD = 0.000000E-01	NEW =
-14.024		
# 13	OLD = 0.000000E-01	NEW =
-16.657		
# 14	OLD = 0.000000E-01	NEW =
-18.590		
# 15	OLD = 0.000000E-01	NEW =
-20.056		
# 16	OLD = 0.000000E-01	NEW =
-21.173		
# 17	OLD = 0.000000E-01	NEW =
-22.015		
# 18	OLD = 0.000000E-01	NEW =
-22.627		
# 19	OLD = 0.000000E-01	NEW =
-23.038		
# 20	OLD = 0.000000E-01	NEW =
-23.256		
# 21	OLD = 0.000000E-01	NEW =
-23.277		
# 22	OLD = 0.000000E-01	NEW =
-23.081		
# 23	OLD = 0.000000E-01	NEW =
-22.632		
# 24	OLD = 0.000000E-01	NEW =
-21.883		
# 25	OLD = 0.000000E-01	NEW =
-20.796		
# 26	OLD = 0.000000E-01	NEW =
-19.474		
# 27	OLD = 0.000000E-01	NEW =
-18.411		
# 28	OLD = 0.000000E-01	NEW =
-17.937		
# 29	OLD = 0.000000E-01	NEW =
-17.995		
# 30	OLD = 0.000000E-01	NEW =
-18.517		
# 31	OLD = 0.000000E-01	NEW =
-19.510		
# 32	OLD = 0.000000E-01	NEW =
-21.074		
# 33	OLD = 0.000000E-01	NEW =
-23.504		
# 34	OLD = 0.000000E-01	NEW =
-27.095		
# 35	OLD = 0.000000E-01	NEW =
-30.578		
# 36	OLD = 0.000000E-01	NEW =
-33.522		
# 37	OLD = 0.000000E-01	NEW =
-36.059		
# 38	OLD = 0.000000E-01	NEW =
-38.283		

# 39	OLD = 0.000000E-01	NEW =
-40.252		
# 40	OLD = 0.000000E-01	NEW =
-42.009		
# 41	OLD = 0.000000E-01	NEW =
-43.582		
# 42	OLD = 0.000000E-01	NEW =
-44.992		
# 43	OLD = 0.000000E-01	NEW =
-46.256		
# 44	OLD = 0.000000E-01	NEW =
-47.387		
# 45	OLD = 0.000000E-01	NEW =
-48.395		
# 46	OLD = 0.000000E-01	NEW =
-49.288		
# 47	OLD = 0.000000E-01	NEW =
-50.068		
# 48	OLD = 0.000000E-01	NEW =
-50.743		
# 49	OLD = 0.000000E-01	NEW =
-51.315		
# 50	OLD = 0.000000E-01	NEW =
-51.786		
# 51	OLD = 0.000000E-01	NEW =
-52.156		
# 52	OLD = 0.000000E-01	NEW =
-52.428		
# 53	OLD = 0.000000E-01	NEW =
-52.603		
# 54	OLD = 0.000000E-01	NEW =
-52.680		
# 55	OLD = 0.000000E-01	NEW =
-52.66		
# 56	OLD = 0.000000E-01	NEW =
-52.545		
# 57	OLD = 0.000000E-01	NEW =
-52.335		
# 58	OLD = 0.000000E-01	NEW =
-52.031		
# 59	OLD = 0.000000E-01	NEW =
-51.634		
# 60	OLD = 0.000000E-01	NEW =
-51.147		
# 61	OLD = 0.000000E-01	NEW =
-50.572		
# 62	OLD = 0.000000E-01	NEW =
-49.912		
# 63	OLD = 0.000000E-01	NEW =
-49.172		
# 64	OLD = 0.000000E-01	NEW =
-48.355		
# 65	OLD = 0.000000E-01	NEW =
-47.468		

```

# 66 OLD = 0.000000E-01 NEW =
-46.517
# 67 OLD = 0.000000E-01 NEW =
-45.509
# 68 OLD = 0.000000E-01 NEW =
-44.448
# 69 OLD = 0.000000E-01 NEW =
-43.341
# 70 OLD = 0.000000E-01 NEW =
-42.188
# 71 OLD = 0.000000E-01 NEW =
-40.991
# 72 OLD = 0.000000E-01 NEW =
-39.742
# 73 OLD = 0.000000E-01 NEW =
-38.433
# 74 OLD = 0.000000E-01 NEW =
-37.047
# 75 OLD = 0.000000E-01 NEW =
-35.564
# 76 OLD = 0.000000E-01 NEW =
-33.955
# 77 OLD = 0.000000E-01 NEW =
-32.181
# 78 OLD = 0.000000E-01 NEW =
-30.196
# 79 OLD = 0.000000E-01 NEW =
-27.931
# 80 OLD = 0.000000E-01 NEW =
-25.286
# 81 OLD = 0.000000E-01 NEW =
-22.079
# 82 OLD = 0.000000E-01 NEW =
-17.785
# 83 OLD = 0.000000E-01 NEW =
-13.204
# 84 OLD = 0.000000E-01 NEW =
-10.795
# 85 OLD = 0.000000E-01 NEW =
-9.042
# 86 OLD = 0.000000E-01 NEW =
-7.663
# 87 OLD = 0.000000E-01 NEW =
-6.535
# 88 OLD = 0.000000E-01 NEW =
-5.591
# 89 OLD = 0.000000E-01 NEW =
-4.785
# 90 OLD = 0.000000E-01 NEW =
-4.090

```

```

ESTAT ---OPTION # (I)=
EDIT----OPTION # (I):: 1
HAS THE WORK FILE CHANGED?
Y

```

MASTER--OPTION # (I)= 4
 LIST----OPTION # (I)= 3
 * STATION DATA *
 THEORETICAL MODEL FROM SNOW
 UNITS OF DISTANCE IS KILOM
 STATION # OR MATCH PT IS 1
 THE TOTAL SUM OF SQUARES IS 104375.641
 INPUT RANGE OF STATIONS TO BE PRINTED
 AS START INDEX, END INDEX
 0,0 WILL PRINT ALL

0,0

Type <CR> to continue

STATION	DISTANCE TO STATION	ELEVATION	COMPUTED GRAVITY	OBSERVED GRAVITY	DIFFERENCE OBS-COMP
1	0.000	0.000	0.000	0.000	0.000
2	0.200	0.000	-0.294	-0.294	0.294
3	0.400	0.000	-0.633	-0.633	0.633
4	0.600	0.000	-1.029	-1.029	1.029
5	0.800	0.000	-1.499	-1.499	1.499
6	1.000	0.000	-2.067	-2.067	2.067
7	1.200	0.000	-2.770	-2.770	2.770
8	1.400	0.000	-3.664	-3.664	3.664
9	1.600	0.000	-4.854	-4.854	4.854
10	1.800	0.000	-6.562	-6.562	6.562
11	2.000	0.000	-9.789	-9.789	9.789
12	2.200	0.000	-14.024	-14.024	14.024
13	2.400	0.000	-16.657	-16.657	16.657
14	2.600	0.000	-18.590	-18.590	18.590
15	2.800	0.000	-20.056	-20.056	20.056
16	3.000	0.000	-21.173	-21.173	21.173
17	3.200	0.000	-22.015	-22.015	22.015
18	3.400	0.000	-22.627	-22.627	22.627

Type <CR> to continue

19	3.600	0.000	-23.038	-23.038	23.038
20	3.800	0.000	-23.256	-23.256	23.256
21	4.000	0.000	-23.277	-23.277	23.277
22	4.200	0.000	-23.081	-23.081	23.081
23	4.400	0.000	-22.632	-22.632	22.632
24	4.600	0.000	-21.883	-21.883	21.883
25	4.800	0.000	-20.796	-20.796	20.796
26	5.000	0.000	-19.474	-19.474	19.474
27	5.200	0.000	-18.411	-18.411	18.411
28	5.400	0.000	-17.937	-17.937	17.937
29	5.600	0.000	-17.995	-17.995	17.995
30	5.800	0.000	-18.517	-18.517	18.517
31	6.000	0.000	-19.510	-19.510	19.510
32	6.200	0.000	-21.074	-21.074	21.074
33	6.400	0.000	-23.504	-23.504	23.504
34	6.600	0.000	-27.095	-27.095	27.095
35	6.800	0.000	-30.578	-30.578	30.578
36	7.000	0.000	-33.522	-33.522	33.522
37	7.200	0.000	-36.059	-36.059	36.059
38	7.400	0.000	-38.283	-38.283	38.283

Type <CR> to continue

39	7.600	0.000	-40.252	-40.252	40.252
40	7.800	0.000	-42.009	-42.009	42.009
41	8.000	0.000	-43.582	-43.582	43.582
42	8.200	0.000	-44.992	-44.992	44.992
43	8.400	0.000	-46.256	-46.256	46.256
44	8.600	0.000	-47.387	-47.387	47.387
45	8.800	0.000	-48.395	-48.395	48.395
46	9.000	0.000	-49.288	-49.288	49.288
47	9.200	0.000	-50.068	-50.068	50.068
48	9.400	0.000	-50.743	-50.743	50.743
49	9.600	0.000	-51.315	-51.315	51.315
50	9.800	0.000	-51.786	-51.786	51.786
51	10.000	0.000	-52.156	-52.156	52.156
52	10.200	0.000	-52.428	-52.428	52.428
53	10.400	0.000	-52.603	-52.603	52.603
54	10.600	0.000	-52.680	-52.680	52.680
55	10.800	0.000	-52.660	-52.660	52.660
56	11.000	0.000	-52.545	-52.545	52.545
57	11.200	0.000	-52.335	-52.335	52.335
58	11.400	0.000	-52.031	-52.031	52.031
Type<CR> to continue					
59	11.600	0.000	-51.634	-51.634	51.634
60	11.800	0.000	-51.147	-51.147	51.147
61	12.000	0.000	-50.572	-50.572	50.572
62	12.200	0.000	-49.912	-49.912	49.912
63	12.400	0.000	-49.172	-49.172	49.172
64	12.600	0.000	-48.355	-48.355	48.355
65	12.800	0.000	-47.468	-47.468	47.468
66	13.000	0.000	-46.517	-46.517	46.517
67	13.200	0.000	-45.509	-45.509	45.509
68	13.400	0.000	-44.448	-44.448	44.448
69	13.600	0.000	-43.341	-43.341	43.341
70	13.800	0.000	-42.188	-42.188	42.188
71	14.000	0.000	-40.991	-40.991	40.991
72	14.200	0.000	-39.742	-39.742	39.742
73	14.400	0.000	-38.433	-38.433	38.433
74	14.600	0.000	-37.047	-37.047	37.047
75	14.800	0.000	-35.564	-35.564	35.564
76	15.000	0.000	-33.955	-33.955	33.955
77	15.200	0.000	-32.181	-32.181	32.181
78	15.400	0.000	-30.196	-30.196	30.196
Type<CR> to continue					
79	15.600	0.000	-27.931	-27.931	27.931
80	15.800	0.000	-25.286	-25.286	25.286
81	16.000	0.000	-22.079	-22.079	22.079
82	16.200	0.000	-17.785	-17.785	17.785
83	16.400	0.000	-13.204	-13.204	13.204
84	16.600	0.000	-10.795	-10.795	10.795
85	16.800	0.000	-9.042	-9.042	9.042
86	17.000	0.000	-7.663	-7.663	7.663
87	17.200	0.000	-6.535	-6.535	6.535
88	17.400	0.000	-5.591	-5.591	5.591
89	17.600	0.000	-4.785	-4.785	4.785
90	17.800	0.000	-4.090	-4.090	4.090

```

LIST----OPTION # (I)= 1
MASTER--OPTION # (I)= 3
EDIT----OPTION # (I)= 0
    1 RETURN TO MASTER OPTIONS
    2 EDIT WORK FILE HEADER
    3 EDIT STATION DATA
    4 EDIT MODEL DATA
    5 EDIT SEARCH/INVERSN DATA
    6 EDIT PLOT DATA

```

```

EDIT----OPTION # (I)= 4
    EMODEL--OPTION # (I)= 0
        1 RETURN TO EDIT OPTIONS
        2 EDIT NO. OF POLYGON
        3 EDIT # OF SIDES OF POLY.
        4 EDIT DENSITY CONTRASTS
        5 EDIT STRIKE LENGTH OUT
        6 EDIT STRIKE LENGTH IN
        7 EDIT HOR. COORDINATES
        8 EDIT VERT. COORDINATES

```

```

                EMODEL--OPTION # (I)= 7      | change model      |
CHANGE-HORZ. COORDINATES                    | to initial guess |
-----|-----|-----|-----|-----|-----|-----|-----|-----|

```

```

-1.000000E 02 1.185000E 02 1.185000E 02 1.625000E 01 1.550000E 01
 1.350000E 01 1.200000E 01 9.500000E 00 8.500000E 00 7.500000E 00
 6.500000E 00 5.000000E 00 4.500000E 00 2.500000E 00 2.000000E 00
-1.000000E 02-1.000000E 02

```

CHANGE, ADD, DELETE OR RETURN?CHANGE

PARAMETER # (I, J)=-1, -1

```

# 1 1 OLD =-1.000000E 02 NEW =
-100.
# 1 2 OLD = 1.185000E 02 NEW =
118.5
# 1 3 OLD = 1.185000E 02 NEW =
118.5
# 1 4 OLD = 1.625000E 01 NEW =
16.75
# 1 5 OLD = 1.550000E 01 NEW =
15.75
# 1 6 OLD = 1.350000E 01 NEW =
12.5
# 1 7 OLD = 1.200000E 01 NEW =
11.25
# 1 8 OLD = 9.500000E 00 NEW =
9.5
# 1 9 OLD = 8.500000E 00 NEW =
8.5
# 1 10 OLD = 7.500000E 00 NEW =
7.25
# 1 11 OLD = 6.500000E 00 NEW =
6.37
# 1 12 OLD = 5.000000E 00 NEW =
5.

```

```

#      1      13  OLD = 4.500000E 00  NEW =
4.
#      1      14  OLD = 2.500000E 00  NEW =
2.
#      1      15  OLD = 2.000000E 00  NEW =
1.5
#      1      16  OLD =-1.000000E 02  NEW =
-100.
#      1      17  OLD =-1.000000E 02  NEW =
-100.
-1.000000E 02 1.185000E 02 1.185000E 02 1.675000E 01 1.575000E 01
1.250000E 01 1.125000E 01 9.500000E 00 8.500000E 00 7.250000E 00
6.370000E 00 5.000000E 00 4.000000E 00 2.000000E 00 1.500000E 00
-1.000000E 02-1.000000E 02
CHANGE, ADD, DELETE OR RETURN?RETURN
EMODEL--OPTION # (I)=      B
CHANGE--VERT. COORDINATES
0.000000E-01 0.000000E-01 1.000000E-02 1.000000E-02 2.000000E 00
2.000000E 00 4.750000E 00 5.000000E 00 2.920000E 00 3.000000E 00
1.250000E-01 2.500000E-01 1.420000E 00 1.500000E 00 1.000000E-02
1.000000E-02 0.000000E-01
CHANGE, ADD, DELETE OR RETURN?CHANGE
PARAMETER # (I, J)=-1, -1
#      1      1  OLD = 0.000000E-01  NEW =
0.
#      1      2  OLD = 0.000000E-01  NEW =
0.
#      1      3  OLD = 1.000000E-02  NEW =
#      1      4  OLD = 1.000000E-02  NEW =
#      1      5  OLD = 2.000000E 00  NEW =
1.25
#      1      6  OLD = 2.000000E 00  NEW =
1.25
#      1      7  OLD = 4.750000E 00  NEW =
4.
#      1      8  OLD = 5.000000E 00  NEW =
4.
#      1      9  OLD = 2.920000E 00  NEW =
2.
#      1     10  OLD = 3.000000E 00  NEW =
2.
#      1     11  OLD = 1.250000E-01  NEW =
#      1     12  OLD = 2.500000E-01  NEW =
#      1     13  OLD = 1.420000E 00  NEW =
2.
#      1     14  OLD = 1.500000E 00  NEW =
2.
#      1     15  OLD = 1.000000E-02  NEW =
#      1     16  OLD = 1.000000E-02  NEW =
#      1     17  OLD = 0.000000E-01  NEW =
0.
0.000000E-01 0.000000E-01 1.000000E-02 1.000000E-02 1.250000E 00
1.250000E 00 4.000000E 00 4.000000E 00 2.000000E 00 2.000000E 00
1.250000E-01 2.500000E-01 2.000000E 00 2.000000E 00 1.000000E-02

```

1. 000000E-02 0. 000000E-01

CHANGE, ADD, DELETE OR RETURN?RETURN

EMODEL--OPTION # (I)= 0

- 1 RETURN TO EDIT OPTIONS
- 2 EDIT NO. OF POLYGON
- 3 EDIT # OF SIDES OF POLY.
- 4 EDIT DENSITY CONTRASTS
- 5 EDIT STRIKE LENGTH OUT
- 6 EDIT STRIKE LENGTH IN
- 7 EDIT HOR. COORDINATES
- 8 EDIT VERT. COORDINATES

EMODEL--OPTION # (I)= 1

EDIT----OPTION # (I)= 0

- 1 RETURN TO MASTER OPTIONS
- 2 EDIT WORK FILE HEADER
- 3 EDIT STATION DATA
- 4 EDIT MODEL DATA
- 5 EDIT SEARCH/INVERSN DATA
- 6 EDIT PLOT DATA

EDIT----OPTION # (I)= 5

ESEARCH-OPTION # (I)= 0

- 1 RETURN TO EDIT OPTIONS
- 2 EDIT # OF ITERATIONS
- 3 EDIT # OF VERTEX SEARCH DIR.
- 4 EDIT # OF DENSITY SEARCH DIR
- 5 EDIT DENSITY SEARCH #S
- 6 EDIT VERT. SEARCH #S(VERTEX)
- 7 EDIT HORZ. SEARCH #S(VERTEX)
- 8 EDIT TOLERANCES FOR SEARCH
- 9 EDIT STEP SIZES FOR SEARCH

ESEARCH-OPTION # (I)= 2

CHANGE-# ITERATIONS

OLD= 0 NEW=

4

ESEARCH-OPTION # (I)= 3

CHANGE-# VERTX SEARCH DIR. S

OLD= 0 NEW=

7

ESEARCH-OPTION # (I)= 6

CHANGE-VERT. SEARCH #S

0	0	0	0	0
0	0	0	0	0
0	0	0	0	0
0	0			

CHANGE, ADD, DELETE OR RETURN?CHANGE

PARAMETER # (I, J)=-1, -1

1 1 OLD = 0 NEW =

0

1 2 OLD = 0 NEW =

0

1 3 OLD = 0 NEW =

```

0
# 1 4 OLD = 0 NEW =
0
# 1 5 OLD = 0 NEW =
6
# 1 6 OLD = 0 NEW =
6
# 1 7 OLD = 0 NEW =
3
# 1 8 OLD = 0 NEW =
3
# 1 9 OLD = 0 NEW =
3
# 1 10 OLD = 0 NEW =
3
# 1 11 OLD = 0 NEW =
0
# 1 12 OLD = 0 NEW =
0
# 1 13 OLD = 0 NEW =
1
# 1 14 OLD = 0 NEW =
1
# 1 15 OLD = 0 NEW =
0
# 1 16 OLD = 0 NEW =
0
# 1 17 OLD = 0 NEW =
0

```

```

0 0 0 0 6
6 3 3 3 3
0 0 1 1 0
0 0

```

```

CHANGE, ADD, DELETE OR RETURN?RETURN
      ESEARCH-OPTION # (I)= 7
CHANGE-HORZ. SEARCH #S

```

```

0 0 0 0 0
0 0 0 0 0
0 0 0 0 0
0 0

```

```

CHANGE, ADD, DELETE OR RETURN?CHANGE
PARAMETER # (I, J)=-1, -1

```

```

# 1 1 OLD = 0 NEW =
0
# 1 2 OLD = 0 NEW =
0
# 1 3 OLD = 0 NEW =
0
# 1 4 OLD = 0 NEW =
7
# 1 5 OLD = 0 NEW =
7
# 1 6 OLD = 0 NEW =
7

```

```

# 1 7 OLD = 0 NEW =
5
# 1 8 OLD = 0 NEW =
4
# 1 9 OLD = 0 NEW =
4
# 1 10 OLD = 0 NEW =
0
# 1 11 OLD = 0 NEW =
0
# 1 12 OLD = 0 NEW =
0
# 1 13 OLD = 0 NEW =
0
# 1 14 OLD = 0 NEW =
2
# 1 15 OLD = 0 NEW =
2
# 1 16 OLD = 0 NEW =
0
# 1 17 OLD = 0 NEW =
0

```

```

0 0 0 7 7
7 5 4 4 0
0 0 0 2 2
0 0

```

CHANGE, ADD, DELETE OR RETURN?CHANGE

PARAMETER # (I, J)=1, 6

```

# 1 6 OLD = 7 NEW =
5

```

```

-----
! change incorrectly !
! typed number      !
-----

```

```

0 0 0 7 7
5 5 4 4 0
0 0 0 2 2
0 0

```

CHANGE, ADD, DELETE OR RETURN?RETURN

ESEARCH-OPTION # (I)= 0

- 1 RETURN TO EDIT OPTIONS
- 2 EDIT # OF ITERATIONS
- 3 EDIT # OF VERTEX SEARCH DIR.
- 4 EDIT # OF DENSITY SEARCH DIR
- 5 EDIT DENSITY SEARCH #S
- 6 EDIT VERT. SEARCH #S(VERTEX)
- 7 EDIT HORZ. SEARCH #S(VERTEX)
- 8 EDIT TOLERANCES FOR SEARCH
- 9 EDIT STEP SIZES FOR SEARCH

ESEARCH-OPTION # (I)= 8

CHANGE-TOLERANCES

```

0.000000E-01 0.000000E-01 0.000000E-01 0.000000E-01 0.000000E-01
0.000000E-01 0.000000E-01

```

PARAMETER # (I)=-1

```

# 1 OLD = 0.000000E-01 NEW =
1.
# 2 OLD = 0.000000E-01 NEW =

```

1.
 # 3 OLD = 0.000000E-01 NEW =
 1.
 # 4 OLD = 0.000000E-01 NEW =
 1.
 # 5 OLD = 0.000000E-01 NEW =
 1.
 # 6 OLD = 0.000000E-01 NEW =
 1.
 # 7 OLD = 0.000000E-01 NEW =
 1.

ESEARCH-OPTION # (I)= 9

CHANGE-STEP SIZES

0.000000E-01 0.000000E-01 0.000000E-01 0.000000E-01 0.000000E-01
 0.000000E-01 0.000000E-01

PARAMETER # (I)=-1

1 OLD = 0.000000E-01 NEW =
 # 2 OLD = 0.000000E-01 NEW =
 # 3 OLD = 0.000000E-01 NEW =
 # 4 OLD = 0.000000E-01 NEW =
 # 5 OLD = 0.000000E-01 NEW =
 # 6 OLD = 0.000000E-01 NEW =
 # 7 OLD = 0.000000E-01 NEW =

ESEARCH-OPTION # (I)= 1

EDIT----OPTION # (I)= 1

HAS THE WORK FILE CHANGED?

Y

MASTER--OPTION # (I)= 4

LIST----OPTION # (I)= 4

* MODEL DATA *

POLYGON NO. 1 DENSITY = -0.50000

STRIKE LENGTH 1 = 10.00000

STRIKE LENGTH 2 = 10.00000

SEARCH NO. = 0

X VERTICE	Z VERTICE	VERT. SEARCH NO.	HOR. SEARCH NO.
-100.000	0.000	0	0
118.500	0.000	0	0
118.500	0.010	0	0
16.750	0.010	0	7
15.750	1.250	6	7
12.500	1.250	6	5
11.250	4.000	3	5
9.500	4.000	3	4
8.500	2.000	3	4
7.250	2.000	3	0
6.370	0.125	0	0
5.000	0.250	0	0
4.000	2.000	1	0
2.000	2.000	1	2
1.500	0.010	0	2

Type <CR> to continue

-100.000 0.010 0 0

-100.000 0.000 0 0

Type <CR> to continue

LIST----OPTION # (I)= 5
 * SEARCH DATA *
 NO. OF ITERATIONS FOR INVERSION IS 4
 TOTAL NO. OF VERTEX SEARCH DIRECTIONS IS 7
 TOTAL NO. OF DENSITY CONTRAST SEARCH DIRECTIONS IS 0
 Type <CR> to continue

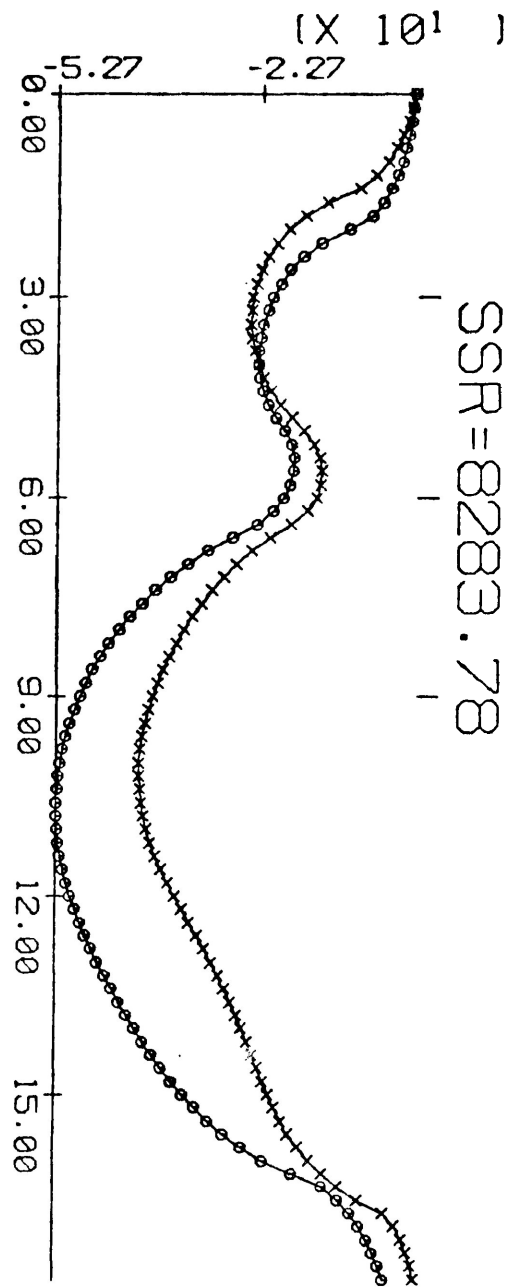
	TOLERANCE	STEP SIZE
1	1.00000	0.25000
2	1.00000	0.25000
3	1.00000	0.25000
4	1.00000	0.25000
5	1.00000	0.25000
6	1.00000	0.25000
7	1.00000	0.25000

LIST----OPTION # (I)= 1
 MASTER--OPTION # (I)= 3
 EDIT----OPTION # (I)= 5
 ESEARCH-OPTION # (I)= 3
 CHANGE-# VERTEX SEARCH DIR. S
 OLD= 7 NEW=
 0

ESEARCH-OPTION # (I)=
 EDIT----OPTION # (I)= 1
 HAS THE WORK FILE CHANGED?
 Y
 MASTER--OPTION # (I)= 5 | STEP 3 |
 XQT-----OPTION # (I)= 2 |-----|
 OUTPUT--OPTION # (I)= 1
 THE TOTAL SUM OF SQUARES (SSR) = 8283.779
 0 SEARCHES LEFT
 XQT-----OPTION # (I)= 1
 MASTER--OPTION # (I)= 7
 PLOT----OPTION # (I)= 0
 1 RETURN TO MASTER OPTIONS
 2 PLOT CURRENT MODEL
 3 PLOT MULTIPLE SAVED MODELS

PLOT----OPTION # (I)= 2
 CURRENT MODEL PLOT
 DEVICE--OPTION # (I)= 0
 1 TEKTRONIX GRAPHICS PLOT
 2 STATUS PLOT
 3 UUCS CALCOMP PLOT

DEVICE--OPTION # (I)= 2
 # OF VECTORS= 2364
 PLOT----OPTION # (I)= 1
 MASTER--OPTION # (I)= 3
 EDIT----OPTION # (I)= 5
 ESEARCH-OPTION # (I)= 3
 CHANGE-# VERTEX SEARCH DIR. S
 OLD= 0 NEW=



SSR=8283.78

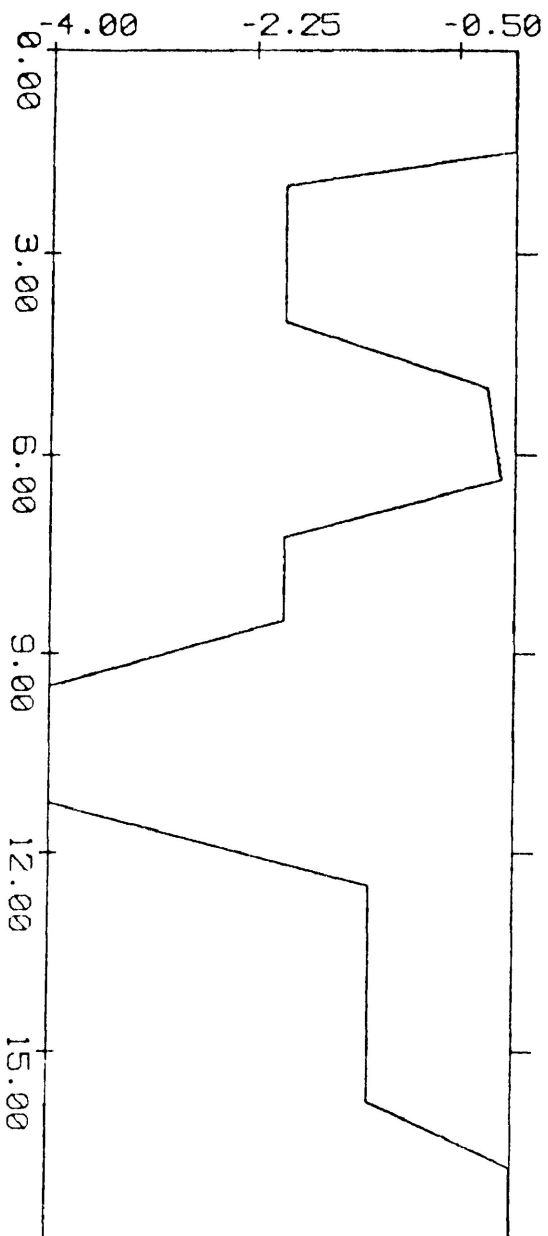


FIGURE 1 INITIAL GUESS

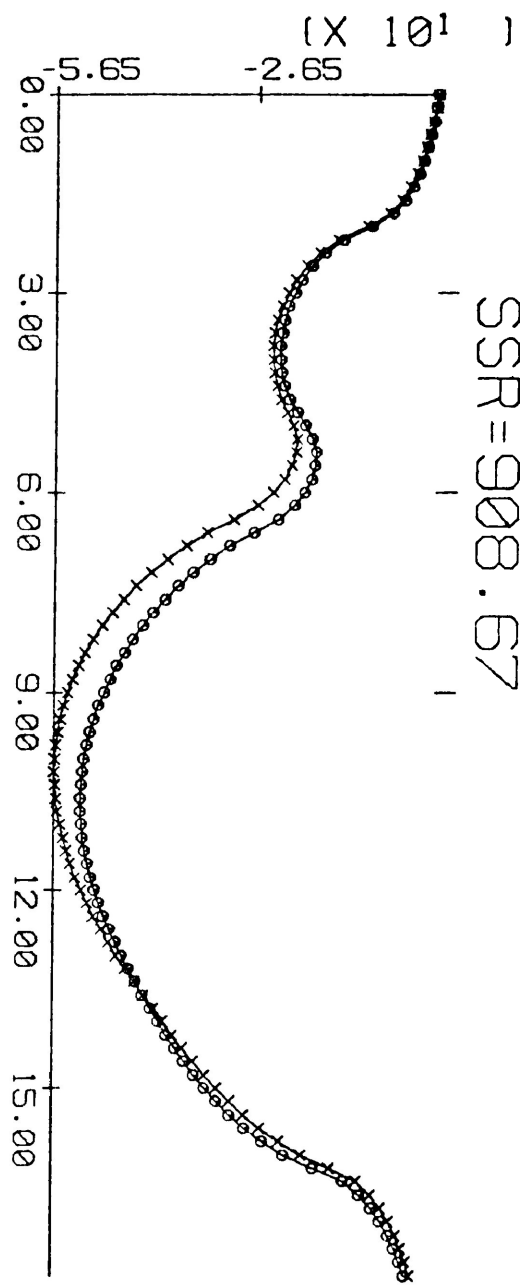
POLYGON NO.	DENSITY CONTRAST
1	-0.50000

```

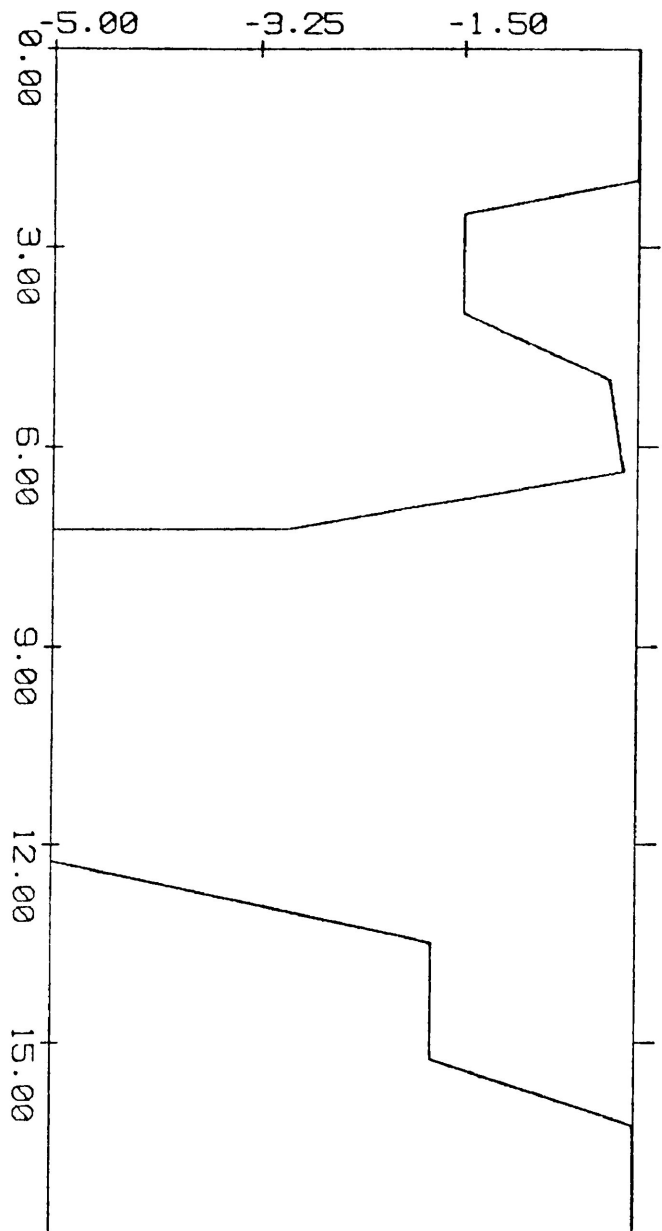
      ESEARCH-OPTION # (I)=
    EDIT-----OPTION # (I)= 1
HAS THE WORK FILE CHANGED?
N
MASTER---OPTION # (I)= 5          | STEP 4 |
  XQT-----OPTION # (I)= 2
    OUTPUT--OPTION # (I)= 1
THE TOTAL SUM OF SQUARES (SSR) = 8283.779
  0 SEARCHES LEFT
THE TOTAL SUM OF SQUARES (SSR) = 6935.303
  6 SEARCHES LEFT
THE TOTAL SUM OF SQUARES (SSR) = 6008.625
  5 SEARCHES LEFT
THE TOTAL SUM OF SQUARES (SSR) = 2553.403
  4 SEARCHES LEFT
THE TOTAL SUM OF SQUARES (SSR) = 2258.706
  3 SEARCHES LEFT
THE TOTAL SUM OF SQUARES (SSR) = 992.981
  2 SEARCHES LEFT
THE TOTAL SUM OF SQUARES (SSR) = 1026.183
  1 SEARCHES LEFT
THE TOTAL SUM OF SQUARES (SSR) = 908.666
  0 SEARCHES LEFT
DO YOU WANT THIS SAVED?
YES
  XQT-----OPTION # (I)= 1
MASTER---OPTION # (I)= 7
  PLOT-----OPTION # (I)= 2
*CURRENT MODEL PLOT*
  DEVICE--OPTION # (I)= 2
# OF VECTORS= 2362
  PLOT-----OPTION # (I)= 1          | STEP 5 |
MASTER---OPTION # (I)= 5
  XQT-----OPTION # (I)= 0
    1 RETURN TO MASTER
    2 XQT SEARCH
    3 XQT INVERSION

  XQT-----OPTION # (I)= 3
    OUTPUT--OPTION # (I)= 1
THE TOTAL SUM OF SQUARES IS 908.664
  4 ITERATIONS LEFT
THE TOTAL SUM OF SQUARES IS 48.659
  3 ITERATIONS LEFT
THE TOTAL SUM OF SQUARES IS 24.613
  2 ITERATIONS LEFT
THE TOTAL SUM OF SQUARES IS 17.496
  1 ITERATIONS LEFT
THE TOTAL SUM OF SQUARES IS 17.164
  0 ITERATIONS LEFT
DO YOU WANT THIS SAVED?
YES

```



ORIGINAL = O
 NEW = X



POLYCON NO.	DENSITY CONTRAST
1	-0.50000

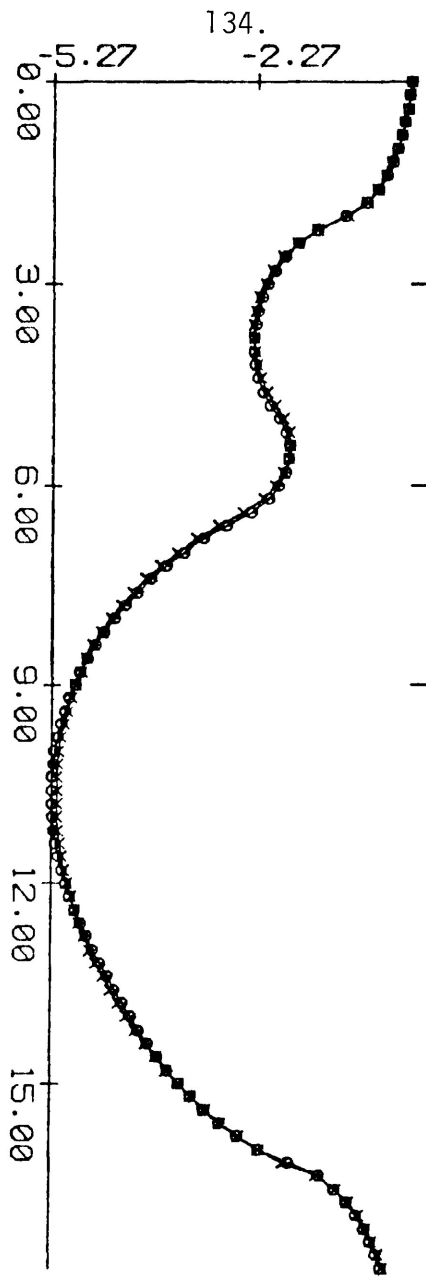
```

XQT-----OPTION # (I)=
MASTER--OPTION # (I)= 6
*FILE MAINTENANCE*
FMAIN---OPTION # (I)= 2
TEST FILES FOR DEBUGGING G2HSER
*SUBFILE# 1
SOUTH LINE - HILL AIRFORCE BASE - WITH D.P.
HILL AIRFORCE BASE SOUTH LINE
*SUBFILE# 2
NORTH LINE - HILL AIRFORCE BASE - WITH D.P.
HILL AIRFORCE BASE NORTH LINE
*SUBFILE# 3
TEST OF RONS FILE
BALTAZOR L-3 1ST CUT
*SUBFILE# 4
EXAMPLE ONE
HILL AIRFORCE BASE SOUTH LINE
*SUBFILE# 5
TEST OF AUTOMATIC SEARCH ON THEORETICAL MODEL
THEORETICAL MODEL FROM SNOW
Type <CR> to continue
*SUBFILE# 6
TEST OF INVERSION ON THEORETICAL MODEL AFTER SEARCH
THEORETICAL MODEL FROM SNOW
*SUBFILE# 7
M2 INV
LINE M2 GRAV
FMAIN---OPTION # (I)= 0
1 RETURN TO MASTER PROGRAM
2 LIST MERGED FILE DIRECTORY
3 SAVE WORK FILE ON MERGED FILE
4 RESTORE WORK FILE FROM MERGED FILE
5 DELETE AND PACK MERGED FILE
6 INITIALIZE MERGE FILE
7 SEND MERGE FILE CONTENTS TO PRINTER

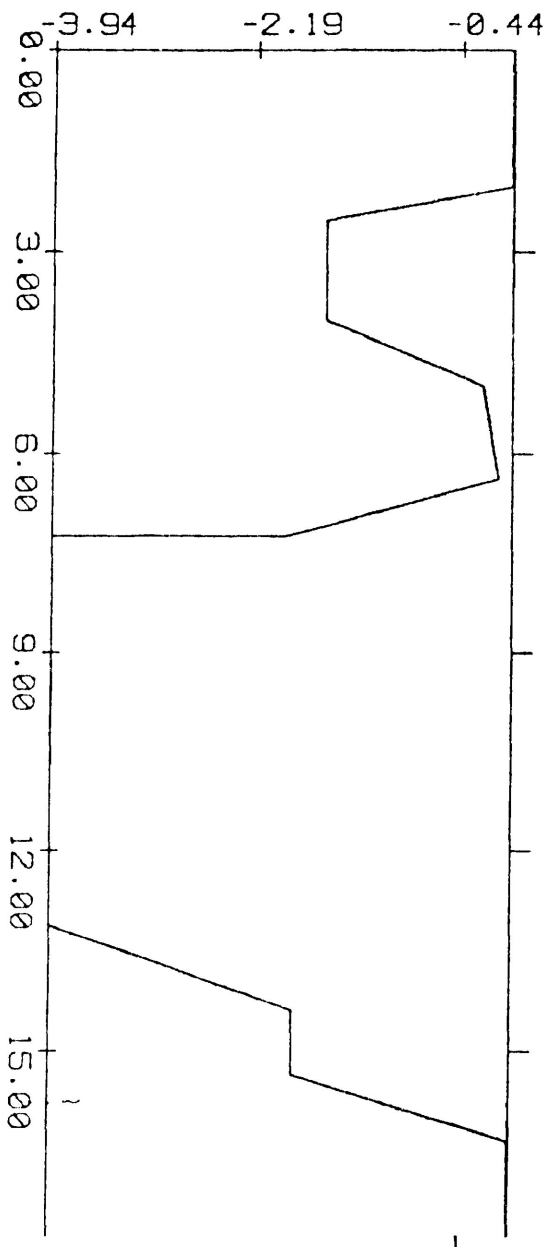
FMAIN---OPTION # (I)= 3
*SAVE WORK FILE*
WORK FILE SAVED AS SUBFILE# 8
FMAIN---OPTION # (I)= 1
MASTER--OPTION # (I)= 7
PLOT----OPTION # (I)= 2
*CURRENT MODEL PLOT*
DEVICE--OPTION # (I)= 2
# OF VECTORS= 2293
PLOT----OPTION # (I)= 1
MASTER--OPTION # (I)= 1

```

SSR = 17.50



ORIGINAL = O
NEW = X



POLYGON NO.	DENSITY CONTRAST
1	-0.50000

FIGURE 3 GRAVITY MODEL AFTER INVERSION

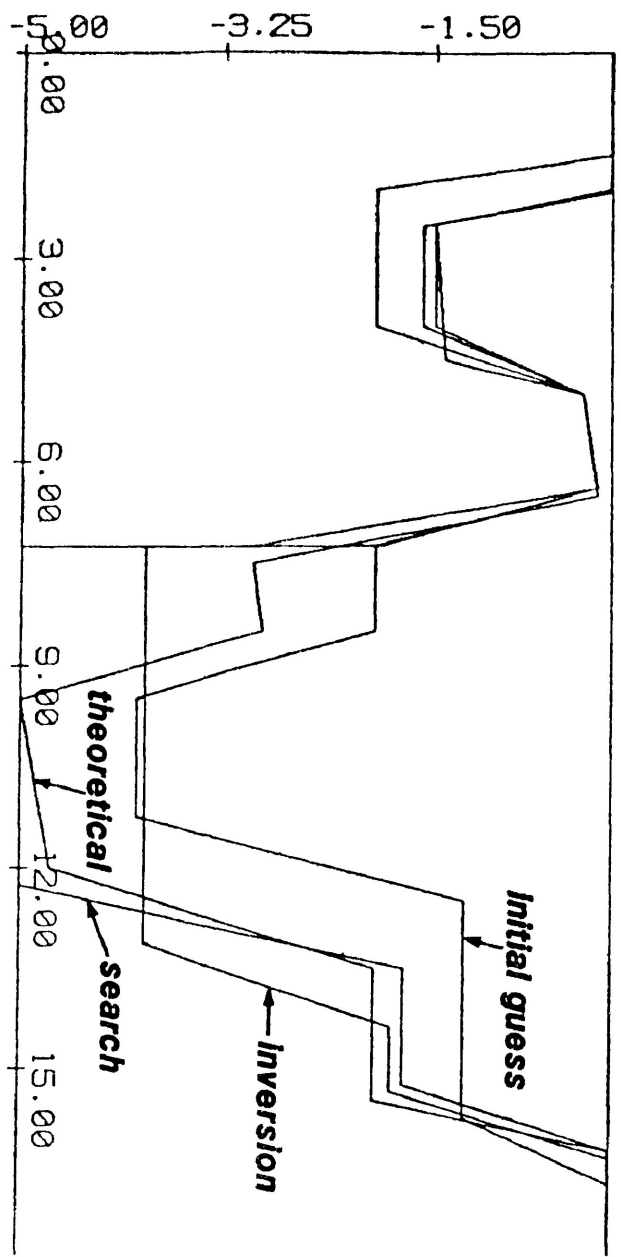
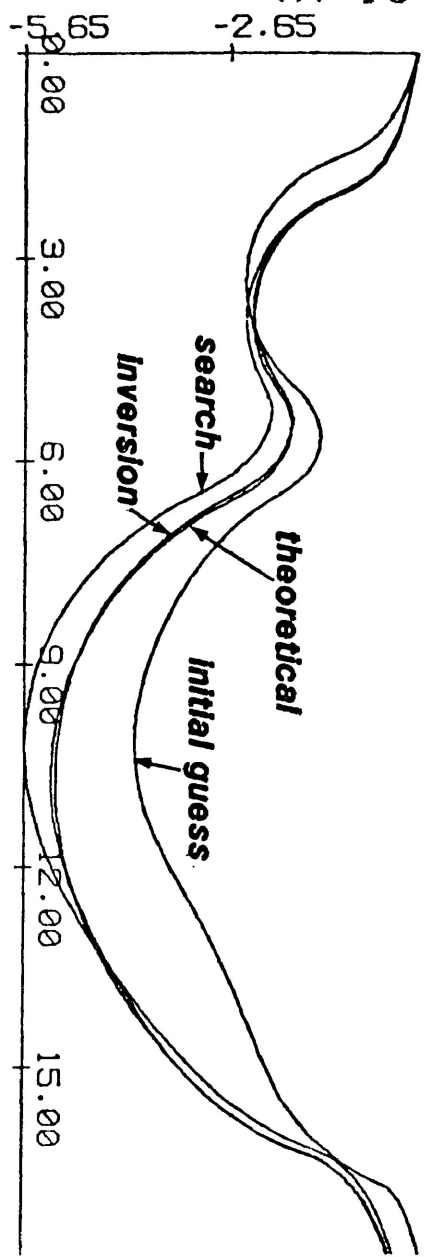


FIGURE 4 COMPARISON OF 3 PREVIOUS GRAVITY MODELS WITH THEORETICAL MODEL

OK, T
2'48 8'11 0'27
OK, COMD -END

: Time since LOGIN :
: explained below :

Note Time since LOGIN

2 hrs. 48 min. of connect time
8 min. 11 sec. of CPU time
0 min. 27 sec. of disc I/O time

Approx breakdown

STEP 3 (forward problem) = 17 sec. CPU time
STEP 4 (search) = 185 sec. CPU time
STEP 5 (inversion) = 160 sec. CPU time

SAMPLE TERMINAL SESSION #2

This terminal session uses a multiple-polygon model.

OK, T

4'06 2'54 0'28

OK, SLIST STATIONS. SOUTH

HILL SOUTH LINE

1

26

150)

-1. 16, . 15, 0. 0
-1. 90, . 30, 0. 0
-3. 17, . 61, 0. 0
-4. 56, . 91, 0. 0
-5. 91, 1. 22, 0. 0
-6. 40, 1. 37, 0. 0
-6. 88, 1. 52, 0. 0
-7. 83, 1. 83, 0. 0
-8. 59, 2. 13, 0. 0
-9. 01, 2. 29, 0. 0
-9. 41, 2. 44, 0. 0
-10. 22, 2. 74, 0. 0
-11. 03, 3. 05, 0. 0
-11. 42, 3. 20, 0. 0
-12. 07, 3. 50, 0. 0
-12. 50, 3. 81, 0. 0
-12. 76, 4. 12, 0. 0
-12. 81, 4. 27, 0. 0
-12. 83, 4. 57, 0. 0
-12. 71, 4. 88, 0. 0
-12. 47, 5. 18, 0. 0
-12. 22, 5. 49, 0. 0
-11. 83, 5. 79, 0. 0
-11. 49, 6. 10, 0. 0
-11. 27, 6. 40, 0. 0
-10. 99, 6. 71, 0. 0
-11. 00, 7. 01, 0. 0
-10. 96, 7. 16, 0. 0
-10. 95, 7. 31, 0. 0
-11. 01, 7. 62, 0. 0
-11. 27, 7. 93, 0. 0
-11. 51, 8. 23, 0. 0
-11. 70, 8. 53, 0. 0
-11. 82, 8. 84, 0. 0
-11. 97, 8. 99, 0. 0
-11. 91, 9. 14, 0. 0
-11. 91, 9. 30, 0. 0
-11. 82, 9. 60, 0. 0
-11. 78, 9. 75, 0. 0
-11. 75, 9. 91, 0. 0
-11. 79, 10. 21, 0. 0
-11. 89, 10. 52, 0. 0
-12. 07, 10. 67, 0. 0
-12. 49, 10. 97, 0. 0
-12. 83, 11. 12, 0. 0
-13. 34, 11. 28, 0. 0
-13. 53, 11. 43, 0. 0

-14.38, 11.74, 0.0
-14.85, 11.89, 0.0
-15.31, 12.04, 0.0
-15.81, 12.19, 0.0
-16.35, 12.34, 0.0
-16.88, 12.50, 0.0
-17.22, 12.65, 0.0
-17.99, 12.80, 0.0
-18.63, 12.95, 0.0
-19.25, 13.11, 0.0
-19.91, 13.26, 0.0
-20.60, 13.41, 0.0
-21.26, 13.56, 0.0
-21.94, 13.72, 0.0
-22.59, 13.87, 0.0
-23.28, 14.02, 0.0
-23.96, 14.17, 0.0
-24.68, 14.33, 0.0
-25.30, 14.48, 0.0
-26.01, 14.63, 0.0
-26.84, 14.78, 0.0
-27.39, 14.93, 0.0
-28.02, 15.09, 0.0
-28.55, 15.24, 0.0
-29.15, 15.39, 0.0
-29.67, 15.54, 0.0
-30.23, 15.70, 0.0
-30.76, 15.85, 0.0
-31.18, 16.00, 0.0
-31.68, 16.15, 0.0
-32.06, 16.31, 0.0
-32.46, 16.46, 0.0
-32.83, 16.61, 0.0
-33.15, 16.76, 0.0
-33.47, 16.92, 0.0
-33.78, 17.07, 0.0
-34.00, 17.22, 0.0
-34.26, 17.37, 0.0
-34.48, 17.53, 0.0
-34.65, 17.68, 0.0
-34.78, 17.83, 0.0
-34.86, 17.98, 0.0
-34.97, 18.14, 0.0
-35.03, 18.29, 0.0
-35.03, 18.44, 0.0
-35.11, 18.59, 0.0
-35.08, 18.74, 0.0
-34.98, 18.90, 0.0
-34.94, 19.05, 0.0
-34.84, 19.20, 0.0
-34.77, 19.36, 0.0
-34.68, 19.51, 0.0
-34.54, 19.66, 0.0
-34.34, 19.81, 0.0

-34.23, 19.96, 0.0
-34.14, 20.12, 0.0
-33.96, 20.27, 0.0
-33.77, 20.42, 0.0
-33.45, 20.57, 0.0
-33.08, 20.73, 0.0
-32.74, 20.88, 0.0
-32.51, 21.03, 0.0
-32.16, 21.28, 0.0
-31.94, 21.49, 0.0
-31.67, 21.64, 0.0
-31.32, 21.79, 0.0
-30.27, 22.25, 0.0
-29.88, 22.40, 0.0
-29.47, 22.56, 0.0
-29.07, 22.71, 0.0
-28.68, 22.86, 0.0
-28.22, 23.01, 0.0
-27.68, 23.16, 0.0
-27.18, 23.32, 0.0
-26.70, 23.47, 0.0
-26.16, 23.62, 0.0
-25.57, 23.77, 0.0
-24.95, 23.93, 0.0
-24.32, 24.08, 0.0
-23.79, 24.23, 0.0
-23.29, 24.38, 0.0
-22.80, 24.54, 0.0
-22.20, 24.69, 0.0
-21.59, 24.84, 0.0
-21.00, 24.99, 0.0
-20.39, 25.15, 0.0
-19.62, 25.30, 0.0
-18.89, 25.45, 0.0
-18.29, 25.61, 0.0
-17.55, 25.76, 0.0
-16.82, 25.92, 0.0
-15.71, 26.06, 0.0
-14.73, 26.18, 0.0
-13.76, 26.37, 0.0
-13.35, 26.52, 0.0
-12.95, 26.66, 0.0
-10.08, 27.58, 0.0
-8.46, 27.89, 0.0
-5.78, 28.13, 0.0
-4.22, 28.37, 0.0
-3.67, 28.54, 0.0
-2.76, 28.78, 0.0

OK, SLIST MODEL3

5

23, --, 50, 10., 10., 17

-2000., 0.000, 0, 0

2000., 0.000, 0, 0

2000. . . 001, 0, 0
 29. 200, . 001, 0, 0
 28. 660, . 3500, 1, 51
 28. 20, . 450, 0, 0
 28. 000, . 550, 0, 0
 27. 40, . 630, 0, 0
 26. 8, . 32, 0, 0
 24. 8, . 480, 0, 0
 24. 6, . 175, 0, 0
 20. 7, . 175, 0, 0
 20. 0, . 75, 0, 0
 16. 2, . 75, 0, 0
 15. 7, . 15, 0, 0
 13. 3, . 16, 0, 0
 12. 5, . 41, 0, 0
 -2000. . . 001, 0, 0
 -2000. . . 000, 0, 0
 29, -. 46, 10. , 10. , 18
 12. 5, . 41, 0, 0
 13. 3, . 160, 0, 0
 15. 7, . 150, 0, 0
 16. 2, . 75, 0, 0
 20. 0, . 75, 0, 0
 20. 7, . 175, 0, 0
 24. 6, . 175, 0, 0
 24. 8, . 480, 0, 0
 26. 8, . 320, 0, 0
 27. 400, . 630, 15, 16
 26. 800, . 950, 13, 14
 25. 60, . 950, 0, 0
 20. 6, . 950, 0, 0
 20. 2, 1. 30, 0, 0
 16. 2, 1. 3, 0, 0
 15. 8, . 85, 0, 0
 15. 00, . 650, 0, 0
 12. 80, . 650, 0, 0
 11. 300, . 750, 11, 8
 10. 850, . 750, 7, 8
 9. 200, . 850, 7, 8
 9. 000, . 950, 0, 0
 8. 100, . 900, 0, 0
 7. 700, . 780, 5, 6
 6. 000, . 860, 5, 6
 4. 400, 1. 18, 1, 4
 2. 950, . 970, 1, 4
 2. 150, . 750, 20, 30
 16, -. 42, 10. , 10. , 19
 11. 300, . 750, 11, 8
 12. 80, . 650, 0, 0
 15. 0, . 650, 0, 0
 15. 80, . 85, 0, 0
 16. 20, 1. 3, 0, 0
 20. 2, 1. 3, 0, 0
 20. 6, . 95, 0, 0

25. 600, . 950, 13, 14
 25. 200, 1. 55, 13, 14
 20. 8, 1. 55, 0, 0
 20. 4, 1. 75, 0, 0
 16. 4, 1. 75, 0, 0
 16. 0, 1. 45, 0, 0
 13. 500, 1. 350, 11, 12
 12. 8, . 90, 0, 0
 11. 30, . 900, 0, 0
 11. 30, . 750, 0, 0
 12, -. 39, 10. , 10. , 20
 13. 500, 1. 350, 11, 12
 16. 0, 1. 45, 0, 0
 16. 4, 1. 75, 0, 0
 20. 4, 1. 75, 0, 0
 20. 8, 1. 55, 0, 0
 25. 200, 1. 550, 13, 14
 23. 600, 1. 900, 13, 14
 21. 40, 2. 100, 0, 0
 21. 20, 2. 400, 0, 0
 16. 4, 2. 40, 0, 0
 16. 0, 2. 20, 0, 0
 14. 600, 2. 200, 11, 12
 13. 500, 1. 350, 11, 12
 9, -. 36, 10. , 10. , 21
 14. 6, 2. 20, 0, 0
 16. 0, 2. 20, 0, 0
 16. 400, 2. 400, 11, 12
 21. 20, 2. 400, 0, 0
 21. 40, 2. 10, 0, 0
 23. 600, 1. 900, 13, 14
 23. 500, 2. 3, 0, 0
 21. 300, 2. 800, 9, 10
 16. 600, 2. 900, 9, 10
 14. 600, 2. 200, 11, 12

OK, GRAV2D

TERMINL-OPTION # (I)= 3

*** GRAV2D MASTER ***

MASTER--OPTION # (I)= 2

INPUT WORK FILE HEADER (80 CHAR.)

EXAMPLE TWO

DO YOU WANT TO INPUT STATION DATA FROM FILE?

YES

INPUT FILENAME (16 CHAR)

STATIONS. SOUTH

INPUT PROFILE ID.

INPUT CODE FOR UNITS: 1 = KILOMETERS

2 = METERS

3 = KILOFEET

INPUT STATION NO. OR MATCH PT.

INPUT NO. OF STATIONS

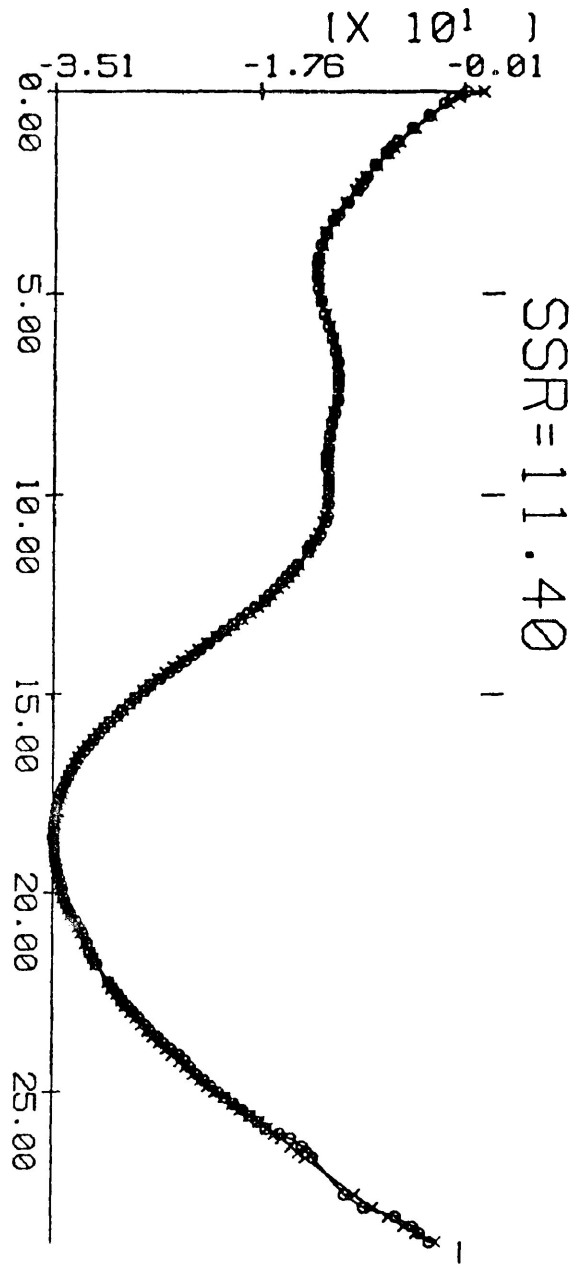
INPUT OBS. GRAVITY, DIST., ELEV. FOR 150 STATIONS

DO YOU WANT TO INPUT MODEL DATA FROM FILE?

```

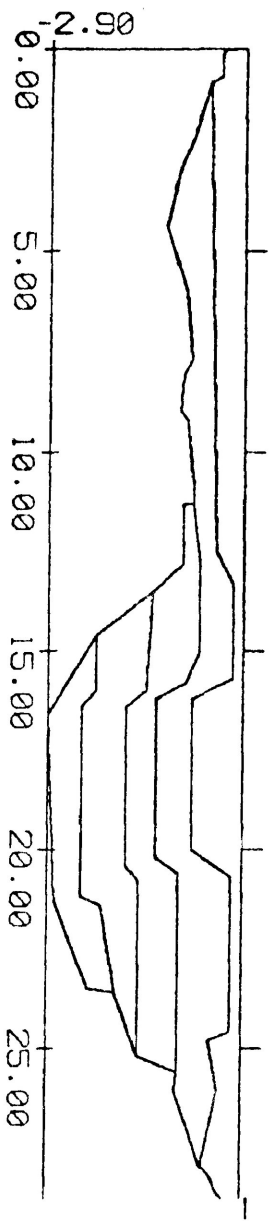
YES
INPUT FILENAME (16 CHAR)
MODEL3
INPUT NO. OF POLYGONS
FOR POLYGON 1 , INPUT:
# OF SIDES(I), DENSITY CONTRAST, STRIKE OUT, STRIKE IN, DENSITY SEARCH #(I)
FOR 24 VERTICES, INPUT:
HORZ. COORD., VERT. COORD., VERT. SEARCH #(I), HORZ. SEARCH #(I)
FOR POLYGON 2 , INPUT:
# OF SIDES(I), DENSITY CONTRAST, STRIKE OUT, STRIKE IN, DENSITY SEARCH #(I)
FOR 30 VERTICES, INPUT:
HORZ. COORD., VERT. COORD., VERT. SEARCH #(I), HORZ. SEARCH #(I)
FOR POLYGON 3 , INPUT:
# OF SIDES(I), DENSITY CONTRAST, STRIKE OUT, STRIKE IN, DENSITY SEARCH #(I)
FOR 17 VERTICES, INPUT:
HORZ. COORD., VERT. COORD., VERT. SEARCH #(I), HORZ. SEARCH #(I)
FOR POLYGON 4 , INPUT:
# OF SIDES(I), DENSITY CONTRAST, STRIKE OUT, STRIKE IN, DENSITY SEARCH #(I)
FOR 13 VERTICES, INPUT:
HORZ. COORD., VERT. COORD., VERT. SEARCH #(I), HORZ. SEARCH #(I)
FOR POLYGON 5 , INPUT:
# OF SIDES(I), DENSITY CONTRAST, STRIKE OUT, STRIKE IN, DENSITY SEARCH #(I)
FOR 10 VERTICES, INPUT:
HORZ. COORD., VERT. COORD., VERT. SEARCH #(I), HORZ. SEARCH #(I)
DO YOU WANT TO INPUT SEARCH DATA FROM FILE?
NO
INPUT # ITERATIONS FOR INVERSION
0
INPUT TOTAL # OF VERTEX SEARCH DIRECTIONS
0
INPUT TOTAL # OF DENSITY CONTRAST SEARCH DIRS.
0
INPUT HOR. SCALE, VER. SCALE(CURVES), VER. SCALE(MODEL)
5., 17.5, 3.
MASTER--OPTION # (I)= 5
XQT-----OPTION # (I)= 2
OUTPUT--OPTION # (I)= 1
THE TOTAL SUM OF SQUARES (SSR) = 11.402
0 SEARCHES LEFT
XQT-----OPTION # (I)= 1
MASTER--OPTION # (I)= 7
PLOT----OPTION # (I)= 2
*CURRENT MODEL PLOT*
DEVICE--OPTION # (I)= 2
# OF VECTORS= 3412
PLOT----OPTION # (I)= 1
MASTER--OPTION # (I)= 1

```



SSR = 11.40

ORIGINAL = O
NEW = X



POLYCON NO.	DENSITY CONTRAST
1	-0.50000
2	-0.46000
3	-0.42000
4	-0.39000
5	-0.36000

FIGURE 5 GRAVITY MODEL

REFERENCES

- Allis, R.G. and Garland, G.D.
 1979 Heat flow measurements under some lakes in the Superior Province of the Canadian Shield, Can. Jour. Earth Sc. Vol. 16, page 1951.
- Brisbin, W.C., and Green, A.G.
 1980 Gravity model of the Aulneau batholith, northwestern Ontario, Can. Jour. Earth Sc. Vol. 17, No. 8, page 968.
- Clendinning, W.
 1981 The geology of tectonism of Archean rocks of Burnt Island and vicinity, East Bay, Dog Lake, Ontario, unpubl. H.B.Sc. thesis, Lakehead University.
- Condie, K.
 1981 Archean Greenstone Belts, Vol. 3, Developments in Precambrian Geology, B.F. Windley, ad. ed. Elsevier Scientific Publ. Co.
- Dunlop, D.J.
 1979 A regional paleomagnetic study of Archean rocks from the Superior Geotraverse area, northwestern Ontario, Can. Jour. Earth Sc. Vol. 16, page 1906.
- Dusanowskyj, T.H., Barlow, R.B., and Wade, D.R.
 1975 Preliminary evaluation of the density control of a gravity survey of the Sturgeon Lake Metavolcanic Belt, Geotraverse Workshop paper no. 20.
- Earth Physics Branch, Dept. of Energy, Mines and Resources
 1970 Ignace-Fort William Gravity Map Series No. 83.
- Gibb, R.A.
 1968 The densities of Precambrian rocks from northern Manitoba, Can. Jour. Earth Sc. Vol. 13, page 433.
- Goodwin, A.M.
 1976 Geotraverse Models, Geotraverse Conference paper No. 35.
- Goodwin, A.M., and West, G.F.
 1975 The Superior Geotraverse Project, Geotraverse Workshop paper No. 1.
- Gupta, V.K., Thurston, P.C., and Dusanowskyj, T.H.
 1982 Constraints upon models of greenstone belt evolution by gravity modelling, Birch-Uchi greenstone belt, northern Ontario. Precambrian Res., 16: 233-255.

- Innes, M.J.S.
1960 Gravity and isostasy in northern Ontario and Manitoba. Publication of the Dominion Observatory, 21, No. 6.
- Kehlenbeck, M.M.
1976 Nature of the Quetico-Wabigoon boundary in the de Courcey-Smiley Lakes area, northwestern Ontario, Can. Jour. Earth Sc. Vol. 13, page 737.
- Kehlenbeck, M.M.
1977 The Barnum Lake Pluton, Thunder Bay, Ontario. Can. Jour. Earth Sc. Vol. 14, page 2157.
- Lehto, D.
1975 Structural and Petrological Evolution of the Quetico Gneiss Belt in the Dog-Hawkeye Lakes Area, unpubl. H.B.Sc. thesis, Lakehead University.
- MacDonald, R.D.
1939 Geology of Gorham Township and vicinity, Ontario Dept. of Mines 48th Annual Report, Vol. 48, Part 3.
- Mareschal, J.C. and West, G.F.
1980 A model for Archean tectonism. Part 2. Numerical models of vertical tectonism in greenstone belts. Can. Jour. Earth Sc. Vol. 17, page 60.
- Nutter, C.
1980 GRAV2D: An interactive 2½-Dimensional Gravity Modeling Program, publ. of Earth Science Laboratory, University of Utah Research Institute, Salt Lake City, Utah.
- Ontario Department of Mines
1970 Aeromagnetic Map Series, nos. 2096G, 2097G, 2098G, 2106G and 2108G.
- Perry, G.
1976 The relationship between metamorphism and the magnetic expression of rocks in a portion of the Quetico Gneiss Belt, Thunder Bay, Ontario, unpubl. H.B.Sc. thesis, Lakehead University.
- Pirie, J. and Mackasey, W.O.
1978 Preliminary examination of regional metamorphism in parts of the Quetico metasedimentary belt, Superior Province, Ontario, from Metamorphism in the Canadian Shield, Geological Survey Paper, 78-10, Pages 37 - 47.

- Pye, E.G. and Fenwick, K.
1965 Ontario Division of Mines Geological Compilation
Map Series No. 2065 Atikokan - Lakehead.
- Ramberg, H.
1967 Gravity, Deformation and the Earth's Crust
Academic Press, New York.
- Schwerdtner, W.M., Stone, D, Osadetz, K., Morgan, J., and
Stott, G.M.
1979 Granitoid complexes and the Archean tectonic
record in the southern part of northwestern
Ontario, Can. Jour. Earth Sc. Vol. 16, page 1965.
- Schwerdtner, W.M., and Lumbers, S.,
1980 Major diapiric structures in the Superior and
Grenville Provinces of the Canadian Shield
from The Continental Crust and its Mineral
Deposits. The Geological Association of Canada
Special Paper Number 20, page 149 ed. D.
Strangway.
- Shegelski, R. J.
1980 Archean cratonization, emergence and red bed
development, Lake Shebandowan area, Canada.
Precambrian Research, Vol.12, page 331.
- Stockwell, C.H.
1970 Intro. to Chapter IV; Geology of the Canadian
Shield: in Geology and Economic Minerals of
Canada, R. J. W. Douglas ed. Geol. Surv. Can.,
Econ. Geol. Rept. 1, 5th ed.
- Szewczyk, Z. J. and West, G.F.
1976 Gravity study of an Archean granitic area
northwest of Ignace, Ontario. Can. Jour. Earth
Sc. Vol. 13, page 1119.
- Tarling, D.H.
1980 Lithosphere evolution and changing tectonic
regimes. Journal of the Geological Society,
Vol. 137, Part 4, page 459.
- Telford, W., Geldart, L., Sheriff, R. and Keys, D.
1976 Applied Geophysics, Cambridge University Press,
Cambridge.

- Urquhart, W. and West, G.F.
1975 Linear aeromagnetic anomalies in the metasedimentary gneiss belt. Geotraverse Workshop, paper no. 23.
- West, G.F.
1980 Formation of continental crust, from The Continental Crust and Its Mineral Deposits, Page 117, The Geological Association of Canada Special Paper Number 20.
- West, G.F. and Mareschal, J.C.
1979 A model for Archean tectonism. Part 1. The thermal conditions, Vol. 16, page 1942, Canadian Journal of Earth Sciences.
- Windley, B.F.
1977 The Evolving Continents, publ. John Wiley and Sons, Ltd.
- Winkler, H.
1976 Petrogenesis of Metamorphic Rocks, publ. Springer - Verlag, New York.
- Woollard, G.P.
1979 The new gravity system - changes in international gravity base values and anomaly values. Geophysics, Vol. 44, No. 8, page 1352.

APPENDIX B ENVELOPE

2 $\frac{1}{2}$ -Dimensional GRAV2D Program Model Data Output

Profile A-A'	OUTPUTAA.DAT.1
Profile B-B'	OUTPUTBB.DAT.1
Profile C-C'	OUTPUTCC.DAT.1
Profile D-D'	OUTPUTDD.DAT.1
Profile E-E'	OUTPUTEE.DAT.1
Profile F-F'	OUTPUTFF.DAT.1

3-Dimensional GRAV3D Program Listing

GRAV3D.FOR.1

3-Dimensional GRAV3D Program Model Data Output

OUTPT3D.DAT.1

WORK FILE HEADER:

PAA

THE TOTAL SUM OF SQUARES IS
* THE STATION DATA *

46.661

PROFILE A-A'

UNITS OF DISTANCE IS KILOM
STATION # OR MATCH PT IS
THE TOTAL SUM OF SQUARES IS

1

46.661

COMPUTED

ELEVATION

OBSERVED

DIFFERENCE

OBS-COMP

STATION	TO STATION	DISTANCE	IS KILOM	OR MATCH PT IS	THE TOTAL SUM OF SQUARES IS	COMPUTED GRAVITY	OBSERVED GRAVITY	DIFFERENCE OBS-COMP
1	0.000	0.000	0.000	0.000	0.000	73.000	73.000	0.000
2	1.000	0.000	0.000	0.000	0.000	72.011	72.000	0.011
3	2.000	0.000	0.000	0.000	0.000	70.906	71.000	-0.094
4	3.000	0.000	0.000	0.000	0.000	69.814	70.000	-0.186
5	4.000	0.000	0.000	0.000	0.000	68.757	69.000	-0.243
6	5.000	0.000	0.000	0.000	0.000	67.744	68.000	-0.256
7	6.000	0.000	0.000	0.000	0.000	66.762	67.000	-0.238
8	7.000	0.000	0.000	0.000	0.000	65.787	66.000	-0.213
9	8.000	0.000	0.000	0.000	0.000	64.792	65.000	-0.208
10	9.000	0.000	0.000	0.000	0.000	63.752	64.000	-0.248
11	10.000	0.000	0.000	0.000	0.000	62.658	63.000	-0.342
12	11.000	0.000	0.000	0.000	0.000	61.516	62.000	-0.484
13	12.000	0.000	0.000	0.000	0.000	60.329	61.500	-0.671
14	13.000	0.000	0.000	0.000	0.000	59.077	59.500	-0.423
15	14.000	0.000	0.000	0.000	0.000	57.717	58.000	-0.277
16	15.000	0.000	0.000	0.000	0.000	56.223	56.600	-0.377
17	16.000	0.000	0.000	0.000	0.000	54.638	55.000	-0.362
18	17.000	0.000	0.000	0.000	0.000	53.105	53.800	-0.695
19	18.000	0.000	0.000	0.000	0.000	51.825	52.000	-0.175
20	19.000	0.000	0.000	0.000	0.000	50.992	50.600	0.392
21	20.000	0.000	0.000	0.000	0.000	50.738	47.600	3.138
22	21.000	0.000	0.000	0.000	0.000	51.130	48.500	2.630
23	22.000	0.000	0.000	0.000	0.000	52.230	50.000	2.230
24	23.000	0.000	0.000	0.000	0.000	54.045	54.500	-0.455
25	24.000	0.000	0.000	0.000	0.000	56.738	57.800	-1.062
26	25.000	0.000	0.000	0.000	0.000	58.856	57.800	1.056
27	26.000	0.000	0.000	0.000	0.000	59.888	59.200	0.688
28	27.000	0.000	0.000	0.000	0.000	60.561	60.300	0.261
29	28.000	0.000	0.000	0.000	0.000	61.044	61.400	-0.356
30	29.000	0.000	0.000	0.000	0.000	61.452	62.400	-0.948
31	30.000	0.000	0.000	0.000	0.000	62.262	62.400	-0.138
32	31.000	0.000	0.000	0.000	0.000	63.951	62.600	1.351
33	32.000	0.000	0.000	0.000	0.000	64.600	62.800	1.800
34	33.000	0.000	0.000	0.000	0.000	65.267	63.500	1.767
35	34.000	0.000	0.000	0.000	0.000	65.989	65.500	0.489
36	35.000	0.000	0.000	0.000	0.000	66.782	66.500	0.282
37	36.000	0.000	0.000	0.000	0.000	67.631	67.200	0.431
38	37.000	0.000	0.000	0.000	0.000	68.457	68.700	-0.243
39	38.000	0.000	0.000	0.000	0.000	69.122	68.300	0.822
40	39.000	0.000	0.000	0.000	0.000	69.574	69.000	0.574
41	40.000	0.000	0.000	0.000	0.000	69.932	70.200	-0.268
42	41.000	0.000	0.000	0.000	0.000	69.405	69.200	0.205
43	42.000	0.000	0.000	0.000	0.000	68.879	68.600	0.279
44	43.000	0.000	0.000	0.000	0.000	67.438	67.800	-0.362
45	44.000	0.000	0.000	0.000	0.000	67.133	66.500	0.633
46	45.000	0.000	0.000	0.000	0.000	66.999	66.500	0.499
47	46.000	0.000	0.000	0.000	0.000	66.666	66.500	0.166
48	47.000	0.000	0.000	0.000	0.000	66.666	66.500	0.166
49	48.000	0.000	0.000	0.000	0.000	66.666	66.500	0.166
50	49.000	0.000	0.000	0.000	0.000	66.666	66.500	0.166

51 0.000
52 0.000
53 0.000
54 0.000
55 0.000
56 0.000
57 0.000
58 0.000
59 0.000
60 0.000

-67.300
-67.600
-67.800
-68.300
-69.500
-70.000
-69.500
-68.800
-68.500

-67.149
-67.439
-67.828
-68.284
-68.776
-69.277
-69.771
-70.240
-70.673
-71.066

0.000
0.000
0.000
0.000
0.000
0.000
0.000
0.000
0.000
0.000

50.000
51.000
52.000
53.000
54.000
55.000
56.000
57.000
58.000
59.000

* MODEL DATA *

POLYGON NO. 1

DENSITY = 0.12000
STRIKE LENGTH 1 = 10.00000
STRIKE LENGTH 2 = 10.00000
SEARCH NO. = 0

X VERTICE	Z VERTICE	VERT. SEARCH NO.	HOR. SEARCH NO.
-100.000	0.000	0	0
0.000	0.000	0	0
24.000	0.000	0	0
24.000	0.500	0	0
20.000	1.000	1	0
15.000	1.000	1	0
10.000	1.000	1	0
5.000	1.500	1	0
0.000	0.010	0	0
-100.000	0.000	0	0

POLYGON NO. 2

DENSITY = 0.17000
STRIKE LENGTH 1 = 10.00000
STRIKE LENGTH 2 = 10.00000
SEARCH NO. = 0

X VERTICE	Z VERTICE	VERT. SEARCH NO.	HOR. SEARCH NO.
0.000	0.500	0	0
5.000	1.000	1	0
10.000	1.000	1	0
15.000	1.000	1	0
20.000	1.000	1	0
24.000	0.500	0	0
22.500	13.000	1	0
20.500	13.000	1	0
19.000	17.500	1	0
17.000	3.500	1	0
15.000	2.750	1	0
12.000	2.500	1	0
19.000	2.000	1	0
5.000	1.500	1	0
0.000	0.500	0	0

POLYGON NO. 3

DENSITY = 0.08000
STRIKE LENGTH 1 = 10.00000
STRIKE LENGTH 2 = 10.00000
SEARCH NO. = 0

X VERTICE	Z VERTICE	VERT. SEARCH NO.	HOR. SEARCH NO.
24.000	0.000	0	0
160.000	0.000	0	0
160.000	0.010	0	0
29.000	0.010	0	0

35.000
 37.000
 39.000
 37.000
 35.000
 32.500
 30.000
 27.000
 22.500
 24.000
 24.000

POLYGON NO. 4

DENSITY = 0.12000
 STRIKE LENGTH 1 = 10.00000
 STRIKE LENGTH 2 = 10.00000
 SEARCH NO. = 0

X	VERTICE	Z	VERTICE	VERT. SEARCH NO.	HOR. SEARCH	NO.
44.000	44.000	4.000	1	1	0	0
50.000	4.000	4.000	1	1	0	0
56.000	6.000	6.000	1	1	0	0
58.000	8.000	8.000	1	1	0	0
60.000	10.000	10.000	0	0	0	0
58.000	8.000	8.000	0	0	0	0
54.000	6.000	6.000	0	0	0	0
50.000	4.000	4.000	0	0	0	0
40.000	9.000	9.000	0	0	0	0
35.000	10.000	10.000	1	1	0	0
41.000	9.000	9.000	1	1	0	0
42.000	8.500	8.500	1	1	0	0
43.000	8.000	8.000	1	1	0	0
44.000	6.4.000	6.4.000	1	1	0	0

* SEARCH DATA *

NO. OF ITERATIONS FOR INVERSION IS 0
 TOTAL NO. OF VERTEX SEARCH DIRECTIONS IS 0
 TOTAL NO. OF DENSITY CONTRAST SEARCH DIRECTIONS IS 0
 * PLOT DATA *

HORIZONTAL SCALE (UNITS/INCH) = 1.00000
 VERTICAL SCALE FOR CURVES (MILLIGALS/INCH) = 1.00000
 VERTICAL SCALE FOR MODEL (UNITS/INCH) = 1.00000

WORK FILE HEADER:

23.941

PBB THE TOTAL SUM OF SQUARES IS THE STATION DATA *

PROFILE R H1 UNITS OF DISTANCE IS KILOM STATION # OR MATCH PT IS THE TOTAL SUM OF SQUARES IS TO STATION

23.941

STATION	DISTANCE	SQUARES	ELEVATION	COMPUTED GRAVITY
1	0.000	0.000	0.000	-72.000
2	1.000	1.000	0.000	-70.827
3	2.000	4.000	0.000	-69.200
4	3.000	9.000	0.000	-66.787
5	4.000	16.000	0.000	-63.518
6	5.000	25.000	0.000	-60.235
7	6.000	36.000	0.000	-57.233
8	7.000	49.000	0.000	-54.638
9	8.000	64.000	0.000	-52.518
10	9.000	81.000	0.000	-50.915
11	10.000	100.000	0.000	-49.803
12	11.000	121.000	0.000	-49.130
13	12.000	144.000	0.000	-48.820
14	13.000	169.000	0.000	-48.780
15	14.000	196.000	0.000	-48.914
16	15.000	225.000	0.000	-49.139
17	16.000	256.000	0.000	-49.402
18	17.000	289.000	0.000	-49.687
19	18.000	324.000	0.000	-49.025
20	19.000	361.000	0.000	-50.502
21	20.000	400.000	0.000	-51.275
22	21.000	441.000	0.000	-52.634
23	22.000	484.000	0.000	-55.134
24	23.000	529.000	0.000	-57.555
25	24.000	576.000	0.000	-58.926
26	25.000	625.000	0.000	-59.934
27	26.000	676.000	0.000	-61.037
28	27.000	729.000	0.000	-62.367
29	28.000	784.000	0.000	-64.068
30	29.000	841.000	0.000	-66.375
31	30.000	900.000	0.000	-67.821
32	31.000	961.000	0.000	-67.868
33	32.000	1024.000	0.000	-67.844
34	33.000	1089.000	0.000	-67.844
35	34.000	1156.000	0.000	-67.764
36	35.000	1225.000	0.000	-67.685
37	36.000	1296.000	0.000	-67.617
38	37.000	1369.000	0.000	-67.563
39	38.000	1444.000	0.000	-67.521
40	39.000	1521.000	0.000	-67.485
41	40.000	1600.000	0.000	-67.450
42	41.000	1681.000	0.000	-67.408
43	42.000	1764.000	0.000	-67.354
44	43.000	1849.000	0.000	-67.288
45	44.000	1936.000	0.000	-67.188
46	45.000	2025.000	0.000	-67.067
47	46.000	2116.000	0.000	-66.916
48	47.000	2209.000	0.000	-66.732
49	48.000	2304.000	0.000	-66.516
50	49.000	2401.000	0.000	-66.267

OBSERVED GRAVITY	DIFFERENCE
-72.000	0.000
-71.000	-0.173
-70.000	-0.800
-69.000	-0.213
-68.500	-0.982
-68.000	-0.265
-67.500	-0.768
-67.000	-0.818
-66.500	-0.215
-66.000	-0.003
-65.500	-0.570
-65.000	-0.780
-64.500	-0.720
-64.000	-0.486
-63.500	-0.361
-63.000	-0.198
-62.500	-0.133
-62.000	-0.225
-61.500	-0.602
-61.000	-0.775
-60.500	-0.105
-60.000	-0.134
-59.500	-0.230
-59.000	-0.355
-58.500	-0.926
-58.000	-0.466
-57.500	-1.433
-57.000	-0.432
-56.500	-1.175
-56.000	-1.821
-55.500	-1.368
-55.000	-0.698
-54.500	-0.344
-54.000	-0.036
-53.500	-0.515
-53.000	-0.837
-52.500	-0.437
-52.000	-0.315
-51.500	-0.250
-51.000	-0.146
-50.500	-0.117
-50.000	-0.112
-49.500	-0.133
-49.000	-0.184
-48.500	-0.268
-48.000	-0.203

51 0.000 0.000 -65.990 65.800 0.190
 52 1.000 0.000 -65.687 65.300 0.387
 53 2.000 0.000 -65.367 64.800 0.567
 54 3.000 0.000 -65.038 64.500 0.538
 55 4.000 0.000 -64.712 64.200 0.512
 56 5.000 0.000 -64.400 63.900 0.500
 57 6.000 0.000 -64.118 63.800 0.318
 58 7.000 0.000 -63.883 63.700 0.183
 59 8.000 0.000 -63.713 63.600 0.113
 60 9.000 0.000 -63.628 63.500 0.128

* MODEL DATA *

POLYGON NO. 1
 DENSITY = 0.12000
 STRIKE LENGTH 1 = 10.00000
 STRIKE LENGTH 2 = 10.00000
 SEARCH NO. = 0

Z VERTICE	VERT. SEARCH NO.	HOR. SEARCH NO.
0.000	0	0
0.000	0	0
0.000	0	0
0.500	0	0
0.500	0	0
0.500	0	0
0.010	0	0
0.000	0	0

POLYGON NO. 2
 DENSITY = 0.17000
 STRIKE LENGTH 1 = 10.00000
 STRIKE LENGTH 2 = 10.00000
 SEARCH NO. = 0

Z VERTICE	VERT. SEARCH NO.	HOR. SEARCH NO.
0.500	0	0
0.500	0	0
0.500	0	0
5.500	0	0
4.500	0	0
4.500	0	0
5.000	0	0
7.000	0	0
9.000	0	0
7.000	0	0
5.250	0	0
2.750	0	0
2.000	0	0
0.750	0	0
0.500	0	0

POLYGON NO. 3
 DENSITY = 0.08000
 STRIKE LENGTH 1 = 10.00000
 STRIKE LENGTH 2 = 10.00000
 SEARCH NO. = 0

Z VERTICE	VERT. SEARCH NO.	HOR. SEARCH NO.
0.000	0	0
0.000	0	0
0.010	0	0
0.250	0	0
1.000	0	0
2.500	0	0

26.000
 25.000
 24.000
 23.000
 21.000
 22.000
 22.000 4
 POLYGON NO.

4.500
 7.500
 6.750
 5.500
 0.500
 0.000
 DENSITY = 0.12000
 STRIKE LENGTH 1 = 10.00000
 STRIKE LENGTH 2 = 10.00000
 SEARCH NO. = 0

0
 0
 0
 0
 0
 0

X	VERTICE	Z	VERT. SEARCH NO.	HOR. SEARCH NO.
25.000	10.000	10.000	0	0
25.000	18.000	0	0	0
29.000	8.000	0	0	0
30.000	5.500	0	0	0
35.000	5.250	0	0	0
40.000	5.000	0	0	0
50.000	4.500	0	0	0
60.000	4.000	0	0	0
60.000	10.000	0	0	0
55.000	18.500	0	0	0
50.000	7.500	0	0	0
45.000	7.500	0	0	0
40.000	8.000	0	0	0
35.000	9.000	0	0	0
25.000	10.000	0	0	0

* SEARCH DATA *

NO. OF ITERATIONS FOR INVERSION IS 0
 TOTAL NO. OF VERTEX SEARCH DIRECTIONS IS 0
 TOTAL NO. OF DENSITY CONTRAST SEARCH DIRECTIONS IS 0
 * PLOT DATA *

HORIZONTAL SCALE (UNITS/INCH) = 0.00000
 VERTICAL SCALE FOR CURVES (MILLIGALS/INCH) = 0.00000
 VERTICAL SCALE FOR MODEL (UNITS/INCH) = 0.00000

51 0.000 0.000 -64.310 -63.700 0.610
 52 51.000 0.000 -63.865 -63.500 0.365
 53 52.000 0.000 -63.395 -63.200 0.195
 54 53.000 0.000 -62.900 -62.500 0.400
 55 54.000 0.000 -62.375 -61.800 0.575
 56 55.000 0.000 -61.813 -61.400 0.413
 57 56.000 0.000 -61.224 -60.800 0.424
 58 57.000 0.000 -60.657 -60.300 0.357
 59 58.000 0.000 -60.197 -59.900 0.297
 60 59.000 0.000 -59.930 -59.800 0.130

* MODEL DATA *

POLYGON NO. 1

DENSITY = 0.12000
 STRIKE LENGTH 1 = 10.00000
 STRIKE LENGTH 2 = 10.00000
 SEARCH NO. = 0

X VERTICE	Z VERTICE	VERT. SEARCH NO.	HOR. SEARCH NO.
-100.000	0.000	0	0
0.000	0.000	0	0
20.000	0.000	0	0
20.000	0.500	0	0
15.000	0.500	0	0
10.000	0.500	0	0
5.000	0.500	0	0
0.000	0.500	0	0
0.000	0.010	0	0
-100.000	0.010	0	0
-100.000	0.000	0	0

POLYGON NO. 2

DENSITY = 0.17000
 STRIKE LENGTH 1 = 10.00000
 STRIKE LENGTH 2 = 10.00000
 SEARCH NO. = 0

X VERTICE	Z VERTICE	VERT. SEARCH NO.	HOR. SEARCH NO.
0.000	0.500	0	0
5.000	0.500	0	0
10.000	0.500	0	0
15.000	0.500	0	0
20.000	0.500	0	0
18.000	1.500	0	0
16.500	2.500	0	0
15.000	6.500	0	0
13.000	7.000	0	0
11.000	6.500	0	0
9.000	5.500	0	0
7.000	4.500	0	0
5.000	2.500	0	0
3.500	0.800	0	0
1.500	0.600	0	0
0.000	0.500	0	0

POLYGON NO. 3

DENSITY = 0.08000
 STRIKE LENGTH 1 = 10.00000
 STRIKE LENGTH 2 = 10.00000
 SEARCH NO. = 0

X VERTICE	Z VERTICE	VERT. SEARCH NO.	HOR. SEARCH NO.
20.000	0.000	0	0
160.000	0.000	0	0
160.000	0.010	0	0
128.000	0.010	0	0

26.000
 24.000
 22.000
 20.000
 18.000
 20.000
 20.000
 POLYGON NO. 4

2.500
 3.000
 3.500
 2.500
 1.500
 0.500
 0.000
 DENSITY = 0.12000
 STRIKE LENGTH 1 = 10.00000
 STRIKE LENGTH 2 = 10.00000
 SEARCH NO. = 0

0
 0
 0
 0
 0
 0

X	Z	VERT. SEARCH NO.	HOR. SEARCH NO.
25.000	8.000	0	0
30.000	3.750	0	0
35.000	3.500	0	0
40.000	3.000	0	0
45.000	2.500	0	0
50.000	2.500	0	0
55.000	2.500	0	0
58.000	2.000	0	0
60.000	2.000	0	0
60.000	8.000	0	0
50.000	5.500	0	0
45.000	5.000	0	0
40.000	5.000	0	0
32.500	7.000	0	0
25.000	8.000	0	0

* SEARCH DATA *

NO. OF ITERATIONS FOR INVERSION IS 0
 TOTAL NO. OF VERTEX SEARCH DIRECTIONS IS 0
 TOTAL NO. OF DENSITY CONTRAST SEARCH DIRECTIONS IS 0
 * PLOT DATA *

HORIZONTAL SCALE (UNITS/INCH) = 0.00000
 VERTICAL SCALE FOR CURVES (MILLIGALS/INCH) = 0.00000
 VERTICAL SCALE FOR MODEL (UNITS/INCH) = 0.00000

WORK FILE HEADER:

22.111

POD THE TOTAL SUM OF SQUARES IS
* THE STATION DATA *

PROFILE D-D,
UNITS OF DISTANCE IS KILOM
STATION # OR MATCH PT IS
THE TOTAL SUM OF SQUARES IS
TO STATION DISTANCE IS
1

22.111

STATION	DISTANCE	SQUARES	ELEVATION	COMPUTED GRAVITY
1	0.000	0.000	0.000	-75.500
2	1.000	1.000	0.000	-75.250
3	2.000	4.000	0.000	-74.893
4	3.000	9.000	0.000	-74.361
5	4.000	16.000	0.000	-73.505
6	5.000	25.000	0.000	-71.914
7	6.000	36.000	0.000	-67.425
8	7.000	49.000	0.000	-62.057
9	8.000	64.000	0.000	-58.748
10	9.000	81.000	0.000	-56.498
11	10.000	100.000	0.000	-55.420
12	11.000	121.000	0.000	-55.701
13	12.000	144.000	0.000	-63.509
14	13.000	169.000	0.000	-62.403
15	14.000	196.000	0.000	-65.429
16	15.000	225.000	0.000	-68.706
17	16.000	256.000	0.000	-69.451
18	17.000	289.000	0.000	-68.944
19	18.000	324.000	0.000	-68.392
20	19.000	361.000	0.000	-68.930
21	20.000	400.000	0.000	-70.221
22	21.000	441.000	0.000	-72.466
23	22.000	484.000	0.000	-73.021
24	23.000	529.000	0.000	-73.373
25	24.000	576.000	0.000	-73.682
26	25.000	625.000	0.000	-73.979
27	26.000	676.000	0.000	-74.259
28	27.000	729.000	0.000	-74.531
29	28.000	784.000	0.000	-74.991
30	29.000	841.000	0.000	-74.408
31	30.000	900.000	0.000	-73.466
32	31.000	961.000	0.000	-69.552
33	32.000	1024.000	0.000	-68.422
34	33.000	1089.000	0.000	-67.024
35	34.000	1156.000	0.000	-66.983
36	35.000	1225.000	0.000	-65.371
37	36.000	1296.000	0.000	-64.710
38	37.000	1369.000	0.000	-63.143
39	38.000	1444.000	0.000	-63.742
40	39.000	1521.000	0.000	-63.467
41	40.000	1600.000	0.000	-63.263
42	41.000	1681.000	0.000	-63.092
43	42.000	1764.000	0.000	-62.930
44	43.000	1849.000	0.000	-62.760
45	44.000	1936.000	0.000	-62.567
46	45.000	2025.000	0.000	-62.350
47	46.000	2116.000	0.000	-62.110
48	47.000	2209.000	0.000	-61.850
49	48.000	2304.000	0.000	-61.570
50	49.000	2401.000	0.000	-61.270

OBSERVED GRAVITY	DIFFERENCE OBS-COMP
-75.500	0.000
-75.300	-0.200
-75.100	-0.400
-74.300	0.505
-73.000	0.914
-71.000	0.075
-63.000	0.943
-59.000	0.252
-55.500	0.998
-55.600	0.122
-57.500	-1.580
-60.000	-0.299
-62.500	1.009
-67.000	1.597
-69.000	1.571
-68.400	0.294
-67.600	1.051
-67.800	1.344
-68.000	0.592
-70.000	0.221
-71.400	1.066
-72.500	0.521
-73.300	0.073
-73.700	0.018
-74.200	0.221
-74.500	0.241
-74.900	0.369
-75.500	0.509
-74.000	0.408
-73.100	0.258
-69.600	0.468
-68.700	0.280
-68.300	0.678
-67.200	0.676
-66.000	0.688
-64.700	0.017
-63.900	0.671
-63.700	0.810
-63.600	0.443
-63.500	1.423
-63.300	0.037
-63.100	0.008
-62.800	0.160
-62.500	0.000

50.000 0.000 -62.335
 51.000 0.000 -62.348
 52.000 0.000 -61.685
 53.000 0.000 -61.239
 54.000 0.000 -60.726
 55.000 0.000 -60.173
 56.000 0.000 -59.606
 57.000 0.000 -59.029
 58.000 0.000 -58.529
 59.000 0.000 -58.078
 60.000 0.000 -57.600

-62.300
 -62.100
 -61.600
 -61.500
 -59.800
 -59.400
 -59.200
 -59.100

0.033
 -0.052
 0.085
 0.039
 0.226
 0.373
 0.206
 -0.150
 -0.571
 -0.922

* MODEL DATA *

POLYGON NO. 1

DENSITY = -0.03000
 STRIKE LENGTH 1 = 5.00000
 STRIKE LENGTH 2 = 5.00000
 SEARCH NO. = 0

X	VERTICE	Z	VERTICE	VERT. SEARCH NO.	HOR. SEARCH NO.
-10.000	0.000	0.000	0	0	0
0.000	0.000	0.000	0	0	0
6.000	0.010	0.000	0	0	0
6.000	1.500	0.000	0	0	0
7.000	1.500	0.000	0	0	0
8.000	2.000	0.000	0	0	0
9.000	7.000	0.000	0	0	0
7.000	5.000	0.000	0	0	0
5.000	3.000	0.000	0	0	0
-10.000	0.000	0.000	0	0	0
-10.000	0.000	0.000	0	0	0

POLYGON NO. 2

DENSITY = -0.05000
 STRIKE LENGTH 1 = 5.00000
 STRIKE LENGTH 2 = 5.00000
 SEARCH NO. = 0

X	VERTICE	Z	VERTICE	VERT. SEARCH NO.	HOR. SEARCH NO.
12.000	0.000	0.000	0	0	0
14.000	0.000	0.000	0	0	0
13.000	0.500	0.000	0	0	0
13.500	2.000	0.000	0	0	0
14.000	2.000	0.000	0	0	0
15.000	1.000	0.000	0	0	0
15.500	0.500	0.000	0	0	0
18.000	0.500	0.000	0	0	0
18.000	2.000	0.000	0	0	0
17.000	7.000	0.000	0	0	0
15.000	3.000	0.000	0	0	0
13.500	2.000	0.000	0	0	0
13.000	0.500	0.000	0	0	0
12.000	0.000	0.000	0	0	0
12.000	0.000	0.000	0	0	0

POLYGON NO. 3

DENSITY = 0.12000
 STRIKE LENGTH 1 = 5.00000
 STRIKE LENGTH 2 = 5.00000
 SEARCH NO. = 0

X	VERTICE	Z	VERTICE	VERT. SEARCH NO.	HOR. SEARCH NO.
0.000	0.000	0.000	0	0	0
6.000	0.000	0.000	0	0	0
12.000	0.000	0.000	0	0	0
6.000	0.500	0.000	0	0	0

0
0

0
0

0.010
0.000

POLYGON NO. 4

DENSITY = 0.17000
STRIKE LENGTH 1 = 5.00000
STRIKE LENGTH 2 = 5.00000
SEARCH NO. = 0

X VERTICE	Z VERTICE	VERT. SEARCH NO.	HOR. SEARCH NO.
14.000	0.000	0	0
18.000	0.000	0	0
18.000	0.500	0	0
15.000	0.500	0	0
14.000	1.000	0	0
13.500	2.000	0	0
13.000	0.500	0	0
14.000	0.000	0	0

POLYGON NO. 5

DENSITY = 0.17000
STRIKE LENGTH 1 = 5.00000
STRIKE LENGTH 2 = 5.00000
SEARCH NO. = 0

X VERTICE	Z VERTICE	VERT. SEARCH NO.	HOR. SEARCH NO.
6.000	0.500	0	0
12.000	0.500	0	0
13.000	2.000	0	0
11.000	3.000	0	0
10.000	8.000	0	0
9.000	9.000	0	0
8.000	8.500	0	0
7.000	1.500	0	0
6.000	1.000	0	0
6.000	0.500	0	0

POLYGON NO. 6

DENSITY = 0.08000
STRIKE LENGTH 1 = 5.00000
STRIKE LENGTH 2 = 5.00000
SEARCH NO. = 0

X VERTICE	Z VERTICE	VERT. SEARCH NO.	HOR. SEARCH NO.
18.000	0.000	0	0
20.500	0.000	0	0
20.500	2.000	0	0
22.000	4.000	0	0
24.000	4.000	0	0
26.000	5.000	0	0
27.000	7.500	0	0
20.000	6.000	0	0
18.000	2.000	0	0
18.000	0.500	0	0
18.000	0.000	0	0

POLYGON NO. 7

DENSITY = 0.17000
STRIKE LENGTH 1 = 5.00000
STRIKE LENGTH 2 = 5.00000
SEARCH NO. = 0

X VERTICE	Z VERTICE	VERT. SEARCH NO.	HOR. SEARCH NO.
20.500	0.000	0	0
21.000	0.000	0	0
20.500	2.000	0	0
20.000	0.000	0	0

POLYGON NO. 8

DENSITY = -0.02000
STRIKE LENGTH 1 = 4.00000
STRIKE LENGTH 2 = 4.00000
SEARCH NO. = 0

X VERTICE	Z VERTICE	VERT. SEARCH NO.	HOR. SEARCH NO.
21.000	0.000	0	0
29.000	0.000	0	0
27.000	7.500	0	0
26.000	5.000	0	0
24.000	4.000	0	0
22.000	4.000	0	0
20.500	2.000	0	0
21.000	0.000	0	0

POLYGON NO. 9

DENSITY = -0.04000
STRIKE LENGTH 1 = 5.00000
STRIKE LENGTH 2 = 5.00000
SEARCH NO. = 0

X VERTICE	Z VERTICE	VERT. SEARCH NO.	HOR. SEARCH NO.
29.000	0.000	0	0
33.000	0.000	0	0
33.000	5.000	0	0
31.500	7.000	0	0
30.000	9.000	0	0
27.000	7.500	0	0
29.000	0.000	0	0

POLYGON NO. 10

DENSITY = 0.12000
STRIKE LENGTH 1 = 10.00000
STRIKE LENGTH 2 = 10.00000
SEARCH NO. = 0

X VERTICE	Z VERTICE	VERT. SEARCH NO.	HOR. SEARCH NO.
30.000	9.000	0	0
33.000	5.000	0	0
33.500	3.500	0	0
37.000	3.500	0	0
40.000	3.000	0	0
41.000	2.000	0	0
52.000	2.000	0	0
60.000	1.500	0	0
160.000	19.000	0	0
160.000	6.000	0	0
52.000	4.500	0	0
39.000	4.500	0	0
38.000	5.500	0	0
33.500	6.500	0	0
33.000	8.000	0	0
30.000	9.000	0	0

* SEARCH DATA *

NO. OF ITERATIONS FOR INVERSION IS 0
TOTAL NO. OF VERTEX SEARCH DIRECTIONS IS 0
TOTAL NO. OF DENSITY CONTRAST SEARCH DIRECTIONS IS 0
* PLOT DATA *

HORIZONTAL SCALE (UNITS/INCH) = 0.00000
VERTICAL SCALE FOR CURVES (MILLIGALS/INCH) = 0.00000
VERTICAL SCALE FOR MODEL (UNITS/INCH) = 0.00000

WORK FILE HEADER:

29.468

THE TOTAL SUM OF SQUARES IS
* THE STATION DATA *

PROFILE E-E'
UNITS OF DISTANCE IS KILOM
STATION # OR MATCH PT IS
THE TOTAL SUM OF SQUARES IS
TO STATION DISTANCE

1

29.468

STATION	DISTANCE	ELEVATION	COMPUTED GRAVITY
1	0.000	0.000	-75.500
2	1.000	0.000	-75.440
3	2.000	0.000	-75.365
4	3.000	0.000	-75.269
5	4.000	0.000	-75.142
6	5.000	0.000	-74.967
7	6.000	0.000	-74.712
8	7.000	0.000	-74.307
9	8.000	0.000	-73.615
10	9.000	0.000	-72.644
11	10.000	0.000	-71.632
12	11.000	0.000	-70.508
13	12.000	0.000	-69.204
14	13.000	0.000	-67.894
15	14.000	0.000	-65.908
16	15.000	0.000	-63.784
17	16.000	0.000	-62.004
18	17.000	0.000	-61.173
19	18.000	0.000	-61.406
20	19.000	0.000	-62.923
21	20.000	0.000	-65.145
22	21.000	0.000	-66.729
23	22.000	0.000	-66.417
24	23.000	0.000	-65.364
25	24.000	0.000	-65.032
26	25.000	0.000	-65.371
27	26.000	0.000	-66.051
28	27.000	0.000	-67.352
29	28.000	0.000	-70.992
30	29.000	0.000	-68.737
31	30.000	0.000	-66.755
32	31.000	0.000	-67.842
33	32.000	0.000	-69.367
34	33.000	0.000	-69.615
35	34.000	0.000	-69.416
36	35.000	0.000	-68.914
37	36.000	0.000	-68.175
38	37.000	0.000	-67.251
39	38.000	0.000	-66.108
40	39.000	0.000	-65.140
41	40.000	0.000	-64.079
42	41.000	0.000	-62.287
43	42.000	0.000	-61.175
44	43.000	0.000	-60.451
45	44.000	0.000	-60.189
46	45.000	0.000	-60.189
47	46.000	0.000	-60.189
48	47.000	0.000	-60.189
49	48.000	0.000	-60.189
50	49.000	0.000	-60.189

OBSERVED GRAVITY
-75.500
-75.400
-75.300
-75.200
-75.100
-74.500
-73.500
-72.800
-72.300
-71.500
-70.800
-68.300
-65.500
-62.500
-60.500
-61.000
-63.000
-64.300
-65.600
-64.800
-64.700
-66.000
-66.500
-67.500
-69.000
-70.000
-67.800
-67.700
-68.500
-69.500
-69.500
-69.200
-68.600
-67.700
-66.500
-65.000
-63.200
-62.000
-61.200
-60.800
-60.500
-60.500

DIFFERENCE OBS-COMP
0.000
0.040
0.065
0.069
0.042
0.033
0.212
0.807
0.815
0.344
0.132
0.508
0.404
0.594
0.408
1.784
1.504
1.173
-1.594
-1.377
0.129
1.617
0.664
0.968
-1.829
-0.449
0.352
-1.292
0.937
0.945
0.658
0.167
0.115
0.084
0.286
0.425
0.449
0.297
0.108
0.840
0.579
0.288
0.067
0.025
0.024
0.149
0.131

STRIKE LENGTH 1 = 10.00000
STRIKE LENGTH 2 = 10.00000
SEARCH NO. = 0

Z VERTICE
0.000
0.000
2.000
2.000
5.000
6.000
5.000
1.500
1.000
0.500
0.000
0.000

HOR. SEARCH NO.
0
0
0
0
0
0
0
0
0
0
0
0

VERT. SEARCH NO.
0
0
0
0
0
0
0
0
0
0
0
0

DENSITY = -0.02000
STRIKE LENGTH 1 = 4.00000
STRIKE LENGTH 2 = 2.00000
SEARCH NO. = 0

X VERTICE
21.000
28.000
28.000
26.000
24.000
23.000
22.000
21.000
22.000
23.000
21.000
21.000

POLYGON NO. 5

Z VERTICE
0.000
0.000
2.000
6.000
6.000
2.000
0.000

HOR. SEARCH NO.
0
0
0
0
0
0
0

VERT. SEARCH NO.
0
0
0
0
0
0
0

DENSITY = 0.08000
STRIKE LENGTH 1 = 5.00000
STRIKE LENGTH 2 = 10.00000
SEARCH NO. = 0

X VERTICE
28.000
31.000
31.000
30.000
29.000
28.000
28.000

POLYGON NO. 6

Z VERTICE
0.000
0.000
3.000
6.000
6.000
2.000
0.000

HOR. SEARCH NO.
0
0
0
0
0
0
0

VERT. SEARCH NO.
0
0
0
0
0
0
0

DENSITY = 0.12000
STRIKE LENGTH 1 = 10.00000
STRIKE LENGTH 2 = 10.00000
SEARCH NO. = 0

X VERTICE
31.000
33.000
33.000
32.000
30.000
31.000
31.000

POLYGON NO. 7

Z VERTICE
9.000
7.000
5.000
3.000
2.000
1.500
1.000
0.000
8.000
6.500
6.500

HOR. SEARCH NO.
0
0
0
0
0
0
0
0
0
0
0

VERT. SEARCH NO.
0
0
0
0
0
0
0
0
0
0
0

X VERTICE
30.000
33.000
37.000
40.000
43.000
50.000
90.000
90.000
60.000
55.000
50.000

50.000
51.000
52.000
53.000
54.000
55.000
56.000
57.000
58.000
59.000
60.000

-59.985
-59.830
-59.700
-59.560
-59.375
-59.119
-58.779
-58.361
-57.887
-57.385

0.000
0.000
0.000
0.000
0.000
0.000
0.000
0.000
0.000
0.000
0.000

-60.400
-60.200
-60.100
-59.700
-59.400
-58.900
-58.200
-57.800
-57.600
-57.500

-0.415
-0.370
-0.400
-0.140
-0.025
0.219
0.579
0.561
0.287
-0.115

* MODEL DATA *

POLYGON NO. 1

DENSITY = -0.03000
STRIKE LENGTH 1 = 10.00000
STRIKE LENGTH 2 = 5.00000
SEARCH NO. = 0

X VERTICE
8.000
14.000
12.000
10.000
9.000
8.000

Z VERTICE
0.000
0.000
0.500
1.000
0.500
0.000

VERT. SEARCH NO.
0
0
0
0
0
0

HOR. SEARCH NO.
0
0
0
0
0
0

POLYGON NO. 2

DENSITY = 0.12000
STRIKE LENGTH 1 = 10.00000
STRIKE LENGTH 2 = 10.00000
SEARCH NO. = 0

X VERTICE
14.000
21.000
21.000
19.000
21.000
17.000
16.000
15.000
14.000
12.000
9.000
9.000
10.000
12.000
14.000

Z VERTICE
0.000
0.000
0.500
1.000
4.000
5.000
7.000
1.500
0.500
2.000
2.000
0.500
1.000
0.500
0.000

VERT. SEARCH NO.
0
0
0
0
0
0
0
0
0
0
0
0
0
0
0

HOR. SEARCH NO.
0
0
0
0
0
0
0
0
0
0
0
0
0
0
0

POLYGON NO. 3

DENSITY = -0.05000
STRIKE LENGTH 1 = 5.00000
STRIKE LENGTH 2 = 5.00000
SEARCH NO. = 0

X VERTICE
19.000
21.000
23.000
21.000
20.000
19.000

Z VERTICE
1.000
0.500
1.500
2.000
5.000
1.000

VERT. SEARCH NO.
0
0
0
0
0
0

HOR. SEARCH NO.
0
0
0
0
0
0

POLYGON NO. 4

DENSITY = 0.08000

0
0
0

0
0
0

6.000
6.000
9.000
9.000

40.000
36.000
33.000
30.000

* SEARCH DATA *

NO. OF ITERATIONS FOR INVERSION IS 0
TOTAL NO. OF VERTEX SEARCH DIRECTIONS IS 0
TOTAL NO. OF DENSITY CONTRAST SEARCH DIRECTIONS IS 0
* PLOT DATA *

HORIZONTAL SCALE (UNITS/INCH) = 0.00000
VERTICAL SCALE FOR CURVES (MILLIGALS/INCH) = 0.00000
VERTICAL SCALE FOR MODEL (UNITS/INCH) = 0.00000

WORK FILE HEADER:

22.806

FF THE TOTAL SUM OF SQUARES IS
* STATION DATA *

PROFILE F-F'
UNITS OF DISTANCE IS KILOM
STATION # OR MATCH PT IS
THE TOTAL SUM OF SQUARES IS

22.806

STATION	DISTANCE TO STATION	ELEVATION	COMPUTED GRAVITY
1	0.000	0.000	-75.500
2	1.000	0.000	-75.376
3	2.000	0.000	-75.213
4	3.000	0.000	-74.993
5	4.000	0.000	-74.690
6	5.000	0.000	-74.257
7	6.000	0.000	-73.621
8	7.000	0.000	-72.683
9	8.000	0.000	-71.384
10	9.000	0.000	-69.840
11	10.000	0.000	-68.236
12	11.000	0.000	-66.541
13	12.000	0.000	-63.531
14	13.000	0.000	-60.734
15	14.000	0.000	-59.528
16	15.000	0.000	-58.596
17	16.000	0.000	-57.898
18	17.000	0.000	-57.580
19	18.000	0.000	-57.003
20	19.000	0.000	-61.266
21	20.000	0.000	-65.043
22	21.000	0.000	-65.621
23	22.000	0.000	-65.481
24	23.000	0.000	-65.757
25	24.000	0.000	-65.457
26	25.000	0.000	-65.449
27	26.000	0.000	-66.314
28	27.000	0.000	-67.853
29	28.000	0.000	-68.119
30	29.000	0.000	-68.188
31	30.000	0.000	-68.115
32	31.000	0.000	-68.944
33	32.000	0.000	-67.745
34	33.000	0.000	-67.675
35	34.000	0.000	-67.994
36	35.000	0.000	-69.058
37	36.000	0.000	-68.743
38	37.000	0.000	-67.690
39	38.000	0.000	-66.552
40	39.000	0.000	-64.366
41	40.000	0.000	-63.153
42	41.000	0.000	-61.724
43	42.000	0.000	-59.604
44	43.000	0.000	-58.568
45	44.000	0.000	-57.528
46	45.000	0.000	-56.276
47	46.000	0.000	-56.000
48	47.000	0.000	-56.000
49	48.000	0.000	-56.000
50	49.000	0.000	-56.000

OBSERVED GRAVITY
-75.500
-75.400
-75.300
-75.200
-75.100
-74.300
-73.200
-72.800
-70.340
-69.500
-67.400
-64.000
-61.500
-59.300
-57.500
-57.700
-57.800
-60.000
-62.800
-63.800
-64.500
-65.000
-65.800
-65.600
-66.400
-67.900
-68.500
-68.500
-68.000
-67.000
-67.900
-69.200
-69.600
-69.200
-68.000
-66.500
-65.000
-63.500
-62.500
-61.800
-59.700
-58.800
-57.500
-56.000

DIFFERENCE OBS-COMP
0.000
-0.024
-0.087
-0.207
-0.410
-0.043
0.683
0.584
0.340
0.436
0.141
-0.469
-0.766
0.228
1.302
-0.120
0.203
1.266
1.243
1.821
0.981
0.757
0.078
-0.343
-0.151
-0.086
-0.047
-0.381
0.312
0.115
0.944
0.745
0.226
-1.206
-0.542
-0.564
-0.190
0.152
0.866
0.653
0.327
-0.076
-0.096
-0.232
-0.610
-0.772
-0.624

50.000 0.000 -56.050 -56.500 -0.450
 51.000 0.000 -55.905 -56.000 -0.095
 52.000 0.000 -55.816 -56.100 -0.284
 53.000 0.000 -55.863 -56.200 -0.337
 54.000 0.000 -55.923 -56.000 -0.077
 55.000 0.000 -55.949 -56.900 -0.049
 56.000 0.000 -55.926 -55.800 -0.126
 57.000 0.000 -55.855 -55.700 -0.155
 58.000 0.000 -55.744 -55.600 -0.144
 59.000 0.000 -55.610 -55.500 -0.110
 60.000 0.000 -55.610 -55.500 -0.110

* MODEL DATA *

POLYGON NO. 1
 DENSITY = 0.12000
 STRIKE LENGTH 1 = 10.00000
 STRIKE LENGTH 2 = 10.00000
 SEARCH NO. = 0
 Z VERTICE VERT. SEARCH NO. HOR. SEARCH NO. POLYGON NO.
 -100.000 0.000 0 0
 12.000 0.000 0 0
 19.000 0.000 0 0
 19.000 1.000 0 0
 12.000 1.000 0 0
 12.000 0.010 0 0
 -100.000 0.000 0 0

POLYGON NO. 2
 DENSITY = 0.12000
 STRIKE LENGTH 1 = 10.00000
 STRIKE LENGTH 2 = 10.00000
 SEARCH NO. = 0
 Z VERTICE VERT. SEARCH NO. HOR. SEARCH NO. POLYGON NO.
 12.000 1.000 0 0
 19.000 0.500 0 0
 21.000 5.000 0 0
 22.000 6.000 0 0
 19.000 5.000 0 0
 16.000 5.500 0 0
 14.000 3.000 0 0
 10.000 4.000 0 0
 8.000 3.000 0 0
 10.000 2.000 0 0
 12.000 1.500 0 0
 12.000 1.000 0 0

POLYGON NO. 3
 DENSITY = -0.03000
 STRIKE LENGTH 1 = 10.00000
 STRIKE LENGTH 2 = 10.00000
 SEARCH NO. = 0
 Z VERTICE VERT. SEARCH NO. HOR. SEARCH NO. POLYGON NO.
 19.000 0.000 0 0
 24.000 0.000 0 0
 21.000 0.500 0 0
 19.000 0.500 0 0
 19.000 0.000 0 0

POLYGON NO. 4
 DENSITY = 0.08000
 STRIKE LENGTH 1 = 10.00000
 STRIKE LENGTH 2 = 10.00000
 SEARCH NO. = 0
 Z VERTICE VERT. SEARCH NO. HOR. SEARCH NO. POLYGON NO.
 19.000 0.000 0 0
 24.000 0.000 0 0
 21.000 0.500 0 0
 19.000 0.500 0 0
 19.000 0.000 0 0

24.000
 36.000
 34.000
 32.000
 26.000
 24.000
 22.000
 21.000
 21.000
 24.000
 24.000
 24.000 5
 POLYGON NO.

0.000
 0.000
 1.500
 1.500
 5.000
 6.000
 4.000
 0.500
 0.500
 0.000
 0.000
 0.12000
 DENSITY =
 STRIKE LENGTH 1 = 10.00000
 STRIKE LENGTH 2 = 10.00000
 SEARCH NO. = 0

X	VERTICE	Z	VERTICE	VERT. SEARCH NO.	HOR. SEARCH	NO.
30.000	8.000	8.000	0	0	0	0
35.000	6.500	6.500	0	0	0	0
39.000	3.500	3.500	0	0	0	0
44.000	1.500	1.500	0	0	0	0
46.000	1.000	1.000	0	0	0	0
48.000	0.250	0.250	0	0	0	0
52.000	0.100	0.100	0	0	0	0
60.000	8.000	8.000	0	0	0	0
160.000	5.000	5.000	0	0	0	0
55.000	4.500	4.500	0	0	0	0
50.000	5.500	5.500	0	0	0	0
45.000	6.000	6.000	0	0	0	0
39.000	7.500	7.500	0	0	0	0
35.000	8.000	8.000	0	0	0	0
30.000						

* SEARCH DATA *

NO. OF ITERATIONS FOR INVERSION IS 0
 TOTAL NO. OF VERTEX SEARCH DIRECTIONS IS 0
 TOTAL NO. OF DENSITY CONTRAST SEARCH DIRECTIONS IS 0
 * PLOT DATA *

HORIZONTAL SCALE (UNITS/INCH) = 0.00000
 VERTICAL SCALE FOR CURVES (MILLIGALS/INCH) = 0.00000
 VERTICAL SCALE FOR MODEL (UNITS/INCH) = 0.00000

```

*****ALGORITHM WRITTEN BY Y. LAMONTAGNE.
THIS PROGRAM CALCULATES
A GRAVITY PROFILE ALONG ANY SPECIFIED LINE OF OBSERVATION POINTS.
THE LOCATION OF THE PROFILE IS SPECIFIED BY THE STARTING POINT AND THE
ANGLE BETWEEN THE LINE OF OBSERVATIONS AND THE X AXIS. THE SPACING
BETWEEN OBSERVATION POINTS IS ALSO SPECIFIED. THE MASS IS MADE UP OF
LAYERS, WITH EACH LAYER BEING SPECIFIED BY AN UPPER AND LOWER DEPTH, AND
A POLYGONAL OUTLINE.
THE POLYGON IS SPECIFIED BY INPUTTING THE (X,Y) CO-ORDINATES OF EACH
OF THE VERTICES, IN A CLOCKWISE ORDER.
THE DESIRED PROFILE IS ALSO READ IN, AND IS OUTPUT WITH THE CALCULATE4D
RESPONSE, ALONG WITH THE DIFFERENCES. THE DIFFERENCES, WITH THE MEAN
REMOVED, ARE ALSO LISTED, ALONG WITH THE MEAN AND THE R.M.S. OF THE
DIFFERENCES (WITH MEAN REMOVED).
SAME AS JONES 3D INTEGRATION CONSTANT NECESSARY.
DIMENSION NVTCS(70), X(20,70), Y(20,70), GRAV(60), GRV(60), GDIFF(60),
*ADENS(70), XORS(60), YOBS(60), H1(70), H2(70), GDIFF2(60)
REAL UNIT(12), CFAK(6)
DATA UNIT(1,CM), (2,M), (3,MET), (4,ERS), (5,KM), (6,FEET), (7, )
*(YAR,IDS) 1,0,1.0E2,1.0E5,30.48006, 91.44018, 1.609347 E5 /
REAL CFAK / 1,0,1.0E2,1.0E5,30.48006, 91.44018, 1.609347 E5 /
REAL YPLT(60,CHAR(2))
DIMENSION XCHAR(1,1,1,1,1,1)
DATA XCHAR(1,1,1,1,1,1)
INTEGER NXIN(36)
READ(5,41) BSL
FORMAT(F10.0)
READ(5,42) IUNIT, NP
FORMAT(I2,1X,I2)
CUNIT=6.70E-5*CFAK(IUNIT)
RECORDING OF GEOLOGICAL CONTACTS
DO 4 J=1,NP
READ(5,43) NVTCS(J), H1(J), H2(J), ADENS(J)
FORMAT(I3,T10,F8.0,T20,F8.0,T30,F8.0)
NVT=NVTCS(J)
READ(5,44) X(1,J), Y(1,J), I=1, NVT)
FORMAT(F6F5.0)
DO 4 I=1,NVT
X(I,J)=X(1,J)+0.0
CONTINUE
READ(5,*) INPRF
IF(NP.GT.0) GO TO 4444
DO 445 I=1,N0
GRAV(I)=0.
CONTINUE
READ(5,46) N0, DSPC, DANG, DXST, DYST
FORMAT(I3,T10,F8.0,T20,F8.0,T30,F8.2,T40,F8.2)
READ(5,47) (GRAV(I), I=1, N0)
FORMAT(F6F5.1)
DO 55 I=1,N0
GRAV(I)=GRAV(I)-BSL
DTHETA=DANG*3.14159265/180.
DSPCY=DSPC*COS(DTHETA)
DSPCY=DSPC*SIN(DTHETA)
DO 5 N=1,N0
GRV(N)=0.
CONTINUE
DO 6 J=1,NP
X(NVTCS(J)+1,J)=X(1,J)
Y(NVTCS(J)+1,J)=Y(1,J)

```

CCCCCCCCCCCCCCCC

C

44

4

4444
4444

46

47

55

5


```

HH1=H1(J)*H1(J)
HH2=H2(J)*H2(J)
NVT=NVTC(S(J))
DO 6 I=1,NVT
DX=X(I+1,J)-X(I,J)
DY=Y(I+1,J)-Y(I,J)
R=SSQRT(DX*DX+DY*DY)
AL=DX/R
RE=-DX/R
DO 6 N=1,NO
XX=DXST+DSPCX*FLOAT(N-1)
YY=DYST+DSPCY*FLOAT(N-1)
XORS(N)=XX
YORS(N)=YY
G=0
EX=X(I,J)
EX=X(I+1,J)-XX
FY=Y(I+1,J)-YY
F=-BE*EX+AL*FY
D=AL*EX+RE*FY
AD=ABS(D)
IF(AD.LT.1.F-10)GO TO 8
F=RE*FX-AL*FY
F2=EE
D2=DD
F2=FF*F
R11=SSQRT(E2+D2+HH1)+1.E-20
R12=SSQRT(E2+D2+HH2)+1.E-20
R21=SSQRT(F2+D2+HH1)+1.E-20
R22=SSQRT(F2+D2+HH2)+1.E-20
TN11=D*E*(R11-H1(J))
TD11=(E2*H1(J)+D2*JR11)
TN12=D*E*(R12-H2(J))
TD12=(E2*H2(J)+D2*JR12)
TN21=D*F*(R21-H1(J))
TD21=F2*H1(J)+D2*JR21
TN22=D*F*(R22-H2(J))
TD22=F2*H2(J)+D2*JR22
WN1=TD11*TD21+TN11*TN21
WN2=TN12*TD22+TN12*TN22
WD2=TD12*TD22+TN12*TN22
W1=ATAN2(WN1,WD1)
W2=ATAN2(WN2,WD2)
CHK=((E+R11)+1.E-20)*((F+R22)+1.E-20)/((F+R21)+1.E-20)*((E+R12)
*+1.E-20)
IF(CHK.GT.0.)GO TO 113
CHK=1.
GO TO 66
G=0
CONTINUE
GRV(N)=GRV(N)+G*CVT*ADENS(J)
DO 9 N=1,NO
GDIF(N)=GRV(N)-GRV(N)
CONTINUE
IF(NO.EQ.1)GO TO 11
SUMDI=0
DO 10 N=1,NO

```

113
8
66
6
9

```

10 SUMDIFF=SUMDTF+GDIFF(N)
AVDIFF=SUMDTF/NO
DO 12 N=1,NO
GDIF2(N)=GDIF(N)-AVDIFF
STD=GDIF2(N)*GDIF2(N)+STD
STD=(STD/(NO-1))**.5
CONTINUE
IU1=2*IUNIT-1
IU2=2*IUNIT
IF(INPRF.EQ.1) GO TO 132 UNIT(IU2)
WRITE(6,897) UNIT(IU1)
FORMAT(1H1, 'ALL DISTANCES HAVE UNITS ',2A4)
132 CONTINUE
IF(INPRF.GT.1) GO TO 131
WRITE(6,898)
FORMAT(' LAYER',T10,' DENSITY',T20,' DEPTH TO TOP',T35,' DEPTH TO RD
*TTOM',T90,' VERTICES')
DO 13 J=1,NP
WRITE(6,899) J,ADENS(J),H1(J),H2(J),X(I,J),Y(I,J) I=1,2)
FORMAT(/,T2,I3,T9,F7.3,T18,F15.7,T34,F11.4,/,F11.4,5X
*,F11.4,F11.4)
NVT=NVC(J)
DO 14 KI=3,NVT,2
KK=KI+1
IF(KK.GT.NVT)KK=KI
WRITE(6,900)(X(I,J),Y(I,J),I=KI,KK)
CONTINUE
FORMAT(' T81,F11.4,',F11.4,5X,F11.4,',',F11.4)
14 CONTINUE
WRITE(6,1000)
FORMAT(/, 'ORSERVATION COORDINATES',T35 'MODEL RESPONSE',T65,'D
*ESIRE RESPONSE',T90,'DIFFERENCE',T112,'DIFFERENCE')
WRITE(6,1001) UNIT(IU1),UNIT(IU2)
FORMAT(' T7,2A4,T36,'(MILLIGALS)',T67,'(MILLIGALS)',T89,'(MILLIGALS
*)',T109,'(AVERAGE REMOVED)',/)
WRITE(6,2000)(XOBS(I),YOBS(I),GRV(I),GRV(I),GDIFF(I),GDIFF2(I),I
=1,NO)
FORMAT(T2,F10.3,T15,F10.3,T38,F8.3,T69,F8.3,T92,F8.4,T114,F8.4)
2000 WRITE(6,2002) AVDIFF,STD
FORMAT(/,/, ' THE AVERAGE OF THE DIFFERENCES IS ',F8.4, ' AND THE
* R.M.S. OF THE DIFFERENCES (WITH MEAN REMOVED) IS ',F8.4)
CALL PREP(GRV,GRAV,NO,YPLT,XCHAR)
READ(5,*) INPRF
IF(INPRF.NE.0) GO TO 4444
END
SUBROUTINE PREP(GRV,GRAV,NO,YPLT,XCHAR)
DIMENSION GRV(NO),GRAV(NO),YPLT(NO,2)
DO 66 I=1,NO
YPLT(I,1)=GRAV(I)
YPLT(I,2)=GRV(I)
CONTINUE
CALL SKETCH(YPLT,XCHAR,NO,2)
RETURN
END
SUBROUTINE SKETCH(Y,X,M,N)
THIS SUBROUTINE PLOTS N(NUMBER) PROFILES EACH HAVING 'M' DATA POINTS
X(1),X(2),...,X(N) IS SYMBOL ASSIGNED FOR EACH PROFILE. ARRAY VALUES
C ARE STORED IN MATRIX Y(M,N)

```


ALL DISTANCES HAVE UNITS (KM.)

OBSERVATION (KM.)	COORDINATES	MODEL RESPONSE (MILLIGALS)	DESIRED RESPONSE (MILLIGALS)	DIFFERENCE (MILLIGALS)	DIFFERENCE (AVERAGE REMOVED)
7.500	12.750	15.262	15.000	-0.2624	0.5433
8.440	13.092	16.821	17.400	0.5785	1.3842
9.379	13.434	18.472	19.500	1.0283	1.8340
10.319	13.776	20.109	22.400	2.2914	3.0971
11.259	14.118	21.614	24.500	2.8864	3.6921
12.198	14.460	22.880	25.200	2.3196	3.1253
13.138	14.802	23.871	25.300	1.4292	2.2349
14.078	15.144	24.589	25.400	0.8106	1.6163
15.018	15.486	25.055	25.500	0.4454	1.2511
15.957	15.828	25.288	25.400	0.1125	0.9182
16.897	16.170	25.300	25.300	0.0001	0.8058
17.837	16.512	25.086	25.200	0.1141	0.9198
18.776	16.854	24.610	25.100	0.4900	1.2958
19.716	17.196	23.865	24.700	0.8349	1.6406
20.656	17.538	22.830	24.100	1.2698	2.0755
21.595	17.880	21.522	22.500	0.9783	1.7840
22.535	18.222	20.025	20.800	0.7754	1.5811
23.475	18.564	18.454	19.300	0.8455	1.6513
24.414	18.906	16.872	18.000	1.1279	1.9336
25.354	19.248	15.073	16.500	1.4269	2.2326
26.294	19.590	13.756	15.000	1.2437	2.0494
27.234	19.932	12.978	13.000	0.0219	0.8276
28.173	20.274	12.450	10.200	-2.2497	-1.4440
29.113	20.616	12.073	8.800	-3.2734	-2.4677
30.053	20.958	11.786	8.700	-3.0858	-2.2801
30.992	21.301	11.541	8.600	-2.9411	-2.1354
31.932	21.643	11.320	8.500	-2.8199	-2.0142
32.872	21.985	11.102	8.400	-2.7020	-1.8963
33.811	22.327	10.872	8.300	-2.5717	-1.7660
34.751	22.669	10.611	8.200	-2.4115	-1.6057
35.691	23.011	10.291	8.000	-2.2910	-1.4853
36.630	23.353	9.850	7.000	-2.8498	-2.0441
37.570	23.695	9.143	6.000	-3.1426	-2.3369
38.510	24.037	7.757	5.000	-2.7574	-1.9517
39.450	24.379	4.278	3.000	-1.2784	-0.4727
40.389	24.721	2.807	2.500	-0.3074	0.4983
41.329	25.063	2.158	1.700	-0.4580	0.3477
42.269	25.405	1.837	1.200	-0.6374	0.1683
43.208	25.747	1.707	0.500	-1.2075	-0.4018
44.148	26.089	1.742	-0.200	-1.9424	-1.1367
45.088	26.431	1.995	1.500	-0.4951	0.3107
46.027	26.773	2.663	2.300	-0.3627	0.4431
46.967	27.115	4.704	2.700	-2.0042	-1.1985
47.907	27.457	7.023	3.500	-3.5234	-2.7177
48.846	27.799	7.589	4.500	-3.0893	-2.2836
49.786	28.141	7.783	5.200	-2.5832	-1.7775
50.726	28.483	7.788	5.500	-2.2877	-1.4820
51.666	28.825	7.314	5.200	-2.1142	-1.3085
52.605	29.167	4.896	4.500	-0.3959	0.4098
53.545	29.509	4.367	2.500	-1.8665	-1.0608
54.485	29.851	4.484	5.000	0.5158	1.3215
55.424	30.193	5.031	6.000	0.9692	1.7749
56.364	30.535	6.626	6.200	-0.4262	-0.3795
57.304	30.877	8.761	6.500	-2.2608	-1.4550

*
+

*
+

*
+

*

*

*

*

*

*

*

*

*

*

*

*

+

*

+

++

++

17 ..

18 ..

19 ..

20 ..

21 ..

22 ..

23 ..

24 ..

25 ..

26 ..

27 ..

28 ..

29 ..

30 ..

31 ..

32 ..

33 ..

34 ..

35 ..

36 ..

37 ..

38 .. * +

39 ..*

40 *.

41 .. * +

42 .. **

43 .. *

44 .. *

45 .. ?

46 .. *

47 .. *

48 .. ?

49 .. **

50 ..

51 .. + *

52 .. + *

53 .. * +

54 .. *

55 .. *

56 .. ?

57 .. * +

58

..

*

+

59

..

*

+

60

..

*

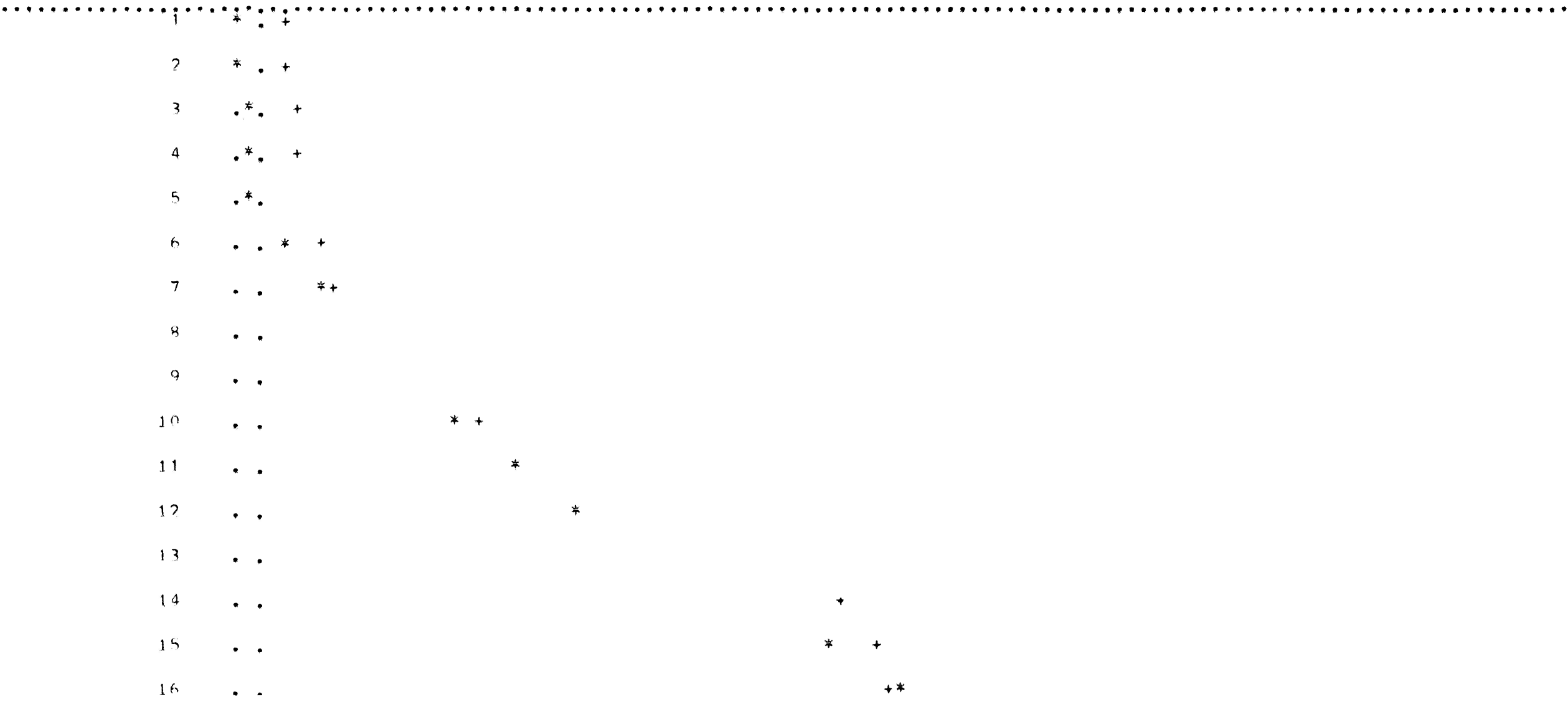
+

ALL DISTANCES HAVE UNITS (KM.)

RESERVATION (KM.)	COORDINATES (KM.)	MODEL RESPONSE (MILLIGALS)	DESIRED RESPONSE (MILLIGALS)	DIFFERENCE (MILLIGALS)	DIFFERENCE (AVERAGE REMOVED)
63.750	0.000	0.811	-0.500	-1.3114	-0.2236
63.750	1.000	0.924	-0.400	-1.3240	-0.2363
63.750	2.000	1.064	-0.300	-1.3640	-0.2762
63.750	3.000	1.245	-0.200	-1.4453	-0.3575
63.750	4.000	1.485	-0.100	-1.5852	-0.4974
63.750	5.000	1.815	0.700	-1.1152	-0.0275
63.750	6.000	2.289	1.800	-0.4889	0.5989
63.750	7.000	3.012	3.000	-0.0125	1.0753
63.750	8.000	4.197	4.200	0.0025	1.0903
63.750	9.000	6.154	5.500	-0.6543	0.4334
63.750	10.000	8.820	7.200	-1.6198	-0.5320
63.750	11.000	13.201	8.600	-4.6009	-3.5131
63.750	12.000	15.023	11.000	-4.0229	-2.9352
63.750	13.000	16.117	13.500	-2.6168	-1.5291
63.750	14.000	16.886	15.700	-1.1861	-0.0983
63.750	15.000	17.440	17.500	0.0595	1.1473
63.750	16.000	17.794	16.800	-0.9942	0.0935
63.750	17.000	17.897	17.300	-0.5970	0.4907
63.750	18.000	17.637	17.200	-0.4372	0.6505
63.750	19.000	15.830	15.000	-0.8297	0.2581
63.750	20.000	13.643	12.200	-1.4429	-0.3552
63.750	21.000	12.152	11.200	-0.9522	0.1356
63.750	22.000	10.689	10.500	-0.1887	0.8991
63.750	23.000	9.632	10.000	0.3684	1.4561
63.750	24.000	9.927	9.600	-0.3275	0.7603
63.750	25.000	10.101	9.200	-0.9005	0.1872
63.750	26.000	9.295	8.400	-0.8954	0.1924
63.750	27.000	8.948	7.600	-1.3479	-0.2602
63.750	28.000	8.699	7.100	-1.5991	-0.5114
63.750	29.000	8.560	6.500	-2.0596	-0.9719
63.750	30.000	8.531	6.500	-2.0305	-0.9428
63.750	31.000	8.595	7.000	-1.5952	-0.5074
63.750	32.000	8.715	8.000	-0.7153	0.3725
63.750	33.000	8.836	8.000	-0.8356	0.2521
63.750	34.000	8.862	7.100	-1.7618	-0.6740
63.750	35.000	8.509	5.800	-2.7091	-1.6214
63.750	36.000	6.789	5.400	-1.3885	-0.3008
63.750	37.000	6.659	5.800	-0.8593	0.2285
63.750	38.000	7.220	7.000	-0.2200	0.8678
63.750	39.000	8.125	8.500	0.3749	1.4627
63.750	40.000	9.231	10.000	0.7692	1.8569
63.750	41.000	10.441	11.500	1.0588	2.1466
63.750	42.000	11.683	12.500	0.8169	1.9046
63.750	43.000	12.865	13.400	0.5350	1.6228
63.750	44.000	14.006	14.200	0.1942	1.2820
63.750	45.000	15.317	15.300	-0.0172	1.0706
63.750	46.000	16.469	16.200	-0.2691	0.8186
63.750	47.000	17.110	16.800	-0.3098	0.7779
63.750	48.000	17.463	17.500	0.0374	1.1252
63.750	49.000	17.694	18.100	0.4056	1.4933
63.750	50.000	17.904	18.500	0.5962	1.6840
63.750	51.000	18.236	19.000	0.7640	1.8518
63.750	52.000	19.657	18.900	-0.7575	1.3303
63.750	53.000	21.881	18.800	-3.0806	-1.9928

53.750	54.000	22.264	19.000	-3.2640	-2.1762
63.750	55.000	22.399	19.100	-3.2992	-2.2114
63.750	56.000	22.448	19.200	-3.2479	-2.1602
63.750	57.000	22.448	19.300	-3.1477	-2.0599
63.750	58.000	22.405	19.400	-3.0054	-1.9177
63.750	59.000	22.315	19.500	-2.8149	-1.7271

THE AVERAGE OF THE DIFFERENCES IS -1.0877, AND THE P.M.S. OF THE DIFFERENCES (WITH MEAN REMOVED) IS 1.2952
 1 DIVISION= 0.330000 MGALS.



38 . . * +

39 . .

40 . . +*

41 . . + *

42 . . + *

43 . . + *

44 . . + *

45 . . +**

46 . .

47 . . +

48 . . **+

49 . . +**

50 . . +**

51 . . + *

52 . . + *

53 . . * +

54 . . *

55 . . *

56 . . * +

57 . . *

58

59

60

• •

*

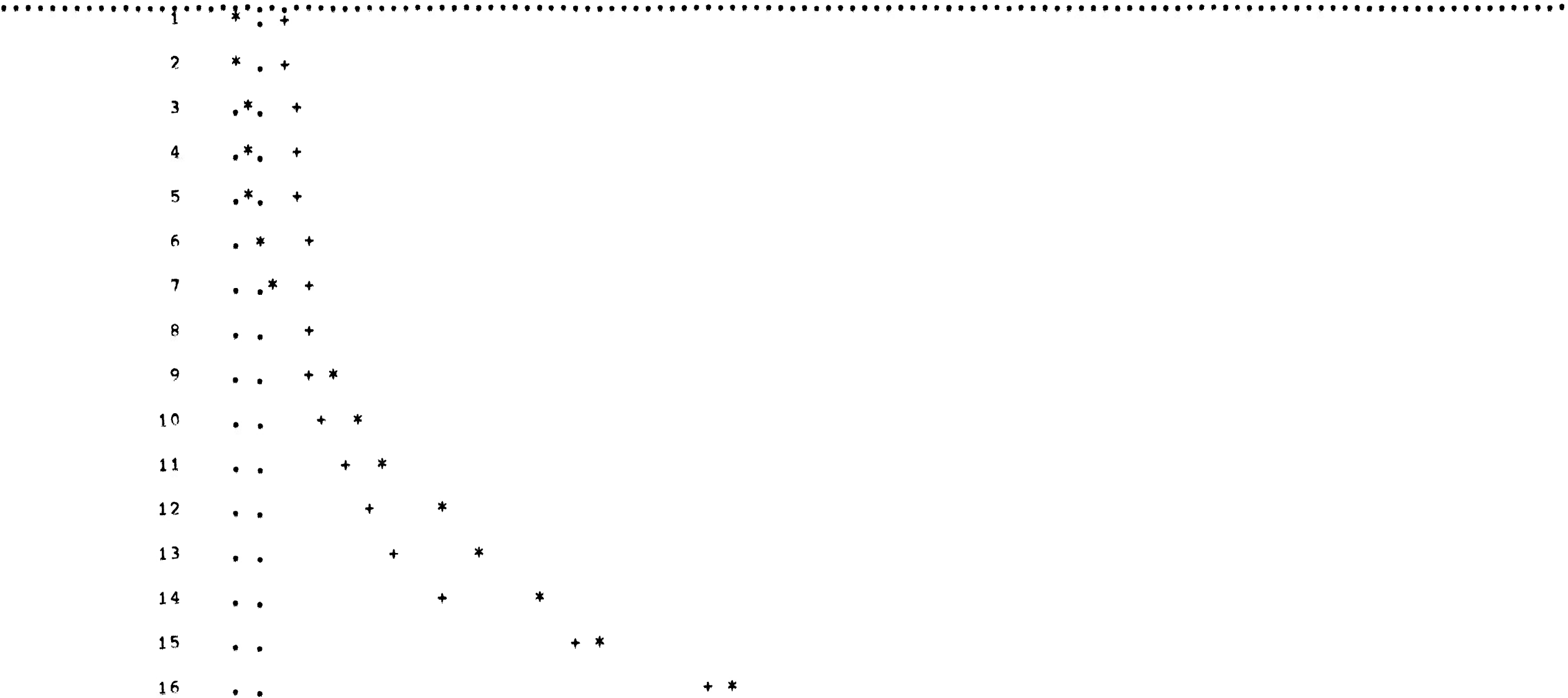
+

ALL DISTANCES HAVE UNITS (KM.)

RESERVATION (KM.)	COORDINATES	MODEL RESPONSE (MILLIGALS)	DESIRED RESPONSE (MILLIGALS)	DIFFERENCE (MILLIGALS)	DIFFERENCE (AVERAGE REMOVED)
53.0000	0.0000	0.868	-0.500	-1.3680	-0.5713
53.0000	1.0000	0.949	-0.400	-1.3493	-0.5526
53.0000	2.0000	1.042	-0.300	-1.3416	-0.5450
53.0000	3.0000	1.147	-0.200	-1.3467	-0.5500
53.0000	4.0000	1.268	-0.100	-1.3675	-0.5708
53.0000	5.0000	1.405	0.000	-1.4055	-0.6088
53.0000	6.0000	1.547	0.500	-1.0472	-0.2505
53.0000	7.0000	1.590	1.500	-0.0902	0.7065
53.0000	8.0000	1.380	2.200	0.8203	1.6170
53.0000	9.0000	1.786	2.700	0.9139	1.7106
53.0000	10.0000	2.387	3.500	1.1130	1.9097
53.0000	11.0000	3.077	5.000	1.9233	2.7200
53.0000	12.0000	3.904	6.200	2.2963	3.0930
53.0000	13.0000	5.176	7.700	2.5239	3.3206
53.0000	14.0000	8.718	9.500	0.7824	1.5791
53.0000	15.0000	12.426	13.000	0.5740	1.3707
53.0000	16.0000	13.834	14.500	0.6660	1.4627
53.0000	17.0000	14.415	14.000	-0.4152	0.3815
53.0000	18.0000	14.211	12.000	-2.2106	-1.4140
53.0000	19.0000	13.017	10.700	-2.3172	-1.5206
53.0000	20.0000	10.012	10.200	0.1881	0.9848
53.0000	21.0000	8.198	9.400	1.2021	1.9987
53.0000	22.0000	9.812	10.200	0.3878	1.1845
53.0000	23.0000	11.332	10.300	-1.0323	-0.2356
53.0000	24.0000	11.372	9.000	-2.3725	-1.5758
53.0000	25.0000	10.827	7.800	-3.0266	-2.2299
53.0000	26.0000	9.974	8.500	-1.4741	-0.6774
53.0000	27.0000	8.942	7.500	-1.4416	-0.6449
53.0000	28.0000	6.925	6.000	-0.9250	-0.1283
53.0000	29.0000	4.699	2.500	-2.1987	-1.4021
53.0000	30.0000	4.788	5.000	0.2124	1.0091
53.0000	31.0000	7.297	7.200	-0.0967	0.7000
53.0000	32.0000	7.534	7.300	-0.2335	0.5631
53.0000	33.0000	5.019	6.500	1.4810	2.2777
53.0000	34.0000	4.788	5.800	1.0120	1.8087
53.0000	35.0000	6.145	5.500	-0.6454	0.1513
53.0000	36.0000	7.378	5.500	-1.8783	-1.0817
53.0000	37.0000	8.286	5.800	-2.4863	-1.6896
53.0000	38.0000	9.106	6.400	-2.7058	-1.9092
53.0000	39.0000	9.871	7.300	-2.5714	-1.7748
53.0000	40.0000	10.591	8.500	-2.0909	-1.2942
53.0000	41.0000	11.273	10.000	-1.2728	-0.4762
53.0000	42.0000	11.940	11.800	-0.1403	0.6564
53.0000	43.0000	12.624	12.500	-0.1243	0.6724
53.0000	44.0000	13.292	13.000	-0.2923	0.5044
53.0000	45.0000	13.833	13.400	-0.4326	0.3640
53.0000	46.0000	14.220	13.800	-0.4201	0.3766
53.0000	47.0000	14.541	14.200	-0.3414	0.4552
53.0000	48.0000	14.919	14.400	-0.5185	0.2782
53.0000	49.0000	15.504	14.500	-1.0038	-0.2071
53.0000	50.0000	16.397	14.600	-1.7973	-1.0006
53.0000	51.0000	17.253	14.800	-2.4527	-1.6560
53.0000	52.0000	17.791	14.900	-2.8905	-2.0938
53.0000	53.0000	18.119	15.300	-2.8192	-2.0225

53,000	54,000	18,340	15,600	-2.7403	-1.9436
53,000	55,000	18,497	16,100	-2.3970	-1.6003
53,000	56,000	18,598	16,800	-1.7978	-1.0011
53,000	57,000	18,617	17,200	-1.4173	-0.6206
53,000	58,000	18,477	17,400	-1.0767	-0.2800
53,000	59,000	18,024	17,500	-0.5241	0.2725

THE AVERAGE OF THE DIFFERENCES IS -0.7967, AND THE R.M.S. OF THE DIFFERENCES (WITH MEAN REMOVED) IS 1.3793
 1 DIVISION= 0.330000 MGALS.



38 . . . *

39 . . . *

40 . . . *

41 . . . *

42 . . . *

43 . . . *

44 . . . *

45 . . . *

46 . . . *

47 . . . *

48 . . . *

49 . . . *

50 . . . *

51 . . . *

52 . . . *

53 . . . *

54 . . . *

55 . . . *

56 . . . *

57 . . . *

58

59

60

• •

* +

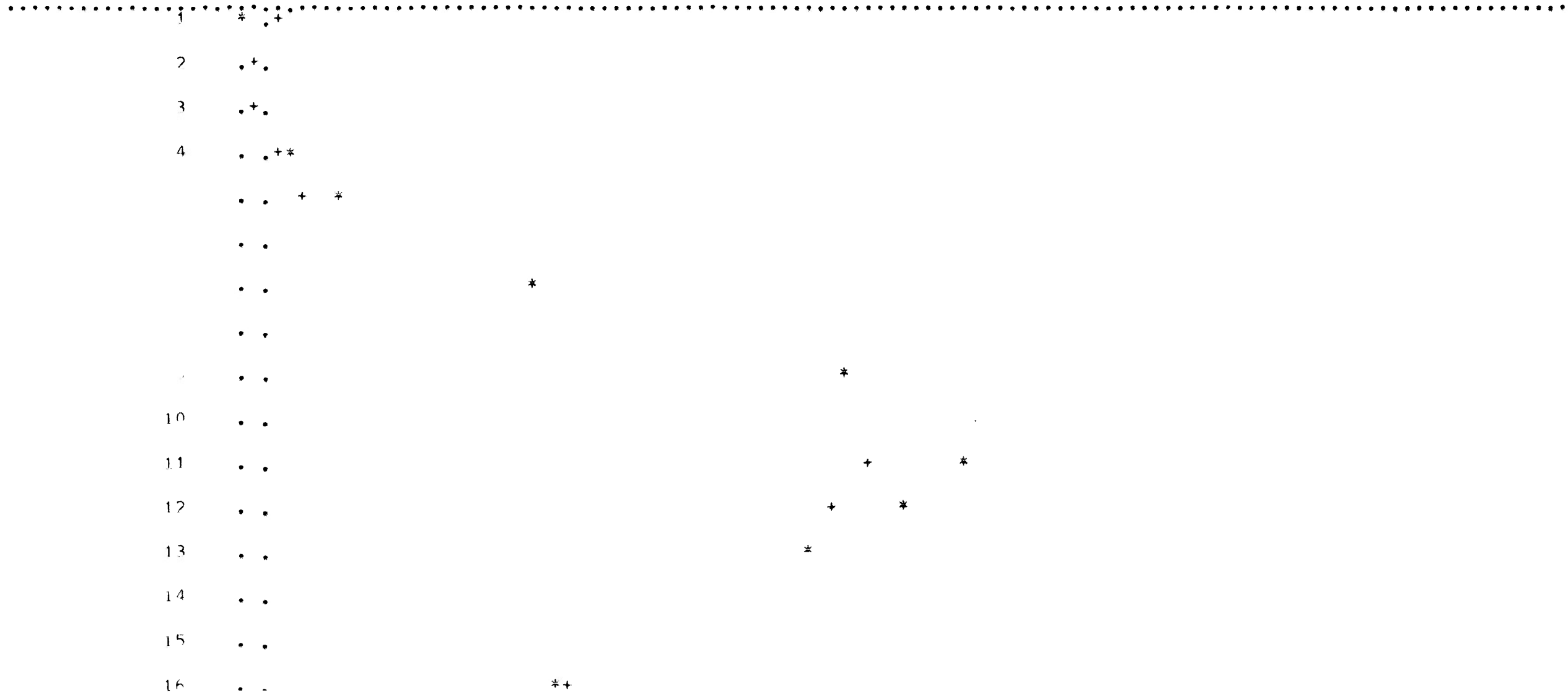
* *

ALL DISTANCES HAVE UNITS (KM.)

RESERVATION COORDINATES (KM.)	MODEL RESPONSE (MILLIGALS)	DESIRED RESPONSE (MILLIGALS)	DIFFERENCE (MILLIGALS)	DIFFERENCE (AVERAGE REMOVED)
41.750	0.000	-0.500	-0.8668	-0.1882
41.750	1.000	-0.300	-0.1802	0.4984
41.750	2.000	-0.100	-0.0896	0.5890
41.750	3.000	0.387	0.3129	0.9915
41.750	4.000	2.000	0.9139	1.5925
41.750	5.000	4.000	1.7626	2.4412
41.750	6.000	7.500	3.1299	3.8085
41.750	7.000	12.000	2.3074	2.9860
41.750	8.000	16.000	2.6677	3.3463
41.750	9.000	19.500	3.7661	4.4447
41.750	10.000	19.400	2.8396	3.5182
41.750	11.000	17.500	1.9396	2.6182
41.750	12.000	15.000	2.6510	3.3296
41.750	13.000	12.500	4.7646	5.4432
41.750	14.000	11.000	2.6414	3.3200
41.750	15.000	8.000	-0.2703	0.4083
41.750	16.000	6.000	-2.1447	-1.4661
41.750	17.000	6.600	-2.0783	-1.3997
41.750	18.000	7.400	-1.9308	-1.2522
41.750	19.000	7.200	-2.5208	-1.8422
41.750	20.000	6.300	-3.8393	-3.1607
41.750	21.000	5.000	-2.9765	-2.2979
41.750	22.000	3.600	-1.2747	-0.5961
41.750	23.000	2.500	-1.1330	-0.4544
41.750	24.000	1.700	-1.0841	-0.4055
41.750	25.000	1.300	-0.8131	-0.1345
41.750	26.000	0.800	-0.7713	-0.0927
41.750	27.000	0.500	-0.6473	0.0313
41.750	28.000	0.100	-0.6725	0.0061
41.750	29.000	-0.500	-0.9248	-0.2462
41.750	30.000	-0.500	-1.3141	-0.6355
41.750	31.000	1.000	-0.6954	-0.0168
41.750	32.000	1.900	-1.1460	-0.4674
41.750	33.000	4.000	-1.3182	-0.6396
41.750	34.000	5.400	-1.4610	-0.7824
41.750	35.000	6.300	-1.6148	-0.9362
41.750	36.000	6.700	-1.9983	-1.3197
41.750	37.000	7.300	-2.0235	-1.3449
41.750	38.000	7.800	-2.0981	-1.4195
41.750	39.000	9.000	-1.5253	-0.8467
41.750	40.000	10.300	-0.9497	-0.2711
41.750	41.000	11.100	-0.8665	-0.1879
41.750	42.000	11.300	-1.2468	-0.5682
41.750	43.000	11.400	-1.5813	-0.9027
41.750	44.000	11.500	-1.8136	-1.1350
41.750	45.000	11.700	-1.8824	-1.2038
41.750	46.000	11.900	-1.9159	-1.2373
41.750	47.000	12.200	-1.8328	-1.1541
41.750	48.000	12.400	-1.8473	-1.1687
41.750	49.000	12.500	-1.9708	-1.2922
41.750	50.000	12.700	-2.0120	-1.3334
41.750	51.000	12.900	-2.0776	-1.3990
41.750	52.000	13.400	-1.8700	-1.1914
41.750	53.000	13.800	-1.7861	-1.1075

41.750	54.000	15.916	14.500	-1.4157	-0.7370
41.750	55.000	16.240	15.200	-1.0399	-0.3613
41.750	56.000	16.535	15.600	-0.9353	-0.2567
41.750	57.000	16.777	15.800	-0.9770	-0.2984
41.750	58.000	16.947	15.500	-1.4474	-0.7688
41.750	59.000	17.032	15.500	-1.5322	-0.8536

THE AVERAGE OF THE DIFFERENCES IS -0.6786, AND THE R.M.S. OF THE DIFFERENCES (WITH MEAN REMOVED) IS 1.7850
 1 DIVISION = 0.330000 MGALS.



18 .
 19 . .
 20 . . *
 21 . .
 22 . . *
 23 . .
 24 . .
 25 . . * +
 26 . . * +
 27 . . * +
 28 . . * +
 29 . . * +
 30 * . +
 31 * . +
 32 . . * +
 33 . .
 34 . .
 35 . .
 36 . . *
 37 . . * +

38 . . . *

39 . . . *

40 . . . *

41 . . . * +

42 . . . * +

43 . . . *

44 . . . *

45 . . . *

46 . . . *

47 . . . *

48 . . . *

49 . . . *

50 . . . *

51 . . . *

52 . . . *

53 . . . *

54 . . . *

55 . . . *

56 . . . * +

57 . . . * +

58

+

59

*

*

60

→

• •

ALL DISTANCES HAVE UNITS (KM.)

RESERVATION (KM.)	COORDINATES	MODEL RESPONSE (MILLIGALS)	DESIRED RESPONSE (MILLIGALS)	DIFFERENCE (MILLIGALS)	DIFFERENCE (AVERAGE REMOVED)
22.500	0.000	5.140	2.000	-3.1404	-1.6710
22.776	0.961	7.527	2.500	-5.0271	-3.5577
23.051	1.923	8.562	3.500	-5.1623	-3.6929
23.327	2.884	9.936	6.500	-3.4359	-1.9665
23.603	3.845	11.718	12.500	0.7817	2.2510
23.878	4.806	14.380	16.000	1.6195	3.0889
24.154	5.768	17.597	18.500	0.9030	2.3723
24.429	6.729	20.443	20.700	0.2568	1.7262
24.705	7.690	22.706	22.500	-0.2065	1.2629
24.981	8.651	24.372	23.500	-0.8717	0.5976
25.256	9.613	25.455	25.200	-0.2545	1.2148
25.532	10.574	25.991	25.500	-0.4911	0.9782
25.808	11.535	26.019	25.300	-0.7188	0.7506
26.083	12.496	25.563	24.800	-0.7633	0.7060
26.359	13.458	24.622	23.800	-0.8221	0.6473
26.635	14.419	23.184	22.300	-0.8841	0.5853
26.910	15.380	21.308	20.500	-0.8082	0.6612
27.186	16.341	19.220	19.200	-0.0195	1.4498
27.461	17.303	17.139	17.000	-0.1394	1.3300
27.737	18.264	15.152	14.500	-0.6515	0.8178
28.013	19.225	13.160	12.200	-0.9597	0.5096
28.288	20.186	12.445	9.500	-2.9450	-1.4757
28.564	21.148	12.085	9.200	-2.8848	-1.4154
28.840	22.109	11.782	10.000	-1.7820	-0.3127
29.115	23.070	11.435	10.200	-1.2345	0.2348
29.391	24.032	10.976	9.400	-1.5756	-0.1062
29.667	24.993	10.319	8.600	-1.7187	-0.2494
29.942	25.954	9.399	8.200	-1.1991	0.2703
30.218	26.915	8.160	7.200	-0.9604	0.5089
30.493	27.877	6.305	6.800	0.4947	1.9641
30.769	28.838	6.188	6.600	0.4118	1.8811
31.045	29.799	6.420	6.500	0.0804	1.5498
31.320	30.760	6.761	6.400	-0.3614	1.1079
31.596	31.722	7.127	6.300	-0.8275	0.6419
31.872	32.683	7.479	6.200	-1.2789	0.1904
32.147	33.644	7.818	6.100	-1.7176	-0.2482
32.423	34.605	8.161	6.500	-1.6610	-0.1916
32.699	35.567	8.518	6.800	-1.7182	-0.2489
32.974	36.528	8.875	7.300	-1.5752	-0.1059
33.250	37.489	9.208	7.600	-1.6077	-0.1384
33.525	38.450	9.512	8.000	-1.5125	-0.0431
33.801	39.412	9.799	8.300	-1.4996	-0.0296
34.077	40.373	10.093	8.500	-1.5927	-0.1234
34.352	41.334	10.428	8.700	-1.7284	-0.2591
34.628	42.296	10.848	8.900	-1.9476	-0.4782
34.904	43.257	11.390	9.200	-2.1905	-0.7211
35.179	44.218	12.041	9.500	-2.5414	-1.0721
35.455	45.179	12.688	9.800	-2.8877	-1.4184
35.731	46.141	13.229	10.400	-2.8292	-1.3599
36.006	47.102	13.669	10.800	-2.8690	-1.3997
36.282	48.063	14.048	11.300	-2.7478	-1.2785
36.558	49.024	14.398	11.500	-2.8981	-1.4287
36.833	49.986	14.737	11.800	-2.9375	-1.4682
37.109	50.947	15.073	12.500	-2.5728	-1.1035

37,584
37,660
37,936
38,211
38,487
38,763

51,908
52,869
53,831
54,792
55,753
56,714

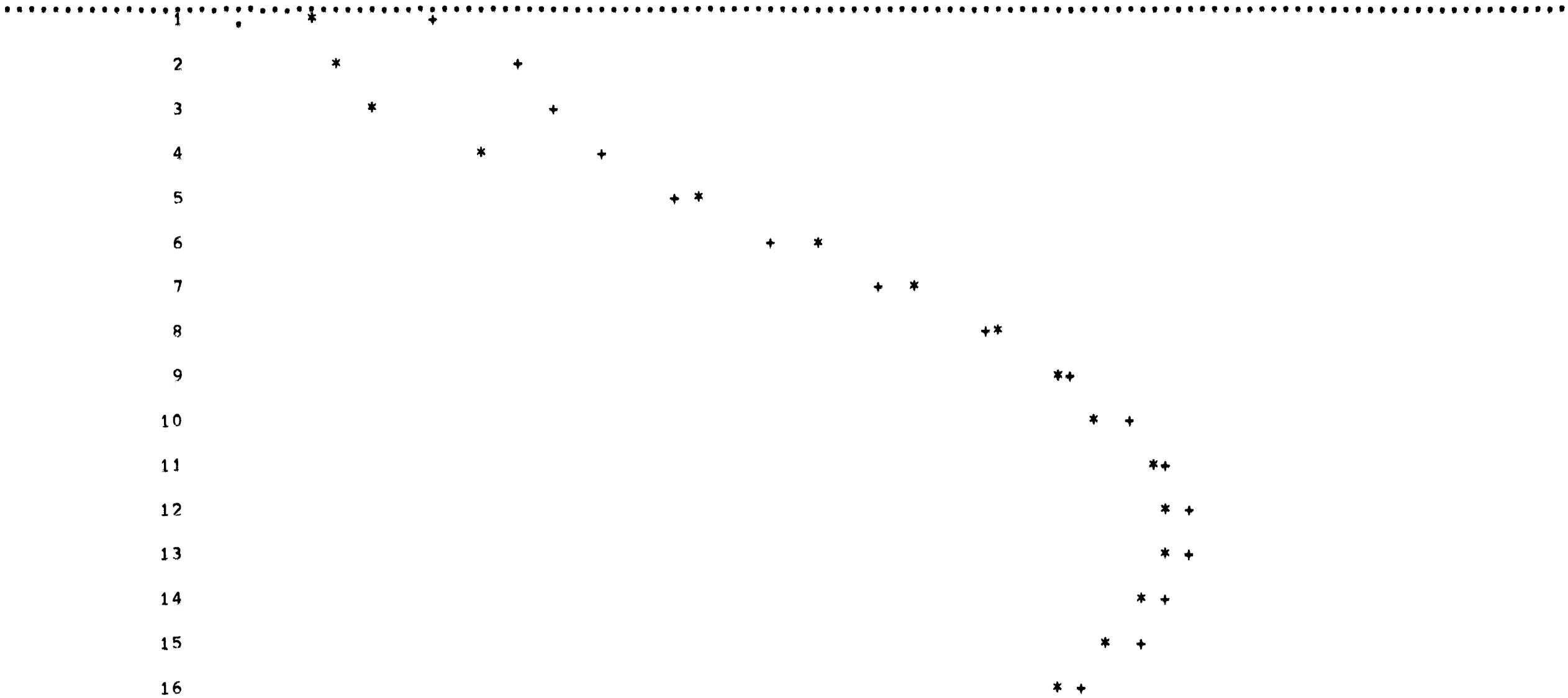
15,403
15,720
16,014
16,274
16,489
16,651

13,200
13,600
14,200
14,700
15,100
15,200

-2,2028
-2,1201
-1,8142
-1,5740
-1,3887
-1,4508

-0,7335
-0,6508
-0,3449
-0,1046
0,0806
0,0185

THE AVERAGE OF THE DIFFERENCES IS -1.4693, AND THE R.M.S. OF THE DIFFERENCES (WITH MEAN REMOVED) IS 1.3017
1 DIVISION= 0,330000 MGALS.



17

* +

18

19

20

* +

21

* +

22

23

*

24

*

25

*

26

*

27

*

28

* +

29

* +

30

+ *

31

+ *

32

+ *

33

* +

34

* +

35

*

36

*

37

* +

.

38

*

39

*

40

*

41

*

42

*

43

*

44

*

45

*

46

*

47

*

48

*

49

*

50

*

51

*

52

*

53

*

54

*

55

*

56

*

57

*

58

59

60

*

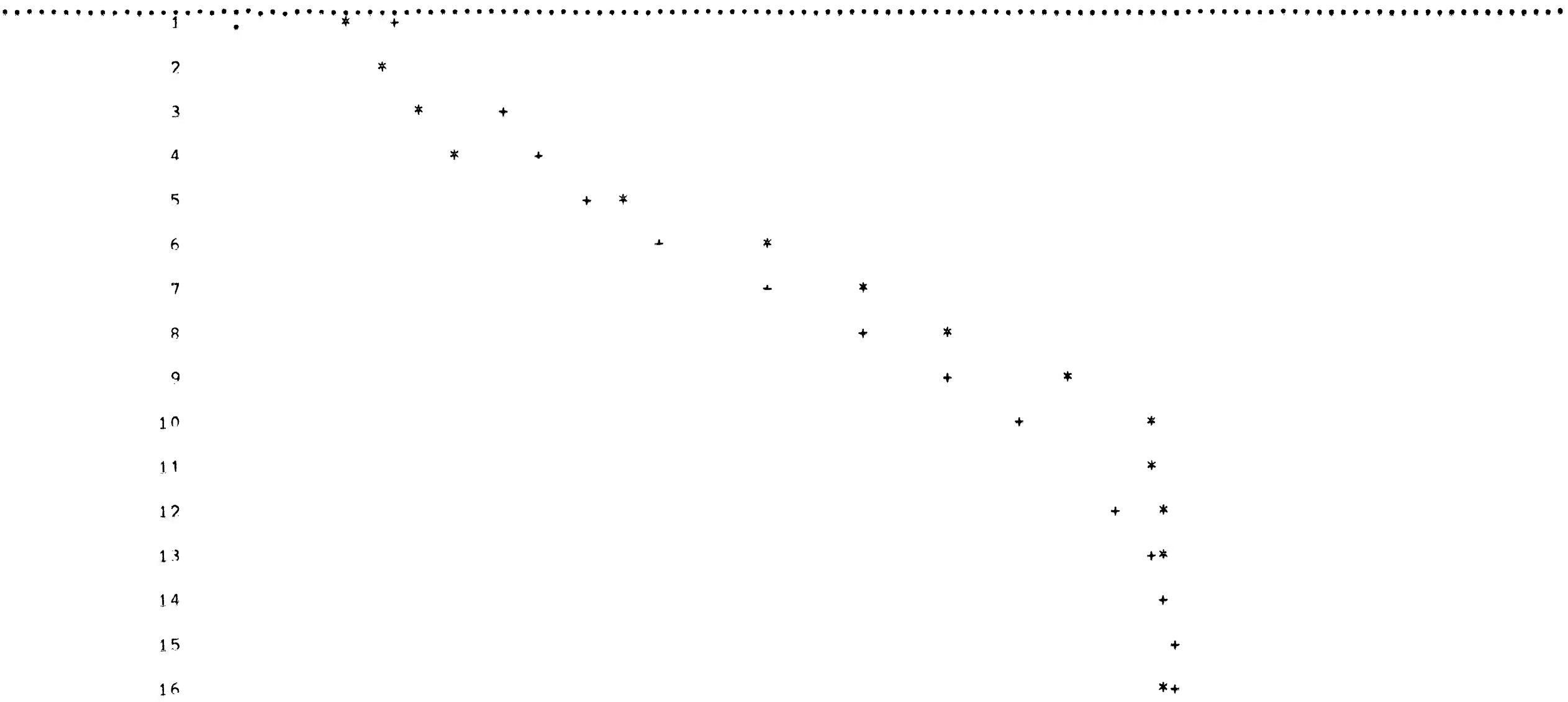
*

ALL DISTANCES HAVE UNITS (KM.)

RESERVATION (KM.)	COORDINATES	MODEL RESPONSE (MILLIGALS)	DESIRED RESPONSE (MILLIGALS)	DIFFERENCE (MILLIGALS)	DIFFERENCE (AVERAGE REMOVED)
12.250	0.000	4.134	3.000	-1.1341	-1.0308
12.526	0.961	6.311	4.000	-2.3108	-2.2075
12.801	1.923	7.180	5.000	-2.1800	-2.0768
13.077	2.884	8.114	6.000	-2.1135	-2.0102
13.353	3.845	9.473	10.500	1.0270	1.1303
13.628	4.806	11.691	14.500	2.8090	2.9123
13.904	5.768	14.568	17.000	2.4320	2.5353
14.179	6.729	17.267	19.500	2.2331	2.3364
14.455	7.690	19.615	22.700	3.0851	3.1884
14.731	8.651	21.561	25.000	3.4389	3.5422
15.006	9.613	23.079	25.200	2.1208	2.2241
15.282	10.574	24.203	25.300	1.0967	1.2000
15.558	11.535	24.972	25.400	0.4282	0.5315
15.833	12.496	25.448	25.500	-0.0519	0.1552
16.109	13.458	25.688	25.600	-0.0876	0.0157
16.385	14.419	25.727	25.500	-0.2267	-0.1234
16.660	15.380	25.575	25.400	-0.1752	-0.0719
16.936	16.341	25.219	25.300	0.0807	0.1840
17.211	17.303	24.624	25.200	0.5765	0.6798
17.487	18.264	23.742	25.100	1.3580	1.4612
17.763	19.225	22.528	24.500	1.9720	2.0753
18.038	20.186	20.931	22.500	1.5690	1.6723
18.314	21.148	18.843	20.000	1.1575	1.2608
18.590	22.109	16.557	18.700	2.1428	2.2461
18.865	23.070	15.326	17.500	2.1740	2.2773
19.141	24.032	14.233	16.000	1.7672	1.8705
19.417	24.993	13.015	13.500	0.4855	0.5888
19.692	25.954	11.583	11.200	-0.3830	-0.2797
19.968	26.915	10.240	10.500	0.2604	0.3637
20.243	27.877	9.022	9.800	0.7781	0.8814
20.519	28.838	7.010	9.200	2.1900	2.2933
20.795	29.799	6.781	8.500	1.7187	1.8220
21.070	30.760	6.995	7.800	0.8047	0.9080
21.346	31.722	7.396	7.500	0.1045	0.2078
21.622	32.683	7.859	7.200	-0.6590	-0.5558
21.897	33.644	8.305	6.800	-1.5048	-1.4015
22.173	34.605	8.693	6.500	-2.1926	-2.0893
22.449	35.567	9.008	7.000	-2.0081	-1.9048
22.724	36.528	9.254	7.100	-2.1543	-2.0511
23.000	37.489	9.442	7.200	-2.2416	-2.1383
23.275	38.450	9.583	7.300	-2.2833	-2.1800
23.551	39.412	9.695	7.400	-2.2947	-2.1915
23.827	40.373	9.790	7.500	-2.2903	-2.1870
24.102	41.334	9.881	7.600	-2.2815	-2.1782
24.378	42.295	9.978	7.700	-2.2781	-2.1748
24.654	43.257	10.083	7.800	-2.2831	-2.1798
24.929	44.218	10.198	7.900	-2.2982	-2.1949
25.205	45.179	10.325	8.000	-2.3254	-2.2221
25.481	46.141	10.464	8.400	-2.0640	-1.9607
25.756	47.102	10.610	8.700	-1.9103	-1.8070
26.032	48.063	10.753	9.200	-1.5532	-1.4499
26.308	49.024	10.881	9.700	-1.1811	-1.0778
26.583	49.986	10.983	10.200	-0.7828	-0.6796
26.859	50.947	11.053	10.500	-0.5527	-0.4495

27.410	52.869	11.082	11.100	0.2687	0.1854
27.686	53.831	11.037	11.200	0.0177	0.2663
27.961	54.792	10.949	11.300	0.1630	0.4540
28.237	55.753	10.817	11.400	0.3507	0.6866
28.513	56.714	10.638	11.500	0.5833	0.9658
				0.8625	

THE AVERAGE OF THE DIFFERENCES IS -0.1033, AND THE R.M.S. OF THE DIFFERENCES (WITH MEAN REMOVED) IS 1.7041
 1 DIVISION= 0.330000 MGALS.



17 **+

18 +**

19 +*

20 + *

21 r *

22 r *

23 *
r *

24 + *

25 *

26 r *

27 + *
+

28 **+

29 +**

30 + *

31 *

32 r *

33 + *

34 +**

35 * +

36 *

37 * + •

38

*

39

*

40

*

41

*

42

*

43

*

44

*

45

*

46

*

47

*

48

*

49

*

50

*

51

*

52

*

53

* +

54

* +

55

* +

56

57

* +

LAYER	DENSITY	DEPTH TO TOP	DEPTH TO BOTTOM	VERTICES			
1	0.120	0.0000000	1.0000000	0.0000,	26.0000	5.0000,	24.0000
				13.0000,	23.0000	26.0000,	19.0000
				32.0000,	18.0000	44.0000,	18.0000
				42.0000,	14.0000	41.0000,	13.0000
				42.0000,	12.0000	49.0000,	11.0000
				31.0000,	0.0000	10.0000,	0.0000
				0.0000,	10.0000		
2	0.170	1.0000000	2.0000000	0.0000,	25.0000	7.0000,	23.0000
				18.0000,	21.0000	27.0000,	18.0000
				43.0000,	11.0000	47.0000,	10.5000
				37.0000,	5.0000	13.0000,	5.0000
				0.0000,	12.0000		
3	0.170	2.0000000	3.0000000	0.0000,	24.0000	19.0000,	20.0000
				26.0000,	16.0000	43.0000,	11.5000
				46.0000,	10.0000	37.0000,	6.0000
				14.0000,	6.0000	7.5000,	13.0000
				0.0000,	17.0000		
4	0.170	3.0000000	5.0000000	0.0000,	23.5000	17.0000,	20.0000
				26.0000,	15.0000	43.0000,	12.5000
				45.0000,	10.0000	38.0000,	7.0000
				14.0000,	7.0000	8.0000,	17.0000
				0.0000,	18.0000		
5	0.170	5.0000000	9.0000000	0.0000,	23.0000	7.5000,	12.0000
				15.0000,	11.0000	43.0000,	11.0000
				44.0000,	10.0000	43.0000,	9.0000
				14.0000,	9.0000	7.5000,	19.0000
				0.0000,	20.0000		
6	0.080	0.0000000	1.0000000	0.0000,	30.0000	6.0000,	29.0000
				14.0000,	30.0000	21.0000,	28.0000
				32.0000,	27.0000	38.0000,	26.0000
				41.0000,	21.0000	41.0000,	20.0000
				49.0000,	20.0000	44.0000,	18.0000
				32.0000,	18.0000	26.0000,	19.0000
				13.0000,	23.0000	5.0000,	24.0000
				0.0000,	26.0000		
7	0.080	1.0000000	2.0000000	0.0000,	35.0000	7.5000,	35.0000
				19.0000,	26.0000	38.0000,	26.0000
				41.0000,	20.0000	49.0000,	20.0000
				44.0000,	18.0000	32.0000,	16.0000
				27.0000,	18.0000	18.0000,	21.0000
				7.0000,	23.0000	0.0000,	25.0000
8	0.080	2.0000000	3.0000000	0.0000,	38.0000	8.0000,	38.0000
				19.0000,	25.0000	38.5000,	25.0000
				40.0000,	23.0000	40.0000,	18.5000
				28.0000,	20.0000	19.0000,	20.0000
				0.0000,	24.0000		
9	0.080	3.0000000	5.0000000	0.0000,	37.0000	8.0000,	37.0000
				18.0000,	25.0000	25.0000,	23.0000
				25.0000,	21.0000	17.0000,	20.0000
				7.0000,	25.0000	0.0000,	27.0000
				0.0000,	29.0000	7.0000,	28.0000

				11.0000, 0.0000,	28.0000 32.0000	7.0000, 31.0000	
10	0.080	5.0000000	7.0000000	0.0000, 18.0000, 22.0000, 7.0000,	34.0000 24.0000 22.0000 32.0000	7.0000, 22.0000, 18.0000, 0.0000,	34.0000 23.0000 22.0000 33.0000
11	-0.030	0.0000000	3.0000000	31.0000, 48.0000,	0.0000 6.0000	49.0000, 43.0000,	11.0000 0.0000
12	-0.030	0.0000000	1.0000000	43.0000, 49.0000, 41.0000, 54.0000, 54.0000,	0.0000 11.0000 13.0000 14.0000 8.0000	48.0000, 42.0000, 42.0000, 59.0000,	6.0000 12.0000 14.0000 12.0000
13	-0.030	1.0000000	4.0000000	31.0000, 47.0000,	0.0000 10.5000	37.0000, 49.0000,	5.0000 11.0000
14	-0.030	2.0000000	5.0000000	37.0000, 46.0000,	5.0000 10.0000	37.0000, 47.0000,	6.0000 10.5000
15	-0.030	3.0000000	6.0000000	37.0000, 45.0000,	6.0000 10.0000	38.0000, 46.0000,	7.0000 10.0000
16	-0.030	5.0000000	7.0000000	38.0000, 43.0000, 45.0000,	7.0000 9.0000 10.0000	40.0000, 44.0000,	9.0000 10.0000
17	-0.030	1.0000000	2.0000000	54.0000, 43.0000, 44.0000, 51.0000, 56.0000, 57.0000, 51.0000, 47.0000,	9.0000 11.0000 18.0000 21.0000 22.0000 20.0000 19.0000 14.0000	47.0000, 35.0000, 49.0000, 52.0000, 57.0000, 56.0000, 47.0000,	10.5000 16.5000 20.0000 23.0000 21.0000 19.0000 15.0000
18	-0.050	2.0000000	6.0000000	37.0000, 45.0000, 47.0000,	16.0000 17.0000 14.0000	41.0000, 47.0000, 39.0000,	17.0000 15.0000 14.0000
19	-0.030	0.0000000	0.5000000	57.0000, 66.0000, 80.0000, 74.0000, 66.0000, 62.0000,	20.0000 25.0000 24.0000 14.0000 17.0000 19.0000	57.0000, 74.0000, 80.0000, 66.0000, 69.0000,	21.0000 24.0000 15.0000 14.0000 19.0000
20	-0.030	0.0000000	1.0000000	52.0000, 57.0000,	20.0000 21.0000	52.0000, 57.0000,	21.0000 20.0000
21	-0.030	2.0000000	3.0000000	52.0000, 56.0000,	20.0000 21.0000	52.0000, 56.0000,	21.0000 20.0000
22	0.120	0.0000000	1.0000000	54.0000, 44.0000, 51.0000, 66.0000, 57.0000,	14.0000 18.0000 21.0000 26.0000 21.0000	42.0000, 49.0000, 54.0000, 66.0000, 52.0000,	14.0000 20.0000 21.0000 25.0000 21.0000

				52.0000,	20.0000	57.0000,	20.0000
				62.0000,	19.0000	69.0000,	19.0000
				66.0000,	17.0000	66.0000,	14.0000
				74.0000,	14.0000	80.0000,	15.0000
				80.0000,	13.0000	74.0000,	12.0000
				54.0000,	9.0000		
23	0.120	1.0000000	2.0000000	54.0000,	9.0000	54.0000,	14.0000
				47.0000,	15.0000	51.0000,	19.0000
				69.0000,	19.0000	66.0000,	17.0000
				66.0000,	14.0000	74.0000,	14.0000
				80.0000,	15.0000	80.0000,	10.0000
				74.0000,	9.0000		
24	0.120	0.5000000	2.0000000	57.0000,	20.0000	57.0000,	21.0000
				80.0000,	21.0000	80.0000,	15.0000
				74.0000,	14.0000	66.0000,	14.0000
				66.0000,	17.0000	69.0000,	19.0000
				62.0000,	19.0000		
25	0.120	2.0000000	4.0000000	80.0000,	11.0000	74.0000,	10.0000
				63.0000,	10.0000	51.0000,	16.0000
				51.0000,	17.0000	52.0000,	20.0000
				56.0000,	20.0000	56.0000,	21.0000
				80.0000,	21.0000		
26	0.120	4.0000000	6.0000000	74.0000,	16.0000	61.0000,	16.0000
				52.0000,	17.0000	52.0000,	18.0000
				54.0000,	19.0000	74.0000,	19.0000
27	0.120	0.0000000	2.0000000	41.0000,	20.0000	41.0000,	21.0000
				51.0000,	21.0000	49.0000,	20.0000
28	0.080	0.5000000	3.0000000	80.0000,	21.0000	57.0000,	21.0000
				66.0000,	25.0000	74.0000,	24.0000
				80.0000,	24.0000		
29	0.080	0.0000000	2.0000000	80.0000,	24.0000	74.0000,	24.0000
				66.0000,	25.0000	66.0000,	27.0000
				70.0000,	30.0000	70.0000,	32.0000
				80.0000,	32.0000		
30	0.080	0.0000000	2.0000000	45.0000,	21.0000	47.0000,	23.0000
				47.0000,	28.0000	55.0000,	28.0000
				57.0000,	29.0000	57.0000,	30.0000
				56.0000,	31.0000	54.0000,	31.0000
				59.0000,	33.0000	74.0000,	41.0000
				80.0000,	41.0000	80.0000,	32.0000
				70.0000,	32.0000	66.0000,	31.0000
				66.0000,	26.0000	56.0000,	22.0000
				52.0000,	22.0000	51.0000,	21.0000
31	0.080	0.0000000	2.0000000	53.0000,	28.0000	47.0000,	28.0000
				46.0000,	29.0000	52.0000,	32.0000
				52.0000,	29.0000		
32	0.080	0.0000000	4.0000000	52.0000,	30.5000	52.0000,	32.0000
				58.0000,	35.0000	59.0000,	33.0000
				54.0000,	31.0000	53.0000,	30.5000
33	0.080	2.0000000	4.0000000	40.0000,	18.5000	40.0000,	23.0000

				41.0000,	21.0000	45.0000,	21.0000
				47.0000,	23.0000	47.0000,	26.0000
				65.0000,	24.5000	56.0000,	21.0000
				51.0000,	21.0000	49.0000,	20.0000
				44.0000,	18.0000		
34	0.080	4.0000000	6.0000000	42.0000,	19.0000	38.5000,	25.0000
				45.0000,	25.0000	58.0000,	24.0000
				58.0000,	23.0000	54.0000,	22.0000
				46.0000,	19.0000		
35	-0.020	0.0000000	2.0000000	66.0000,	27.0000	66.0000,	31.0000
				70.0000,	32.0000	70.0000,	30.0000
36	-0.020	0.0000000	2.0000000	54.0000,	31.0000	56.0000,	31.0000
				57.0000,	30.0000	57.0000,	29.0000
				55.0000,	28.0000	53.0000,	28.0000
				52.0000,	29.0000	52.0000,	30.0000
37	-0.020	2.0000000	4.0000000	52.0000,	30.5000	55.0000,	30.5000
				56.0000,	30.0000	56.0000,	29.0000
				55.0000,	28.5000	52.0000,	28.5000
				51.0000,	29.0000	51.0000,	30.0000
38	-0.020	0.0000000	4.0000000	41.0000,	21.0000	38.0000,	26.0000
				43.0000,	29.0000	46.0000,	29.0000
				47.0000,	28.0000	47.0000,	23.0000
				45.0000,	21.0000		
39	-0.020	4.0000000	7.0000000	41.0000,	25.0000	40.0000,	26.0000
				42.0000,	28.0000	46.0000,	28.0000
				46.0000,	26.0000	45.0000,	25.0000
40	-0.040	0.0000000	2.0000000	38.0000,	26.0000	33.0000,	30.0000
				36.0000,	32.0000	39.0000,	33.0000
				39.0000,	32.0000	47.0000,	34.0000
				54.0000,	35.0000	58.0000,	35.0000
				46.0000,	29.0000	43.0000,	29.0000
41	-0.040	2.0000000	4.0000000	38.0000,	26.0000	36.0000,	30.0000
				38.0000,	32.0000	40.0000,	31.0000
				51.0000,	34.0000	52.0000,	32.0000
				52.0000,	30.5000	51.0000,	30.0000
				51.0000,	29.0000	52.0000,	28.5000
				53.0000,	28.5000	47.0000,	28.0000
				46.0000,	29.0000	43.0000,	29.0000
42	-0.040	4.0000000	7.0000000	40.0000,	26.0000	37.0000,	30.0000
				39.0000,	31.0000	40.0000,	30.0000
				48.0000,	32.0000	54.0000,	30.0000
				54.0000,	29.0000	45.0000,	25.0000
				46.0000,	26.0000	46.0000,	28.0000
				42.0000,	28.0000		
43	-0.040	7.0000000	9.0000000	42.0000,	27.0000	40.0000,	28.0000
				41.0000,	29.0000	46.0000,	29.0000
				47.0000,	28.0000	45.0000,	27.0000
44	0.120	0.0000000	1.0000000	64.0000,	52.0000	57.0000,	54.0000
				57.0000,	57.0000	73.0000,	70.0000
				80.0000,	70.0000	80.0000,	52.0000

45	0.120	1.0000000	2.0000000	61.0000, 48.0000, 70.0000, 80.0000,	45.0000 57.0000 70.0000 45.0000	48.0000, 58.0000, 80.0000,	53.0000 62.0000 70.0000
46	0.120	2.0000000	3.0000000	64.0000, 43.0000, 33.0000, 36.0000, 80.0000,	42.0000 40.0000 46.0000 62.0000 70.0000	54.0000, 40.0000, 33.0000, 43.0000, 80.0000,	44.0000 40.0000 53.0000 70.0000 42.0000
47	0.120	3.0000000	4.0000000	64.0000, 50.0000, 27.0000, 34.0000, 80.0000,	40.0000 36.0000 42.0000 62.0000 70.0000	54.0000, 36.0000, 27.0000, 40.0000, 80.0000,	41.0000 32.0000 48.0000 70.0000 40.0000
48	0.120	4.0000000	5.0000000	64.0000, 44.0000, 31.0000, 26.0000, 68.0000, 80.0000,	43.0000 35.0000 33.0000 47.0000 70.0000 43.0000	54.0000, 36.0000, 26.0000, 56.0000, 80.0000,	45.0000 33.0000 39.0000 62.0000 70.0000
49	0.120	4.0000000	7.0000000	74.0000, 54.0000, 18.0000, 0.0000, 12.0000, 68.0000, 26.0000, 31.0000, 44.0000, 64.0000, 80.0000,	40.0000 35.0000 32.0000 43.0000 52.0000 70.0000 47.0000 33.0000 35.0000 43.0000 40.0000	57.0000, 30.0000, 10.0000, 0.0000, 38.0000, 56.0000, 26.0000, 36.0000, 54.0000, 80.0000,	38.0000 29.0000 43.0000 52.0000 70.0000 62.0000 39.0000 33.0000 45.0000 43.0000

RESERVATION COORDINATES (KM.)	MODEL RESPONSE (MILLIGALS)	DESIRED RESPONSE (MILLIGALS)	DIFFERENCE (MILLIGALS)	DIFFERENCE (AVERAGE REMOVED)
7.500	0.000	2.000	0.5621	-0.7584
7.500	1.000	3.000	1.1654	-0.1551
7.500	2.000	4.000	1.2936	-0.0268
7.500	3.000	5.000	-0.2703	-1.5907
7.500	4.000	6.000	-0.2587	-1.5792
7.500	5.000	7.000	0.0912	-1.2293
7.500	6.000	8.000	0.3734	-0.9471
7.500	7.000	9.000	0.3473	-0.9731
7.500	8.000	10.000	-0.1663	-1.4867
7.500	9.000	11.000	-0.6806	-2.0010
7.500	10.000	12.000	-0.7731	-2.0935
7.500	11.000	13.000	-0.6588	-1.9792
7.500	12.000	14.000	-0.5433	-1.8637
7.500	13.000	15.500	-0.0135	-1.3339
7.500	14.000	17.000	0.4681	-0.8523
7.500	15.000	18.400	0.8680	-0.4524
7.500	16.000	20.000	1.5029	0.1825
7.500	17.000	21.200	1.7993	0.4788
7.500	18.000	23.000	2.8515	1.5310

7.500	19.000	20.605	25.000	4.3950	3.0746
7.500	20.000	20.655	27.400	6.7450	5.4245
7.500	21.000	20.210	26.500	6.2900	4.9696
7.500	22.000	19.206	25.000	5.7937	4.4732
7.500	23.000	17.669	20.500	2.8312	1.5108
7.500	24.000	15.571	18.000	2.4293	1.1088
7.500	25.000	14.580	17.200	2.6200	1.2995
7.500	26.000	14.092	15.800	1.7077	0.3872
7.500	27.000	13.734	14.700	0.9658	-0.3547
7.500	28.000	13.338	13.600	0.2618	-1.0586
7.500	29.000	12.442	12.800	0.3576	-0.9629
7.500	30.000	10.693	12.600	1.9074	0.5870
7.500	31.000	10.363	12.400	2.0367	0.7163
7.500	32.000	10.151	12.200	2.0493	0.7288
7.500	33.000	9.818	11.500	1.6816	0.3612
7.500	34.000	9.222	9.700	0.4785	-0.8420
7.500	35.000	8.303	8.500	0.1966	-1.1238
7.500	36.000	7.380	7.800	0.4196	-0.9009
7.500	37.000	6.646	7.300	0.6540	-0.6665
7.500	38.000	6.062	6.700	0.6381	-0.6823
7.500	39.000	5.694	6.000	0.3060	-1.0145
7.500	40.000	5.597	4.800	-0.7970	-2.1174
7.500	41.000	5.738	5.000	-0.7380	-2.0584
7.500	42.000	6.046	5.800	-0.2464	-1.5669
7.500	43.000	6.442	6.400	-0.0423	-1.3627
7.500	44.000	6.840	7.000	0.1595	-1.1609
7.500	45.000	7.165	7.800	0.6346	-0.6858
7.500	46.000	7.368	8.200	0.8322	-0.4882
7.500	47.000	7.423	8.500	1.0768	-0.2436
7.500	48.000	7.322	8.800	1.4780	0.1576
7.500	49.000	7.061	8.100	1.0395	-0.2809
7.500	50.000	6.643	7.700	1.0570	-0.2634
7.500	51.000	6.088	7.400	1.3115	-0.0089
7.500	52.000	5.439	7.200	1.7610	0.4405
7.500	53.000	4.759	6.700	1.9411	0.6206
7.500	54.000	4.111	5.500	1.3889	0.0685
7.500	55.000	3.536	5.000	1.4642	0.1438
7.500	56.000	3.047	5.500	2.4532	1.1327
7.500	57.000	2.640	6.000	3.3602	2.0397
7.500	58.000	2.304	6.200	3.8961	2.5756
7.500	59.000	2.026	6.500	4.4735	3.1531

THE AVERAGE OF THE DIFFERENCES IS 1.3204, AND THE R.M.S. OF THE DIFFERENCES (WITH MEAN REMOVED) IS 1.6853
 1 DIVISION = 0.330000 MGALS.



6

+*

7

+*

8

**+

9

*+

10

*+

11

*+

12

**+

13

+

14

+*

15

+*

16

+*

17

+*

18

*

19

*

20

*

21

*

22

*

23

*+

24

+*

25

26 . *
 27 + *
 28 + *
 29 + **
 30 + *
 31 *
 32 *
 33 *
 34 *
 35 + **
 36 + *
 37 + *
 38 + *
 39 + *
 40 + **
 41 * +
 42 * +
 43
 44 * +
 45

46

+ *

47

+ *

48

*

49

*

50

+ *

51

+ *

52

+ *

53

*

54

*

55

*

56

*

57

*

58

*

59

*

60

*